

NEA/WPEC-8

International Evaluation Co-operation

VOLUME 8

PRESENT STATUS OF MINOR ACTINIDE DATA

*A report by the Working Party
on International Evaluation Co-operation
of the NEA Nuclear Science Committee*

CO-ORDINATOR

T. Nakagawa
JAERI
Japan

CO-ORDINATOR

H. Takano
JAERI
Japan

MONITOR

A. Hasegawa
JAERI
Japan

NUCLEAR ENERGY AGENCY
ORGANISATION FOR ECONOMIC CO-OPERATION AND DEVELOPMENT

ORGANISATION FOR ECONOMIC CO-OPERATION AND DEVELOPMENT

Pursuant to Article 1 of the Convention signed in Paris on 14th December 1960, and which came into force on 30th September 1961, the Organisation for Economic Co-operation and Development (OECD) shall promote policies designed:

- to achieve the highest sustainable economic growth and employment and a rising standard of living in Member countries, while maintaining financial stability, and thus to contribute to the development of the world economy;
- to contribute to sound economic expansion in Member as well as non-member countries in the process of economic development; and
- to contribute to the expansion of world trade on a multilateral, non-discriminatory basis in accordance with international obligations.

The original Member countries of the OECD are Austria, Belgium, Canada, Denmark, France, Germany, Greece, Iceland, Ireland, Italy, Luxembourg, the Netherlands, Norway, Portugal, Spain, Sweden, Switzerland, Turkey, the United Kingdom and the United States. The following countries became Members subsequently through accession at the dates indicated hereafter: Japan (28th April 1964), Finland (28th January 1969), Australia (7th June 1971), New Zealand (29th May 1973), Mexico (18th May 1994), the Czech Republic (21st December 1995), Hungary (7th May 1996), Poland (22nd November 1996) and the Republic of Korea (12th December 1996). The Commission of the European Communities takes part in the work of the OECD (Article 13 of the OECD Convention).

NUCLEAR ENERGY AGENCY

The OECD Nuclear Energy Agency (NEA) was established on 1st February 1958 under the name of OEEC European Nuclear Energy Agency. It received its present designation on 20th April 1972, when Japan became its first non-European full Member. NEA membership today consists of all OECD Member countries, except New Zealand and Poland. The Commission of the European Communities takes part in the work of the Agency.

The primary objective of the NEA is to promote co-operation among the governments of its participating countries in furthering the development of nuclear power as a safe, environmentally acceptable and economic energy source.

This is achieved by:

- *encouraging harmonization of national regulatory policies and practices, with particular reference to the safety of nuclear installations, protection of man against ionising radiation and preservation of the environment, radioactive waste management, and nuclear third party liability and insurance;*
- *assessing the contribution of nuclear power to the overall energy supply by keeping under review the technical and economic aspects of nuclear power growth and forecasting demand and supply for the different phases of the nuclear fuel cycle;*
- *developing exchanges of scientific and technical information particularly through participation in common services;*
- *setting up international research and development programmes and joint undertakings.*

In these and related tasks, the NEA works in close collaboration with the International Atomic Energy Agency in Vienna, with which it has concluded a Co-operation Agreement, as well as with other international organisations in the nuclear field.

© OECD 1999

Permission to reproduce a portion of this work for non-commercial purposes or classroom use should be obtained through the Centre français d'exploitation du droit de copie (CCF), 20, rue des Grands-Augustins, 75006 Paris, France, Tel. (33-1) 44 07 47 70, Fax (33-1) 46 34 67 19, for every country except the United States. In the United States permission should be obtained through the Copyright Clearance Center, Customer Service, (508) 750-8400, 222 Rosewood Drive, Danvers, MA 01923, USA, or CCC Online: <http://www.copyright.com/>. All other applications for permission to reproduce or translate all or part of this book should be made to OECD Publications, 2, rue André-Pascal, 75775 Paris Cedex 16, France.

FOREWORD

A Working Party on International Evaluation Co-operation was established under the sponsorship of the OECD/NEA Nuclear Science Committee (NSC) to promote the exchange of information on nuclear data evaluations, validation, and related topics. Its aim is also to provide a framework for co-operative activities between members of the major nuclear data evaluation projects. This includes the possible exchange of scientists in order to encourage co-operation. Requirements for experimental data resulting from this activity are compiled. The working party determines common criteria for evaluated nuclear data files with a view to assessing and improving the quality and completeness of evaluated data.

The parties to the project are: ENDF (United States), JEF/EFF (NEA Data Bank Member countries), and JENDL (Japan). Co-operation with evaluation projects of non-OECD countries, specifically the Russian BROND and Chinese CENDL projects, are organised through the Nuclear Data Section of the International Atomic Energy Agency (IAEA).

Subgroup 8 of the working party was initiated with the objective to review the quality of evaluated nuclear data files for minor actinides. These are currently of increasing importance because of the interest in their transmutation as a method of reducing their long-term environmental impact. The work has been divided into two parts, the first part of which graphically compares available data, and the second part of which benchmarks the data against experiments such as irradiated samples, irradiated fuel and reaction rate measurements in critical facilities.

The opinions expressed in this report are those of the authors only and do not necessarily represent the position of any Member country or international organisation. This report is published on the responsibility of the Secretary-General of the OECD.

TABLE OF CONTENTS

SUMMARY	7
1. Introduction	9
2. Comparison of evaluated data	9
2.1 General description	9
2.2 ²³⁷Np cross-sections	11
2.3 ²⁴¹Am cross-sections	13
2.4 ²⁴³Am cross-sections	14
2.5 ²⁴²Cm cross-sections	16
2.6 ²⁴³Cm cross-sections	17
2.7 ²⁴⁴Cm cross-sections	18
2.8 ²⁴⁵Cm cross-sections	19
2.9 Neutrons per fission	20
2.10 Conclusion of data comparison	21
3. Benchmark tests of minor actinides nuclear data of JENDL-3.2, ENDF/B-VI Release 5 and JEF-2.2	21
3.1 Benchmark calculations	22
3.1.1 Burn-up calculations for PWR	22
3.1.2 Analysis of FCA-IX assemblies	22
3.1.3 Accelerator-driven reactor benchmark	24
3.2 Concluding remarks	24
REFERENCES	27
TABLES	35
FIGURES	43

SUMMARY

The present status of evaluated data for ^{237}Np , ^{241}Am , ^{243}Am , ^{242}Cm , ^{243}Cm , ^{244}Cm and ^{245}Cm has been investigated. Their data for cross-sections and number of neutrons per fission are shown in figures comparing the evaluated data in JENDL-3.2, ENDF/B-VI, JEF-2.2 and evaluations for BROND-3 and the data recently evaluated by Maslov, *et al.* with each other and with experimental data. Short comments are given for each data.

To validate minor actinides (MA) nuclear data is given in three large evaluated nuclear data files: JENDL-3.2, ENDF/B-VI and JEF-2.2. A burn-up analysis of PWR and benchmark calculations for fast critical experiments and for accelerator-driven cores were performed. The burn-up analysis of PWR showed that the results calculated with the three data files are generally in good agreement with the measured data, except for the build-up for ^{238}Pu , $^{242\text{m}}\text{Am}$ and ^{244}Cm . The fission reaction rate ratios for minor actinides of ^{237}Np , ^{241}Am , ^{243}Am and ^{244}Cm measured at the FCA-IX assemblies were analysed with the use of the three different nuclear data files. As a result, the calculated values are almost in agreement with the experimental data in the range of 5% errors, with the exception of all the results for ^{244}Cm and the JEF-2.2 results for ^{241}Am . In the benchmark calculation of accelerator-driven cores with concentrated MA fuels, a remarkable discrepancy between k_{eff} values was observed, the major causes being due to the discrepancies in fission neutron spectrum and fission cross-sections evaluated for MA nuclides.

PRESENT STATUS OF MINOR ACTINIDE DATA

1. Introduction

The nuclear data of minor actinides are important not only for analysis of reactor performance but also for study of treatment of spent fuel. However the data in the current major evaluated nuclear data libraries are not very reliable to meet the requirement from those application fields. Subgroup 8 of the Working Party on Evaluation Co-operation (WPEC) was organised to review the status of the evaluated data for the minor actinides, and to perform benchmark calculations to identify the reliability of the evaluated data.

In the early stage of the work of Subgroup 8, we compared the data for ^{237}Np and ^{241}Am given in ENDF/B-VI, JENDL-3 and JEF-2, and reported our findings at the WPEC meetings. Benchmark calculations concerning minor actinides were also made and reported. For the final report of Subgroup 8, we extended the scope of work to the data of ^{243}Am , ^{242}Cm , ^{243}Cm , ^{244}Cm and ^{245}Cm for the comparison, and included the evaluation made by Ignatyuk, *et al.* [1] for BROND-3 and Maslov, *et al.* [2] under the ISTC (International Science and Technology Centre) project as well as ENDF/B-VI Release 5, JENDL-3.2 and JEF-2.2.

In Section 2, we describe the present status of the evaluated cross-section data and neutron per fission ν for ^{237}Np , ^{241}Am , ^{243}Am , ^{242}Cm , ^{243}Cm , ^{244}Cm and ^{245}Cm in comparison with each other and with experimental data.

In Section 3, the benchmark calculations concerning minor actinide data are given.

2. Comparison of evaluated data

2.1 General description

In this section, the evaluated data for ^{237}Np , ^{241}Am , ^{243}Am , ^{242}Cm , ^{243}Cm , ^{244}Cm and ^{245}Cm are compared. Table 2.1 shows the year of evaluation of data stored in JENDL-3.2, ENDF/B-VI Release 5, JEF-2.2 and recent independent

evaluations. In the last 10 years, only the data of ^{237}Np , and the data of ^{241}Am and ^{243}Am above the unresolved resonance region were re-evaluated for ENDF/B-VI, and the resonance parameters of ^{237}Np for JENDL-3.2. Recently, Maslov, *et al.* evaluated the data of ^{241}Am , ^{243}Am , ^{243}Cm and ^{245}Cm . These data are tentatively named here as “MASLOV”. Additionally, a new evaluation [1] of the data of ^{237}Np , ^{241}Am , ^{243}Am , ^{242}Cm , ^{243}Cm and ^{244}Cm was made for BROND-3. These preliminary data are referred to here as “BROND-3”.

Detailed descriptions of the evaluated data can be found in the following literature:

JENDL-3.2	^{241}Am and ^{243}Am [3,4], Cm isotopes [5]
ENDF/B-VI	Cm isotopes [6], ^{242}Cm and ^{245}Cm [7]
JEF-2.2	^{237}Np [8], ^{242}Cm [9], ^{243}Cm [10], ^{245}Cm [11]
BROND-3	[1]
MASLOV	^{241}Am [12], ^{243}Am [13], ^{243}Cm [14], ^{245}Cm [15]

A short description of each data file is given in MF=1, MT=451. The data for BROND-3, which the authors of the present report received from Ignatyuk, have no descriptive data in MF=1.

The pointwise cross-section data were reconstructed using RESENDD [16] or RECENT89 [17]. The adopted accuracy of the cross-section calculation was 0.5%. The thermal cross-sections and resonance integral were calculated from the pointwise data with INTERN [18]. The resonance integral was calculated in the energy range from 0.5 eV to 20 MeV. They are listed in Tables 2.2 to 2.5 comparing with Mughabghab’s recommendations [19] and experimental data reported after 1980.

In order to make graphs for comparison, the cross-sections in the resolved resonance region were averaged with CRECTJ6 [20] using the energy intervals of the JAERI fast group constant set. No weighting function was considered in the averaging. For all nuclides, the fission, capture, elastic scattering and total cross-sections are compared in this averaged form in the incident neutron energy range from 0.01 eV to 20 MeV. Above the keV region, the graphs comparing the evaluated data with experimental data are prepared for the fission and capture cross-sections. The experimental data available in EXFOR as of January 1998 were translated to NESTOR, which is the neutron data storage and retrieval system being used in the Nuclear Data Centre, JAERI. A few sets of recent experimental data are added at making graphs. If enough room exists, the legend of experimental data is given on first author, year of publication, reference and an EXFOR entry-subentry number. The total inelastic, (n,2n) and (n,3n) reaction, elastic scattering and total cross-sections are also shown in graphs.

The numbers of neutrons per fission are compared in figures. To reduce the number of figures, we show only the total numbers of neutrons (ν_{tot}).

Those figures and tables show the present status of the evaluated data for the nuclides. Only short comments on the evaluated data are given in the following sections. Because of their importance, the fission and capture cross-sections are mainly discussed.

2.2 ^{237}Np cross-sections

Resolved resonance region

The upper boundary of the resolved resonance region is 150 eV for ENDF/B-VI and JEF-2.2, and 130 eV for JENDL-3.2. The BROND-3 evaluation extended it to 600 eV. The evaluated data given in ENDF/B-VI and JEF-2.2 are identical, and were evaluated by Derrien *et al.* [8] The data of JENDL-3.2 were based on the experimental data of Weston and Todd [21], and those of Plattard, *et al.* [22] Then, the fission widths were adjusted so as to reproduce the fission cross-section measured by Yamanaka, *et al.* [23] Figure 2.1 shows the comparison of the experimental data of Yamanaka, *et al.* with the evaluated data and the experimental data of Plattard, *et al.* and Hoffman, *et al.* [24] Yamanaka, *et al.* measured the fission cross-section using a lead slowing-down spectrometer. All the data are broadened with the energy resolution of Yamanaka, *et al.* The data of Yamanaka are somewhat larger than those of Plattard *et al.*, but close to the data of Hoffman, *et al.* JENDL-3.2 and BROND-3 are in good agreement with the data of Yamanaka, *et al.*

Fission cross-section

The thermal fission cross-sections are compared in Table 2.2. JENDL-3.2 and BROND-3 are nearly the same and are in agreement with the recent experimental data [25,26]. The resonance integrals of fission of the evaluated data are consistent with the recommendation by Mughabghab, while the experimental data of 4.70 ± 0.23 barns of Kozharin, *et al.* [26] is about 30% lower than the evaluations. However, the resonance integral of fission is sensitive to the upper boundary of integral. For example, the value of 7.06 barns of JENDL-3.2 becomes 4.87 barns if the upper boundary is 7 MeV. Since the measurement of Kozharin, *et al.* was done in the VVR-M reactor, the evaluated values might be consistent with their experimental value.

Figure 2.2 is the comparison of the fission cross-section in the neutron energy range from 0.01 eV to 20 MeV. It shows large discrepancies among the evaluated data below a few hundreds keV. The recent measurement by Iwasaki, *et al.* [27] is in agreement with the BROND-3 evaluation as shown in Figure 2.3. The data above a few hundred keV are satisfactory because many reliable experimental data are available in this energy region.

Capture cross-section

The thermal capture cross-sections of the evaluated values are larger than the recent experimental data measured by Jurova, *et al.* [28] and Kobayashi, *et al.* [29], while the resonance integrals are in good agreement with Mughabghab's recommendation and the experimental data of Kobayashi, *et al.*

Figure 2.4 shows evaluated data in the energy range from 0.01 eV to 20 MeV. Below 1 MeV, the evaluated cross-section data are in good agreement with each other. They are reproducing well the experimental data as shown in Figure 2.5. However, the data are largely discrepant in the energy region above 3 MeV. JEF-2.2 considered the direct and semi-direct capture cross-section. JENDL-3.2 did not consider it. BROND-3 was based on the systematics of the 14 MeV capture cross-sections.

(n,2n) and (n,3n) reaction cross-sections

The $^{237}\text{Np}(n,2n)$ reaction cross-section is important to estimate the amount of ^{236}Pu in the fission reactors. Since the branching ratio to ^{236}Pu from the ^{236}Np ground state is 48% and that from the ^{236}Np meta-stable state 9%, the ratio of ^{236g}Np and ^{236m}Np productions is also important. Figure 2.6 shows evaluated data and experimental data of the $^{237}\text{Np}(n,2n)$ cross-section and $^{237}\text{Np}(n,2n)^{236m}\text{Np}$ cross-section. JEF-2.2 gives only the ^{236g}Np production cross-section and its values are too large. Around 14 to 15 MeV, the evaluated data reproduce rather well the experimental data. Below 14 MeV, experimental data are not sufficient to judge the reliability of the evaluated data. JENDL-3.2 is based on the experimental data of Nishi *et al.* [30] for the total (n,2n) cross-section and Kornilov, *et al.* [31] for the meta-stable state.

Figure 2.7 displays the (n,2n) and (n,3n) reaction cross-sections. There are large discrepancies among the evaluated (n,3n) cross-sections. JENDL-3.2 has the tendency of the large (n,3n) cross-section for all the nuclides considered here.

Other cross-sections

The total inelastic scattering cross-section is shown in Figure 2.8. The elastic scattering cross-sections are compared in Figure 2.9. JENDL-3.2 is about two times larger than the other evaluations in the thermal energy region. The total cross-sections are shown in Figure 2.10. The data are in good agreement with each other in the whole energy region.

2.3 ²⁴¹Am cross-sections

Fission cross-section

The fission cross-section at 0.0253 eV is compared in Table 2.2. The evaluated data are in good agreement with the recent measurement by Yamamoto, *et al.* [32] except for JENDL-3.2, which seems to be a little smaller.

The fission resonance integrals are in good agreement with Mughabghab's recommendation and the experimental data of Dabbs, *et al.* [33], with the exception of JEF-2.2.

The fission cross-sections are given in Figure 2.11. The data above 100 keV are compared with experimental data in Figure 2.12. All the evaluated data above the resolved resonance region agree well with each other and with the experimental data. JEF-2.2, however, seems to be too large below 10 keV. The evaluated data are shown in Figure 2.13 comparing with the experimental data measured by Yamamoto, *et al.* [32]. This experiment was performed with a lead slowing-down spectrometer. The evaluated data in this figure are broadened with the energy resolution of the spectrometer. In the energy range from 20 eV to 150 eV, the data of JENDL-3.2 are smaller than those found in the experiment. Below 1 eV, the resolution function used in the present work seems to be inadequate.

Capture cross-section

The thermal capture cross-sections given in the evaluated data files are 600 to 619 barns. Maslov's evaluation is in good agreement with Mughabghab's recommendation. The recent measurement made by Shinohara, *et al.* [34], however, is 854 ± 58 barns – 45% larger than Mughabghab's recommendation. This large cross-section is consistent with Belanova's evaluation [35] of 824 ± 20 barns, which is based on the measurements by Bak, *et al.* [36], Gavrilov, *et al.* [37] and Harbour, *et al.* [38] On the other hand, Wisshak, *et al.* [39]

obtained 765 ± 39 barns at 0.01474 eV which is 584 barns at 0.0253 eV if the $1/v$ shape assumed. The total cross-section was measured by Adamchuk, *et al.* [40] in this energy region. The total cross-section is shown in Figure 2.14. The total cross-section of Adamchuk, *et al.* is less than 650 barns at the thermal energy. Further investigation is needed to solve this inconsistency.

The capture resonance integrals agree with Mughabghab's recommendation within the quoted error. JENDL-3.2 is slightly small.

As is shown in Figure 2.15, the evaluated data are in good agreement with each other in the energy range below 100 keV. Above this energy, discrepancies are quite large. The experimental data exist below 400 keV. Figure 2.16 shows the experimental data and the evaluated data in the energy range from 1 keV to 1 MeV. The data for BROND-3 were obtained by fitting theoretical values calculated with GNASH and the data estimated from systematics [41] to the renormalised experimental data. JENDL-3.2 is based on the data of Vanpraet, *et al.* [42] Maslov's data are systematically small below 10 keV.

The branching ratio of $^{241}\text{Am}(n,\gamma)^{242g}\text{Am}$ and $^{241}\text{Am}(n,\gamma)^{242m}\text{Am}$ cross-sections is important. Its evaluated data, however, are only given in ENDF/B-VI. A comparison is illustrated in Figure 2.17. At the thermal energy, Shinohara, *et al.* [34] obtained the ratio of ground to total of 0.90 ± 0.09 , which is in very good agreement with the value of 0.92 ± 0.06 at 0.01475 eV [43] and 0.90 given in ENDF/B-VI. The data in the thermal region are satisfactory, but we need further investigation on this quantity in the higher energy region.

Other cross-sections

Figure 2.18 shows the (n,2n) and (n,3n) cross-sections. The (n,3n) cross-section of JENDL-3.2 is too large. Figure 2.19 is a comparison of the total inelastic scattering. Figures 2.20 and 2.21 show the elastic scattering and total cross-sections, respectively. They are in good agreement.

2.4 ^{243}Am cross-sections

Fission cross-section

The thermal fission cross-sections calculated from the resonance parameters and experimental data are rather discrepant. According to the description given in MF=1, MT=451 of JEF-2.2, the thermal fission cross-section of 0.05 barn given in JEF-2.2 is an arbitrary value. The parameters given in BROND-3 and

Maslov's evaluation are identical, which were determined to reproduce the data of 0.072 barn measured by Hulet, *et al.* [44] ENDF/B-VI is based on the Wagemans' measurement (not referenced). JENDL-3.2 is the value calculated from resonance parameters that were mainly based on the data of Knitter and Budtz-Jørgensen [45]. The recent experimental data of 0.0813 ± 0.0025 barn [46] is close to ENDF/B-VI, and is 60% smaller than what Mughabghab recommends.

The resonance integrals of the fission cross-section calculated from the evaluated data are close to each other except JEF-2.2. The value of Knitter and Budtz-Jørgensen, 3.05 ± 0.15 barns, was obtained in the energy range from 0.5 eV to 30 keV. If the resonance integral is calculated in this energy range, JENDL-3.2 and ENDF/B-VI are 2.24 and 2.12 barns, respectively, which are smaller than the experimental data.

The fission cross-sections are given in Figure 2.22. In the energy range below about 400 keV, the large discrepancies are seen among the evaluated data. In particular, JEF-2.2 is too small in this energy region. Discrepancies among other data are large in the energy range from 10 to 100 eV which is the resolved resonance region. The evaluated resonance parameters are based on the fission cross-section measurements of Knitter and Budtz-Jørgensen [45]. The resonance parameters of BROND-3 and MASLOV are the same. ENDF/B-VI assumed the average fission width of 0.025 meV and JENDL-3.2 that of 0.120 meV to the levels whose fission width was not measured by Knitter and Budtz-Jørgensen. Figure 2.23 shows a comparison of the fission cross-sections with the recent experiment made by Kobayashi, *et al.* [46] In this energy region, the data of JENDL-3.2 are closest to the experimental data.

Figure 2.24 is another comparison with experimental data above 1 keV.

Capture cross-section

The thermal capture cross-sections and resonance integral are in good agreement with each other among the evaluated data.

The capture cross-section is given in Figures 2.25 and 2.26. Below 500 keV, the evaluated data are in very good agreement with each other and with the experimental data. In the higher energy region, the evaluated data are discrepant.

Other cross-sections

Figure 2.27 shows the (n,2n) and (n,3n) cross-sections. Figures 2.28, 2.29 and 2.30 show the inelastic scattering, elastic scattering and total cross-sections, respectively.

2.5 ^{242}Cm cross-sections

Fission cross-section

The thermal fission cross-section is not well known. The recommended value in Ref. [19] is “less than 5 barns” which is based on old data measured by Hanna *et al.* [47]. JENDL-3.2, JEF-2.2 and BROND-3 adopted the maximum value.

The resonance integral of 12.9 ± 0.7 barns was obtained by Alam, *et al.* [48] by integrating their measured fission cross-sections from 0.53 eV to 50.93 keV. The resonance integral of JENDL-3.2 and BROND-3 corresponding to this energy range are 11.0 barns and 13.1 barns, respectively. Therefore BROND-3 is in very good agreement with Alam’s data.

Figure 2.31 shows large discrepancies among the evaluated data. In the evaluation for ENDF/B-VI, only the negative resonance has the fission width. Therefore the fission cross-section in the resonance region below 10 keV is too small. Above 10 keV, the cross-section is based on the statistical model calculation. However, the cross-section is still too small. JEF-2.2 gives the $1/v$ cross-section below several hundreds eV. Above 20 keV, the evaluation seems to be based on experimental data. BROND-3 is based on the systematics, and cannot reproduce the experimental data.

Capture cross-section

Contrary to the fission cross-section, the thermal capture cross-section is well known. The evaluated data agree well with the recommended value of 16 ± 5 barns of Mughabghab. The capture resonance integrals calculated from the evaluated data are also consistent with Mughabghab’s recommendation of 110 ± 20 barns.

As shown in Figure 2.32, large discrepancies exist above the resolved resonance region where no experimental data are available. In the JENDL-3.2 evaluation of the smooth part, the average capture width of 40 meV and the

average level spacing of 18 eV that are consistent with the resolved resonance parameters were used. For the other evaluations, such parameters were not documented well.

Other cross-sections

Figure 2.33 shows the (n,2n) and (n,3n) cross-sections. JEF-2.2 does not give the (n,3n) reaction cross-section. Figure 2.34, 2.35 and 2.36 show the inelastic scattering, elastic scattering and total cross-sections, respectively.

2.6 ²⁴³Cm cross-sections

Fission cross-section

For both the thermal cross-section and resonance integral, Maslov's evaluation is almost the same as JENDL-3.2, which agrees with Mughabghab's recommendations. ENDF/B-VI, JEF-2.2 and BROND-3 differ from the recommendation. The resonance parameters given in BROND-3 are the same as those of ENDF/B-VI.

The resolved resonance parameters of JENDL-3.2 were determined on the basis of Anufriev, *et al.* [49] Those of MASLOV were based on Anufriev, *et al.* below 14 MeV, and on fitting to available fission and transmission data. JEF-2.2 and ENDF/B-VI were based on the old experimental data of Berreth, *et al.* [50]

The evaluated data of the fission cross-section are compared in Figure 2.37. Figure 2.38 shows the evaluated fission cross-sections along with experimental data in the neutron energy range from 100 keV to 20 MeV. JENDL-3.2 was evaluated on the basis of the experimental data of Fomushkin, *et al.* [51] Fursov, *et al.* [52] measured the fission cross-section in the energy region from 145 keV to 7 MeV and at 15 MeV. Their results are nearly the same as Silbert [53] in the 100 keV region and as Fomushkin, *et al.* [51] around 15 MeV. All of the current evaluated data are lower than Fursov, *et al.* except BROND-3, which adopts Fursov's data. Their data seem to be too large comparing with the compound formation cross-section calculated with the optical model.

Capture cross-section

Above about 1 keV, discrepancies among the evaluated data are large, as shown in Figure 2.39. JENDL-3.2 and JEF-2.2 did not take account of the direct and semi-direct process.

Other cross-sections

Figure 2.40 shows the (n,2n) and (n,3n) cross-sections. Figures 2.41, 2.42 and 2.43 show the inelastic scattering, elastic scattering and total cross-sections, respectively.

2.7 ²⁴⁴Cm cross-sections

Fission cross-section

The thermal cross-section of ENDF/B-VI is quite a bit smaller than the recommendation by Mughabghab. The other evaluations reproduce well his recommendation. As to the resonance integral, the recommended value of Mughabghab is smaller than the evaluated data. Mughabghab was based on the experimental data of Thompson, *et al.* [54] In almost the same year, however, Benjamin *et al.* [55] reported the resonance integral of 18.0 ± 1.0 barns. The cut-off energy of Benjamin *et al.* is 0.625 eV. The contribution from the energy range from 0.5 to 0.625 eV is negligible for this nuclide. Discrepancies which exist among the evaluated data come from the parameters of the first resonance at 7.67 eV. For example, JENDL-3.2 gives the fission width of 0.12 meV [56] and ENDF/B-VI that of 0.45 meV.

The fission cross-section in the energy range below 100 keV is discrepant as shown in Figure 2.44. Below 10 eV, the discrepancies are due to differences of the resonance parameters for the 7.67 eV and negative resonances. JEF-2.2 gives large fission widths to the resonances at 646 and 648 eV. ENDF/B-VI is too small in the unresolved resonance region. The preliminary data for BROND-3 has a compilation error at 20 keV.

Figure 2.45 shows the evaluated data and experimental data of the fission cross-section. Above the threshold, the evaluated data agree well with the experimental data. Above about 7 MeV, the evaluated data are again discrepant as a result of an insufficient amount of experimental data.

Capture cross-section

The situation of the thermal capture cross-section is the same as the fission. The capture resonance integral recommended by Mughabghab is well reproduced by the evaluated data. More recent experimental data are not available.

The evaluated data agree rather well (Figure 2.46). The experimental data are available below 10 keV (Figure 2.47).

Other cross-sections

Figure 2.48 shows the (n,2n) and (n,3n) cross-sections. Figures 2.49, 2.50 and 2.51 show the inelastic scattering, elastic scattering and total cross-sections, respectively.

2.8 ²⁴⁵Cm cross-sections

Fission cross-section

The thermal fission cross-section of ²⁴⁵Cm is very large. The recommended value of $2\,145\pm 58$ barns [19] is based on the experimental data of Browne, *et al.* [57] JEF-2.2 and Maslov's evaluation are in good agreement with the recommendation. JENDL-3.2 is slightly small. However there also exists a small experimental data of $1\,900\pm 100$ barns measured by Gavrilov, *et al.* [37]

Concerning the resonance integral, JEF-2.2 is too small compared with Mughabghab's recommendation. The fission cross-section calculated from the resonance parameters given in JEF-2.2 seems to be too small at a few eV as shown in Figure 2.52.

The fission cross-section above 10 keV is shown in Figure 2.53. In this energy range, Maslov's evaluation and JENDL-3.2 reproduce well the experimental data.

Capture cross-section

The thermal capture cross-sections given in the evaluated data are in good agreement with the most recent experimental data of 350 ± 18 barns of Gavrilov and Goncharov [58], while the recommendation of Mughabghab is slightly higher.

The resonance integral of JEF-2.2 is larger than the others. As shown in Figure 2.54, the capture cross-section of JEF-2.2 in the 1 to 10 eV range is larger than the other evaluations.

The convex shape of ENDF/B-VI above 10 keV results from the linear-linear interpolation scheme.

Maslov's evaluation gives the capture cross-section larger than the others below 1 MeV. One of the reasons for this difference is the average level spacing: 1.4 eV adopted for JENDL-3.2 and 0.698 eV for Maslov's evaluation.

Other cross-sections

Figure 2.55 shows the (n,2n) and (n,3n) cross-sections. Figures 2.56, 2.57 and 2.58 show the inelastic scattering, elastic scattering and total cross-sections, respectively.

2.9 Neutrons per fission

The total number of neutrons per fission ν was compared in Figures 2.59 to 2.65. The evaluated data for the total ν and the experimental data for both of the total ν and ν_p are shown in these figures.

The data of ^{237}Np are shown in Figure 2.59. BROND-3 is the same as ENDF/B-VI. JENDL-3.2 adopted the data of Frehaut, *et al.* [59], which are smaller than others. The most recent experimental data were obtained by Boikov, *et al.* [60] at 2.9 and 14.7 MeV. Those results are almost the same as JENDL-3.2 at 2.9 MeV, and much smaller than JENDL-3.2 at 14.7 MeV.

Energy	Boikov, <i>et al.</i>	JENDL-3.2
2.9 MeV	2.98±0.07	2.950
14.7 MeV	4.45±0.08	4.719

Figure 2.60 shows the total ν of ^{241}Am . BROND-3 is the same as ENDF/B-VI. The recent experimental data by Khokhlov, *et al.* [61] are about 5% smaller than JENDL-3.2 at the low energies. There is a compilation error at 4 MeV in MASLOV. If the error is modified, MASLOV is in good agreement with Khokhlov, *et al.* In the case of ^{243}Am in Figure 2.61, the data of Khokhlov, *et al.* [61] are in agreement with the evaluated data of JENDL-3.2, BROND-3 and MASLOV. The energy dependence of ENDF/B-VI and JEF-2.2 are different from the other evaluated data.

The evaluated data for ^{242}Cm in Figure 2.62 has the same energy dependence. There are no experimental data for this nuclide. JENDL-3.2 is based on the systematics developed by Howerton [62]. For ^{243}Cm in Figure 2.63, JENDL-3.2, ENDF/B-VI and BROND-3 give the same data, which were determined from the data of Jaffy and Lener [63] and Zuravlev, *et al.* [64] at the thermal neutron energy and Howerton's systematics. The energy dependence of MASLOV was based on Madland-Nix model [65]. Figure 2.64 shows the total ν of ^{244}Cm . JEF-2.2 is almost the same as JENDL-3.2. There are no experimental data. Figure 2.65 displays the data of ^{245}Cm . JENDL-3.2 and MASLOV are in good agreement with the data of Howe, *et al.* [66] and those of Khokhlov, *et al.* [61].

2.10 Conclusion of data comparison

The evaluated cross-section data of ^{237}Np , ^{241}Am , ^{243}Am , ^{242}Cm , ^{243}Cm , ^{244}Cm and ^{245}Cm were compared with each other and with experimental data. The evaluated data chosen are JENDL-3.2, ENDF/B-VI, JEF-2.2, the recent evaluation for BROND-3 and the evaluation made by Maslov, *et al.* Discrepancies are found in the following quantities:

The status of the evaluated data for the fission cross-sections is satisfactory for many nuclides because experimental data are available. However, large discrepancies are found in ^{242}Cm . Small discrepancies still exist for all the nuclides considered in the present work.

The capture cross-sections in the MeV region are discrepant. A large discrepancy exists among the recent experimental data and the evaluated data of ^{241}Am at the thermal neutron energy. This problem should be solved in the near future. The isomeric ratio of ^{241}Am capture cross-section is also important, and good evaluated data are expected in the energy region from a few eV to 20 MeV.

The (n,2n) and (n,3n) reactions have quite large discrepancies among the evaluations. Even in the $^{237}\text{Np}(n,2n)$ reaction cross-section, discrepancies are found. For other nuclides, we have no experimental data at all. The (n,3n) reaction cross-section of JENDL-3.2 is generally too large. Maslov *et al.* indicated that this defect seems to be caused by the optical potential parameters used in the JENDL evaluation which generate large reactions cross-sections at the incident neutron energies above 10 MeV [15].

The situation of the inelastic scattering cross-section is the same as that of the (n,2n) and (n,3n) reaction cross-sections. Since JENDL-3.2 has not considered the direct process, the cross-section in the MeV region is too small.

The total and elastic scattering cross-sections are in rather good agreement with each other. This suggests that the optical model parameters used in the calculations are not largely different. However, it should be noted that those parameters are based on the data of other nuclides such as ^{238}U . To obtain more reliable parameters, we need experimental data of the total cross-section and elastic scattering.

3. Benchmark tests of minor actinides nuclear data of JENDL-3.2, ENDF/B-VI Release 5 and JEF-2.2

In order to accurately assess a neutronic behaviour of various types of reactors, it is necessary to validate both calculation methods and nuclear data by

analysing integral experimental data. There are still discrepancies found among JENDL-3.2, JEF-2.2 and ENDF/B-VI as shown in the previous section on minor actinides nuclear data. They may be considered to cause significant differences in neutronic characteristics. The benchmark calculations will be made for the PWR burn-up analysis, fast benchmark cores and accelerator-driven subcritical core benchmark. As a result, the effects of the discrepancies between nuclear data of ENDF/B-VI, JEF-2.2 and JENDL-3.2 on nuclear characteristics have appeared.

3.1 Benchmark calculations

Benchmark tests of thermal and fast reactors had been performed [67-70]. Here, the benchmark tests for MA nuclear data are described.

3.1.1 Burn-up calculations for PWR

Burn-up calculations were performed for the spent fuel irradiated in the existing PWR called Mihama in Japan [70]. In the calculations, the SRAC95 [71] nuclear design code was used. The branching ratios of $^{237}\text{Np}(n,2n)$ and $^{241}\text{Am}(n,\gamma)$ reactions were adopted from ENDF/B-VI. The results calculated for the three different nuclear data libraries of JENDL-3.2, ENDF/B-VI.5 and JEF-2.2 are compared with the measured values in Table 3.1. From this table, considerable discrepancies are observed for ^{232}U and ^{236}Pu , and the calculated values of ^{238}Pu , $^{242\text{m}}\text{Am}$ and ^{244}Cm significantly underestimate the measured data.

A large underestimate of ^{232}U build-up by JEF-2.2 is caused by underestimating the ^{236}Pu build-up. This may be attributed to the fact that the capture cross-sections in JEF-2.2 are significantly overestimated.

3.1.2 Analysis of FCA-IX assemblies

The FCA-IX assembly series consists of seven uranium fuelled cores which are built so as to cover the wide range of neutron spectrum shapes as shown in Figure 3.1 and to test the fission and capture cross-sections of higher actinides [72,73]. The assemblies IX-1 to IX-6 were composed with 93% enriched metal uranium, and diluent materials were graphite for assemblies IX-1 to IX-3 and stainless steel for assemblies IX-4 to IX-6. The assembly IX-7 was composed with 20% enriched metal uranium with no diluent materials. By analysing these assemblies we can investigate the relation between integral and nuclear data, depending on neutron spectrum. The integral data measured in

these assemblies are the effective multiplication factors and the central fission reaction rate ratios.

The three different libraries of 70-group cross-sections of JFS-3 type were produced with the processing code TIMS-PGG/NJOY [74].

Effective cross-sections were calculated by using the heterogeneous cell calculation code SLAROM [75]. The integral values calculated with two-dimensional diffusion theory were corrected by the factor obtained with the transport code TWODANT.

Effective multiplication factors

The C/E values of k_{eff} calculated with JENDL-3.2, ENDF/B-VI and JEF-2.2 are shown in Table 3.2. The k_{eff} values calculated with JENDL-3.2 are smaller than the results of ENDF/B-VI and JEF-2.2, and the values of JENDL-3.2 are close to the experimental values. However, all the results over-predict the experiments, and this tendency is remarkable for the cores with SUS moderators.

Central fission reaction rate

The central reaction rate ratios of ^{237}Np , ^{241}Am , ^{243}Am and ^{244}Cm to ^{239}Pu were calculated with the three different data libraries. Tables 3.3 to 3.6 show the comparison of the C/E values as a function of neutron spectral hardness.

- 1) *Fission ratio of ^{237}Np to ^{239}Pu : Table 3.3*
The results of JENDL-3.2 are in a good agreement with the experiments. ENDF/B-VI and JEF-2.2 show underestimates of about 3% and 5%, respectively.
- 2) *Fission ratio of ^{241}Am to ^{239}Pu : Table 3.4*
All the results are underestimated. The JEF-2.2 results are especially remarkable.
- 3) *Fission ratio of ^{243}Am to ^{239}Pu : Table 3.5*
The results of ENDF/B-VI are in good agreement with the experiments. JENDL-3.2 and JEF-2.2 under-predict them.
- 4) *Fission ratio of ^{244}Cm to ^{239}Pu : Table 3.6*
The C/E values depend considerably on the core neutron spectra, and all the calculated results overestimate the experiments.

3.1.3 Accelerator-driven reactor benchmark

A two-dimensional homogeneous benchmark model of an accelerator-driven Na-cooled reactor was proposed [76]. This system consists of beam duct with void, tungsten target divided with two different thickness discs, MA-fuelled core and reflector. The atom number densities are homogenised at each region to simplify the benchmark problem. The present accelerator-driven system is considered to be driven by a proton beam of 1 GeV energy and a current of 10 mA in subcritical state of $k_{\text{eff}} = 0.9$.

The three participants were: JAERI (NMTC/JAERI > 20 MeV, TWODANT with 73 group of JENDL-3.2 < 20 MeV), PSI (HETC-PSI, 15 MeV, TWODANT with 33 group of JEF-2.2 < 15 MeV) and IPPE (TWODANT-SYS with 28 group of ABBN-93). A remarkable discrepancy between k_{eff} -values – one of the most important integral data – has been observed [77].

To investigate the cause of this large discrepancy, we calculated this ADS benchmark problem with the three different libraries (JENDL-3.2, ENDF/B-VI Release 2, JEF-2.2) using a JAERI code system consisting of NMTC/JAERI and TWODANT. The calculated results are shown in Figure 3.2, and large differences are observed among the three libraries. At the initial loading stage, the difference in k_{eff} values between JENDL-3.2 and ENDF/B-VI is about 3%, which is caused by discrepancies in ^{237}Np and ^{241}Am nuclear data. The difference between JENDL-3.2 and JEF-2.2 is about 1%, and this is caused by differences between ^{237}Np cross-sections. Furthermore, we can observe considerably large different tendencies on burn-up reactivity change. The different tendency between JENDL-3.2 and ENDF/B-VI is due to large discrepancies in the fission cross-section of ^{242}Cm as shown in Figure 2.31. And the difference between JENDL-3.2 and JEF-2.2 is due to a discrepancy in the fission spectrum of ^{237}Np .

The major causes are due to fission neutron spectrum and fission cross-sections used for minor actinide nuclides in different nuclear data libraries.

3.2 Concluding remarks

The burn-up calculations for the existing PWR spent fuels showed a comparable agreement between the three different nuclear data libraries (JENDL-3.2, ENDF/B-VI and JEF-2.2) with the exception of several isotopes such as ^{232}U , ^{236}Pu and ^{243}Am .

The fission reaction rate ratios for minor actinides of ^{237}Np , ^{241}Am , ^{243}Am and ^{244}Cm measured at the FCA-IX assemblies were analysed using the three

different nuclear data libraries based on JENDL-3.2, ENDF/B-VI and JEF-2.2. As a result, the calculated values are almost in agreement with the experimental data within the range of 5% deviations, except for all the ^{244}Cm results and the JEF-2.2 results for ^{241}Am .

In the accelerator-driven system benchmark, a remarkable discrepancy between k_{eff} values – one of the most important integral data – was observed, the major causes of which being due to fission neutron spectrum and fission cross-sections used for minor actinide nuclides.

REFERENCES

- [1] A.V. Ignatyuk, S.A. Badikov, A.I. Blokhin, K.I. Zolotarev, V.P. Luney, V.N. Manokhin, G.Ya. Tertychny, V.A. Tolstikov, Yu.N. Shubin and A.M. Tsibulya, "Final Project Technical Report of ISTC 304-95, Measurement and Analysis of Basic Nuclear Data for Minor Actinides", ISTC 304-95, Chapter IV (1997).
- [2] V.M. Maslov, "Final Project Technical Report of ISTC B-003-95, Evaluation of Actinide Nuclear Data", ISTC B-003-95 (1998).
- [3] Y. Kikuchi, "Evaluation of Neutron Nuclear Data for ^{241}Am and ^{243}Am ", JAERI-M 82-096 (1982).
- [4] T. Nakagawa, "Evaluation of Nuclear Data for Americium Isotopes", JAERI-M 89-008 (1989).
- [5] T. Nakagawa, "Evaluation of Neutron Nuclear Data for Curium Isotopes", JAERI-M 90-101 (1990).
- [6] F.M. Mann, R.E. Schenter, "HEDL Evaluation of Actinide Cross-Sections for ENDF/B-V", HEDL-TME 77-54 (1977).
- [7] R.W. Benjamin, "Evaluation and Testing of Actinide Cross-Sections", EPRI NP-1067 (1979).
- [8] H. Derrien, J.P. Doat, E. Fort and D. Lafond, "Evaluation of ^{237}Np Neutron Cross-Sections in the Energy Range from 10^{-5} eV to 14 MeV", INDC(FR)-42/L (1980).
- [9] G. Maino, E. Menapace, M. Motta and M. Vaccari, "Evaluation of ^{242}Cm Neutron Cross-Sections from 10^{-5} eV to 15 MeV", INDC(ITY)-7 (1982).
- [10] G. Maino, T. Martinelli, E. Menapace, M. Motta, M. Vaccari and A. Ventura, "Evaluation of ^{243}Cm Neutron Cross-Sections from 10^{-5} eV to 15 MeV", CNEN-RT/FI(81)23 (1981).

- [11] G. Maino, T. Martinelli, E. Menapace, M. Motta and M. Vaccari, "Evaluation of ^{245}Cm Neutron Cross-Sections from 10^{-5} eV to 15 MeV", CNEN-RT/FI(81)24 (1981).
- [12] V.M. Maslov, E.Sh. Sukhovitskij, Yu.V. Porodzinskij, A.B. Klepatskij and G.B. Morogovskij, "Evaluation of Neutron Data for Americium-241", INDC(BLR)-005/L (1996).
- [13] V.M. Maslov, E.Sh. Sukhovitskij, Yu.V. Porodzinskij, A.B. Klepatskij and G.B. Morogovskij, "Evaluation of Neutron Data for Americium-243", INDC(BLR)-006/L (1996).
- [14] V.M. Maslov, E.Sh. Sukhovitskij, Yu.V. Porodzinskij, A.B. Klepatskij and G.B. Morogovskij, "Evaluation of Neutron Data for Curium-243", INDC(BLR)-002/L (1995).
- [15] V.M. Maslov, E.Sh. Sukhovitskij, Yu.V. Porodzinskij, A.B. Klepatskij and G.B. Morogovskij, "Evaluation of Neutron Data for Curium-245", INDC(BLR)-003/L (1996).
- [16] T. Nakagawa, "Program RESENDD (Version 84-07): A Program for Reconstruction of Resonance Cross-Sections from Evaluated Nuclear Data in the ENDF/B Format (Modified Version of RESEND)", JAERI-M 84-192 (1984).
- [17] D.E. Cullen, "Program RECENT (Version 79-1): Reconstruction of Energy-Dependent Neutron Cross-Sections from Resonance Parameters in the ENDF/B Format", UCRL-50400, Vol. 17, Part C (1979).
- [18] O. Ozer, "Program INTEND: A Program to Integrate ENDF/B Cross-Section Files", BNL-NCS-23498 (1977). INTERN is the revised version of INTER5 made from INTEND.
- [19] S.F. Mughabghab, "Neutron Cross-Sections, Vol. 1, Part B, Z = 61 - 100", Academic Press, Inc. (1984).
- [20] T. Nakagawa, "CRECTJ: A Computer Program for Compilation of Evaluated Nuclear Data", JAERI-Data/Code 99-041 (1999).
- [21] L.W. Weston and J.H. Todd, *Nucl. Sci. Eng.*, 79, 184 (1981).
- [22] S. Plattard, J. Blons and D. Paya, *Nucl. Sci. Eng.*, 61, 477 (1976).

- [23] A. Yamanaka, I. Kimura, S. Kanazawa, K. Kobayashi, S. Yamamoto, Y. Nakagome, Y. Fujita and T. Tamai, *J. Nucl. Sci. Technol.*, 30, 863 (1993).
- [24] M.M. Hoffman, W.M. Sanders and M.D. Semon, *Bull. Am. Phys. Soc.*, 21, 655 (1976).
- [25] C. Wagemans, E. Allaert, F. Cañtucoli, P. D'hondt, G. Barreau and P. Perrin, *Nucl. Phys.*, A369, 1 (1981).
- [26] V.V. Kozharin, S.S. Kovalenko, Yu.A. Selitskii, Yu.A. Nemilov, S.V. Khlebnikov, V.S. Belykh, B.Ya. Galkin, V.Ya. Mishin, V.I. Orlov, E.M. Rubtsov, B.I. Tarler, G.V. Val'skii, G.A. Petrov and Yu.S. Pleva, *Sov. At. Energy*, 60, 498 (1986).
- [27] T. Iwasaki, K. Saito, M. Baba, T. Sanami, Y. Nauchi and N. Hirakawa, *J. Nucl. Sci. Technol.*, 36, 127 (1999).
- [28] L.N. Jurova, A.A. Poljakov V.P. Rukhlo, Ju.E. Titarenko, S.F. Komin, Ju.V. Stogov, O.V. Shvedov, B.F. Mjasoedov A.V. Davydov and S.S. Travnikov, *Yadernye Konstanty*, 1/55, 3 (1984), data were taken from EXFOR 40579.
- [29] K. Kobayashi, A. Yamanaka and I. Kimura, *J. Nucl. Sci. Technol.*, 31, 1239 (1994).
- [30] T. Nishi, I. Fujiwara and N. Imanishi, NEANDC(J)-42L, p.20 (1975).
- [31] N.V. Kornilov, V.Ya. Baryba, A.V. Balitskii, A.P. Rudenko, B.D. Kuz'minov, O.A. Sal'nikov, E.A. Gromova, S.S. Kovalenko, L.D. Preobrazhenskaya, A.V. Stepanov, Yu.A. Nemilov, Yu.A. Selitskii, B.I. Tarler, V.B. Funshtein, V.A. Yakovlev, Sh. Darotsi, P. Raich and I. Chikai, *Sov. At. Energy*, 58, 117 (1985).
- [32] S. Yamamoto, K. Kobayashi, M. Miyoshi, I. Kimura, I. Kanno, N. Shinohara and Y. Fujita, *Nucl. Sci. Eng.*, 126, 201 (1997).
- [33] J.W.T. Dabbs, C.H. Johnson and C.E. Bemis, Jr., *Nucl. Sci. Eng.*, 83, 22 (1983).
- [34] N. Shinohara, Y. Hatsukawa, K. Hata and N. Kohno, *J. Nucl. Sci. Technol.*, 34, 613 (1997).

- [35] T.S. Belanova, “Evaluation of Thermal Neutron Cross-Sections and Resonance Integrals of Protactinium, Americium, Curium and Berkelium Isotopes”, INDC(CCP)-391/L (1994).
- [36] M.A. Bak, *et al.*, *At. Energ.*, 23, 316 (1967).
- [37] V.D. Gavrilov, V.A. Goncharov, V.V. Ivanenko, V.N. Kustov and V.P. Smirnov, *Sov. At. Energ.*, 41, 808 (1976).
- [38] R.M. Harbour, K.W. MacMurdo and F.J. McCrosson, *Nucl. Sci. Eng.*, 50, 364 (1973).
- [39] K. Wisshak, J. Wickenhauser and F. Käppeler, “The Isomeric Ratio in Neutron Capture of ^{241}Am at 14.75 meV and 30 keV”, Proc. 5th All Union Conference on Neutron Physics, Kiev, 15–19 Sept. 1980, Vol. 2, p. 306 (1980).
- [40] Ju.V. Adamchuk, V.F. Gerasimov, B.V. Efimov, V.S. Zenkevich, V.I. Mostovoy, M.I. Pevzner, A.P. Tsitovich, A.A. Chernyshov and S.S. Moskalev, Proc. First International Conf. the Peaceful Uses of Atomic Energy, Geneva, 8-20 Aug. 1955, Vol. 4, p. 259 (1955).
- [41] K.I. Zolotarev, A.V. Ignatyuk, V.A. Tolstikov and G.Ya. Tertychnyj, “Neutron Radiative Capture by the ^{241}Am Nucleus in the Energy Range 1 keV – 20 MeV”, INDC(CCP)-416/L, p. 25 (1998).
- [42] G. Vanpraet, E. Cornelis, S. Raman and G. Rohr, “Neutron Capture Measurements of ^{241}Am ”, Proceedings of International Conference on Nuclear Data for Basic and Applied Science, Santa Fe, New Mexico, USA, 13-17 May 1985, Vol. 1, p. 493 (1986).
- [43] K. Wisshak, J. Wickenhauser, F. Käppeler, G. Reffo and F. Fabbri, *Nucl. Sci. Eng.*, 81, 396 (1982).
- [44] E.K. Hulet, R.W. Hoff, H.R. Bowman and M.C. Michel, *Phys. Rev.*, 107, 1294 (1957).
- [45] H-H. Knitter and C. Budtz-Jørgensen, *Nucl. Sci. Eng.*, 99, 1 (1988).
- [46] K. Kobayashi, T. Kai, S. Yamamoto, H. Cho, Y. Fujita, I. Kimura and N. Shinohara, *J. Nucl. Sci. Technol.*, 36, 20 (1999).
- [47] G.C. Hanna, B.G. Harvey, N. Moss and P.R. Tunncliffe, *Phys. Rev.*, 81, 893 (1951).

- [48] B. Alam, R. Block, R.E. Slovacek and R.W. Hoff, *Nucl. Sci. Eng.*, 99, 267 (1988).
- [49] V.A. Anufriev, S.I. Babich, N.G. Kocherygin, V.M. Lebedev, S.N. Nikol'skii, V.N. Nefedov, V.M. Nikolaev, V.A. Poruchikov and A.A. Elesin, *Sov. At. Energy*, 51, 736 (1982).
- [50] J.R. Berreth, F.B. Simpson and B.C. Rusche, *Nucl. Sci. Eng.*, 49, 145 (1972).
- [51] É.F. Fomushkin, G.F. Novoselov, Yu.I. Vinogradov, V.N. Vyachin, V.V. Gavrilov, A.S. Koshelev, V.N. Polynov, V.M. Surin and A.M. Shvetsov, *Sov. At. Energy*, 62, 337 (1987).
- [52] B.I. Fursov, V.N. Polynov, B.F. Samylin and V.S. Shorin, "Fast Neutron Induced Fission Cross-Sections of Some Minor Actinides", Proc. International Conf. Nuclear Data for Science and Technology, Trieste, Italy, 19-24 May 1997, Part 1, p. 488 (1997).
- [53] M.G. Silbert, "Fission Cross-Section of ^{243}Cm from the Underground Nuclear Explosion, Physics-8, Table of Values", LA-6239-MS (1976).
- [54] M.C. Thompson, M.L. Hyder and R.J. Reuland, *J. Inorg. Nucl. Chem.*, 33, 1553 (1971).
- [55] R.W. Benjamin, K.W. MacMurdo and J.D. Spencer, *Nucl. Sci. Eng.*, 47, 203 (1972).
- [56] H.T. Maguire Jr., C.R.S. Stopa, R.C. Block, D.R. Harris, R.E. Slovacek, J.W.T. Dabbs, R.J. Dougan, R.W. Hoff and R.W. Loughheed, *Nucl. Sci. Eng.*, 89, 293 (1985).
- [57] J.C. Browne, R.W. Benjamin and D.G. Karraker, *Nucl. Sci. Eng.*, 65, 166 (1978).
- [58] V.D. Gavrilov and V.A. Goncharov, *Sov. At. Energy*, 44, 274 (1978).
- [59] J. Fréhaut, A. Bertin and R. Bois, Proc. International Conf. Nuclear Data for Science and Technology, Antwerp, Belgium, 6-10 Sept. 1982, p. 78 (1982) [in French].
- [60] G.S. Boikov, V.D. Dmitriev, M.I. Svirin and G.I. Smirenkin, *Phys. At. Nuclei*, 57, 2047 (1994).

- [61] Yu.A. Khokhlov, A. Ivanin, Yu.I. Vinogradov, V.I. In'kov, L.D. Danilin, V.I. Panin, V.N. Polynov, *Yadernye Konstanty*, 1, (INDC(CCP)-349G) p. 6 (1992) [in Russian].
- [62] R.J. Howerton, *Nucl. Sci. Eng.*, 62, 438 (1977).
- [63] A.H. Jaffey and J.L. Lerner, *Nucl. Phys.*, A145, 1 (1970).
- [64] K.D. Zhuravlev, Yu.S. Zamyatnin and N.I. Kroshkin, Proc. 2nd All Union Conf. Neutron Physics, Kiev, 28 May-1 June 1973, Vol. 4, p.57 (1973) [in Russian].
- [65] D.G. Madland and J.R. Nix, *Nucl. Sci. Eng.*, 81, 213, (1982).
- [66] R.E. Howe, R.M. White, J.C. Browne, J.H. Landrum, R.J. Dougan, R.W. Lougheed and R.J. Dupzyk, *Nucl. Phys.*, A407, 193 (1983).
- [67] H. Takano, H. Akie and Y. Kikuchi, "Benchmark Test of JENDL-3.2 for Thermal and Fast Reactors", Proc. of International Conf. Nuclear Data for Science and Technology, Gatlinburg, Tennessee, USA, 9-13 May 1994, Vol. 2, p.809 (1994).
- [68] H. Takano, H. Akie and K. Kaneko, "Fast and Thermal Reactor Benchmark Test for JENDL-3.2, JEF-2.2 and ENDF/B-VI", Proc. of Intl. Conf. Nuclear Data for Science and Technology, Trieste, Italy, 19-24 May 1997, Part II, p. 1122 (1997).
- [69] H. Takano, H. Akie and K. Kaneko, "Reactor Benchmark Testing for JENDL-3.2, JEF-2.2 and ENDF/B-VI.2", Proc. of International Conf. on the Physics of Nuclear Science and Technology, Long Island, New York, USA, 5-8 Oct. 1998, p. 58 (1998).
- [70] K. Okumura, *et al.*, to be published in *J. Nucl. Sci. Technol.*
- [71] K. Okumura, K. Kaneko and K. Tsuchihashi, "SRAC95: General Purpose Neutronics Code System", JAERI-Data/Code 96-015 (1996) [in Japanese].
- [72] T. Mukaiyama, M. Ohbu, M. Nakano, S. Okajima and T. Koakutsu, "Actinide Integral Measurement in FCA Assemblies", Proc. International Conf. Nuclear Cross-Section for Technology, Santa Fe, New Mexico, USA, 13-17 May 1985, Vol. 1, p.483 (1986).

- [73] S. Okajima, T. Mukaiyama, J. Kim, M. Obu and T. Nemoto, "Evaluation and Adjustment of Actinide Cross-Sections Using Integral Data Measured at FCA", Proc. International Conf. Nuclear Data for Science and Technology, Mito, Japan, 30 May-3 June 1988, p. 983 (1988).
- [74] H. Takano, *et al.*, "A Code System for Producing Group Constants in Fast Neutron Energy Region", JAERI-M 82-072 (1982). This code has been updated by combining with NJOY.
- [75] M. Nakagawa, *et al.*: JAERI-1294 (1984).
- [76] T. Nishida, T. Takizuka and T. Sasa, "JAERI Proposal of Benchmark Problem on Method and Data to Calculate the Nuclear Characteristics in Accelerator-Based Transmutation System With Fast Neutron Flux", OECD/NEA NSC Task Force on Physics Aspects of Different Transmutation Concepts – Benchmark Specifications, NSC/DOC(96)10 (1996).
- [77] H. Takano, R.P. Rulko, C. Broeders, T. Wakabayashi, T. Sasa, T. Iwasaki, D. Lutz, T. Mukaiyama and C. Nordborg, "Benchmark Problems on Transmutation Calculation by the OECD/NEA Task Force on Physics Aspects of Different Transmutation Concepts", Proc. of International Conf. on the Physics of Nuclear Science and Technology, Long Island, New York, USA, 5-8 Oct. 1998, p. 1462 (1998).

TABLES

Table 2.1. Year of evaluations for minor actinides

Nuclide	JENDL-3.2	ENDF/B-VI	JEF-2.2	BROND-3	MASLOV
²³⁷ Np	1978 1987 1993*	1990 1991	1980	1996	–
²⁴¹ Am	1988	1988 (< 30 keV) 1994 (> 30 keV)	1981 1989	1997	1996
²⁴³ Am	1988	1988 (< 42 keV) 1996 (> 42 keV)	1981 1984	1997	1996
²⁴² Cm	1989	1979	1982 1984	1997	–
²⁴³ Cm	1989	1979	1982 1988	1997	1995
²⁴⁴ Cm	1989	1978	1983 1989	1997	–
²⁴⁵ Cm	1989	1979	1983 1989	1997	1996

* Res. only

Table 2.2. Comparison of thermal fission cross-sections

	JENDL-3.2	ENDF/B-VI	JEF-2.2	BROND-3	MASLOV	Mughabghab and recent experiments
²³⁷ Np	0.0225	0.0180	0.0180	0.0221	–	0.0215±0.0024 ^[19] 0.026±0.005 ^[25] 0.020±0.001 ^[26]
²⁴¹ Am	3.02	3.14	3.18	3.14	3.14	3.20±0.09 ^[19] 3.15±0.097 ^[32]
²⁴³ Am	0.116	0.0739	0.0496	0.0638	0.0638	0.1983±0.0043 ^[19] 0.0813±0.0025 ^[46]
²⁴² Cm	5.06	3.02	4.97	5.00	–	< 5 ^[19]
²⁴³ Cm	617	691	431	691	613	617±20 ^[19]
²⁴⁴ Cm	1.04	0.604	1.03	1.03	–	1.04±0.20 ^[19]
²⁴⁵ Cm	2 000	2 220	2 130	–	2 140	2145±58 ^[19]

Unit: barns

Table 2.3. Comparison of thermal capture cross-sections

	JENDL-3.2	ENDF/B-VI	JEF-2.2	BROND-3	MASLOV	Mughabghab and recent experiments
²³⁷ Np	165	181	181	176	–	175.9±2.9 ^[19] 158±4 ^[28] 158±3 ^[29]
²⁴¹ Am	600	619	616	619	585	587±12 ^[19] 854±58 ^[34]
²⁴³ Am	78.5	75.1	75.9	76.7	76.7	75.1±1.8 ^[19]
²⁴² Cm	15.9	16.9	16.5	16.7	–	16±5 ^[19]
²⁴³ Cm	130	58.0	113	58.0	131	130±10 ^[19]
²⁴⁴ Cm	15.1	10.4	14.4	15.3	–	15.2±1.2 ^[19]
²⁴⁵ Cm	346	342	349	–	359	369±17 ^[19]

Unit: barns

Table 2.4. Comparison of fission resonance integral

	JENDL-3.2	ENDF/B-VI	JEF-2.2	BROND-3	MASLOV	Mughabghab and recent experiments
²³⁷ Np	7.06	6.43	6.35	6.95	–	6.9±1.0 ^[19] 4.70±0.23 ^[26]
²⁴¹ Am	13.9	14.9	16.1	14.7	14.5	14.4±1.0 ^[19] 14.1±0.9 ^[33]
²⁴³ Am	7.56	7.38	6.52	7.53	7.44	9±1 ^[19] 3.05±0.15 ^[45]
²⁴² Cm	19.9	6.25	12.4	23.9	–	12.9±0.7 ^[48]
²⁴³ Cm	1560	1950	1780	1960	1540	1570±100 ^[19]
²⁴⁴ Cm	13.2	18.7	20.0	14.6	–	12.5±2.5 ^[19]
²⁴⁵ Cm	800	837	759	–	804	840±40 ^[19]

Unit: barns

Table 2.5. Comparison of capture resonance integral

	JENDL-3.2	ENDF/B-VI	JEF-2.2	BROND-3	MASLOV	Mughabghab and recent experiments
²³⁷ Np	662	654	654	644	–	640±50 ^[19] 730±30 ^[28] 652±24 ^[29]
²⁴¹ Am	1310	1390	1450	1390	1350	1425±100 ^[19]
²⁴³ Am	1820	1780	1810	1790	1790	1820±70 ^[19]
²⁴² Cm	109	111	116	115	–	110±20 ^[19]
²⁴³ Cm	199	249	284	249	212	215±20 ^[19]
²⁴⁴ Cm	661	594	637	643	–	650±30 ^[19]
²⁴⁵ Cm	110	109	123	–	106	101±8 ^[19]

Unit: barns

Table 3.1. Comparison of the C/E-values for burn-up calculations for the existing PWR spent fuel of 34.2GWd/t. The calculations were performed with the SRAC95 code.

Isotope	Exp.	Error (%)	JENDL-3.2	ENDF/B-VI	JEF-2.2
²³² U	3.3890E-11	5.6	0.85	0.81	0.63
²³⁵ U	1.8520E-04	2.0	1.02	1.02	1.03
²³⁶ U	9.6270E-05	1.9	0.97	1.01	0.97
²³⁸ U	2.1450E-02	1.9	1.00	1.00	1.00
²³⁷ Np	1.0690E-05	10.6	0.91	0.93	0.92
²³⁶ Pu	7.6700E-12	3.0	0.97	0.97	0.71
²³⁸ Pu	4.2220E-06	2.2	0.81	0.85	0.85
²³⁹ Pu	1.2050E-04	2.1	0.99	1.00	1.00
²⁴⁰ Pu	5.4800E-05	2.1	0.93	0.93	0.93
²⁴¹ Pu	2.4190E-05	1.9	0.99	1.00	0.98
²⁴² Pu	1.2750E-05	2.0	0.91	0.90	0.90
²⁴¹ Am	7.5480E-06	2.4	0.97	0.98	0.96
^{242m} Am	1.7950E-08	10.0	0.72	0.70	0.67
²⁴³ Am	2.1070E-06	5.3	0.98	1.07	0.95
²⁴² Cm	1.8590E-10	10.8	0.95	0.97	0.95
²⁴³ Cm	6.3830E-09	10.3	1.03	1.04	1.14
²⁴⁴ Cm	6.5920E-07	2.0	0.74	0.82	0.72

Table 3.2. Comparison of the effective multiplication factors

Cores	Exp.	Error (%)	JENDL-3.2		ENDF/B-VI		JEF-2.2	
			Cal.	C/E	Cal.	C/E	Cal.	C/E
FCA-9-1	1.0077	0.07	1.0168	1.009	1.0162	1.008	1.0241	1.016
FCA-9-2	1.0107	0.08	1.0157	1.005	1.0236	1.013	1.0229	1.012
FCA-9-3	1.0086	0.08	1.0121	1.004	1.0237	1.015	1.0196	1.011
FCA-9-4	1.0075	0.07	1.0318	1.024	1.0400	1.032	1.0464	1.039
FCA-9-5	1.0096	0.06	1.0280	1.018	1.0372	1.027	1.0403	1.030
FCA-9-6	1.0082	0.06	1.0164	1.008	1.0278	1.020	1.0227	1.014
FCA-9-7	1.0095	0.06	1.0220	1.012	1.0302	1.021	1.0220	1.012

Table 3.3. Comparison of the fission reaction rate ratios of ^{237}Np to ^{239}Pu

Cores	Exp.	JENDL-3.2		ENDF/B-VI		JEF-2.2	
		Cal.	C/E	Cal.	C/E	Cal.	C/E
FCA-9-1	0.2090	0.2068	0.9894	0.2054	0.9829	0.1974	0.9447
FCA-9-2	0.3208	0.3208	1.0002	0.3172	0.9889	0.3054	0.9522
FCA-9-3	0.3836	0.3841	1.0015	0.3784	0.9863	0.3658	0.9536
FCA-9-4	0.3439	0.3501	1.0182	0.3359	0.9767	0.3244	0.9433
FCA-9-5	0.3982	0.4045	1.0157	0.3898	0.9789	0.3785	0.9506
FCA-9-6	0.4672	0.4652	0.9956	0.4587	0.9819	0.4430	0.9481
FCA-9-7	0.3480	0.3480	1.0001	0.3576	1.0275	0.3328	0.9563

Table 3.4. Comparison of the fission reaction rate ratios of ^{241}Am to ^{239}Pu

Cores	Exp.	JENDL-3.2		ENDF/B-VI		JEF-2.2	
		Cal.	C/E	Cal.	C/E	Cal.	C/E
FCA-9-1	0.2001	0.1898	0.9486	0.1958	0.9784	0.1859	0.9288
FCA-9-2	0.3135	0.2957	0.9432	0.2998	0.9564	0.2848	0.9084
FCA-9-3	0.3677	0.3557	0.9673	0.3576	0.9726	0.3409	0.9272
FCA-9-4	0.2933	0.2836	0.9671	0.2766	0.9430	0.2617	0.8925
FCA-9-5	0.3503	0.3410	0.9734	0.3326	0.9493	0.3170	0.9049
FCA-9-6	0.4321	0.4168	0.9646	0.4153	0.9612	0.3952	0.9146
FCA-9-7	0.2965	0.2840	0.9577	0.2990	1.0085	0.2746	0.9259

Table 3.5 Comparison of the fission reaction rate ratios of ^{243}Am to ^{239}Pu

Cores	Exp.	JENDL-3.2		ENDF/B-VI		JEF-2.2	
		Cal.	C/E	Cal.	C/E	Cal.	C/E
FCA-9-1	0.1539	0.1427	0.9274	0.1484	0.9642	0.1473	0.9572
FCA-9-2	0.2391	0.2241	0.9371	0.2282	0.9544	0.2299	0.9613
FCA-9-3	0.2821	0.2704	0.9586	0.2727	0.9665	0.2768	0.9811
FCA-9-4	0.2207	0.2081	0.9431	0.2022	0.9161	0.2074	0.9396
FCA-9-5	0.2640	0.2533	0.9596	0.2460	0.9318	0.2537	0.9610
FCA-9-6	0.3301	0.3151	0.9546	0.3133	0.9492	0.3204	0.9706
FCA-9-7	0.2191	0.2095	0.9563	0.2207	1.0073	0.2188	0.9987

Table 3.6. Comparison of the fission reaction rate ratios of ^{244}Cm to ^{239}Pu

Cores	Exp.	JENDL-3.2		ENDF/B-VI		JEF-2.2	
		Cal.	C/E	Cal.	C/E	Cal.	C/E
FCA-9-1	0.2629	0.2594	0.9868	0.2657	1.0106	0.2633	1.0016
FCA-9-2	0.3816	0.3904	1.0232	0.3964	1.0389	0.3925	1.0288
FCA-9-3	0.4412	0.4619	1.0471	0.4677	1.0601	0.4648	1.0536
FCA-9-4	0.3978	0.4248	1.0679	0.4232	1.0639	0.4149	1.0430
FCA-9-5	0.4526	0.4870	1.0761	0.4870	1.0761	0.4810	1.0628
FCA-9-6	0.5226	0.5550	1.0620	0.5607	1.0728	0.5590	1.0697
FCA-9-7	0.3975	0.4195	1.0553	0.4464	1.1230	0.4244	1.0676

FIGURES

Figure 2.1. ^{237}Np fission cross-section (comparison with Yamanaka, et al. [23]).
The experimental data of Hoffman, et al. [24] and Plattard, et al. [22]
are also shown with the dotted and dashed line, respectively.

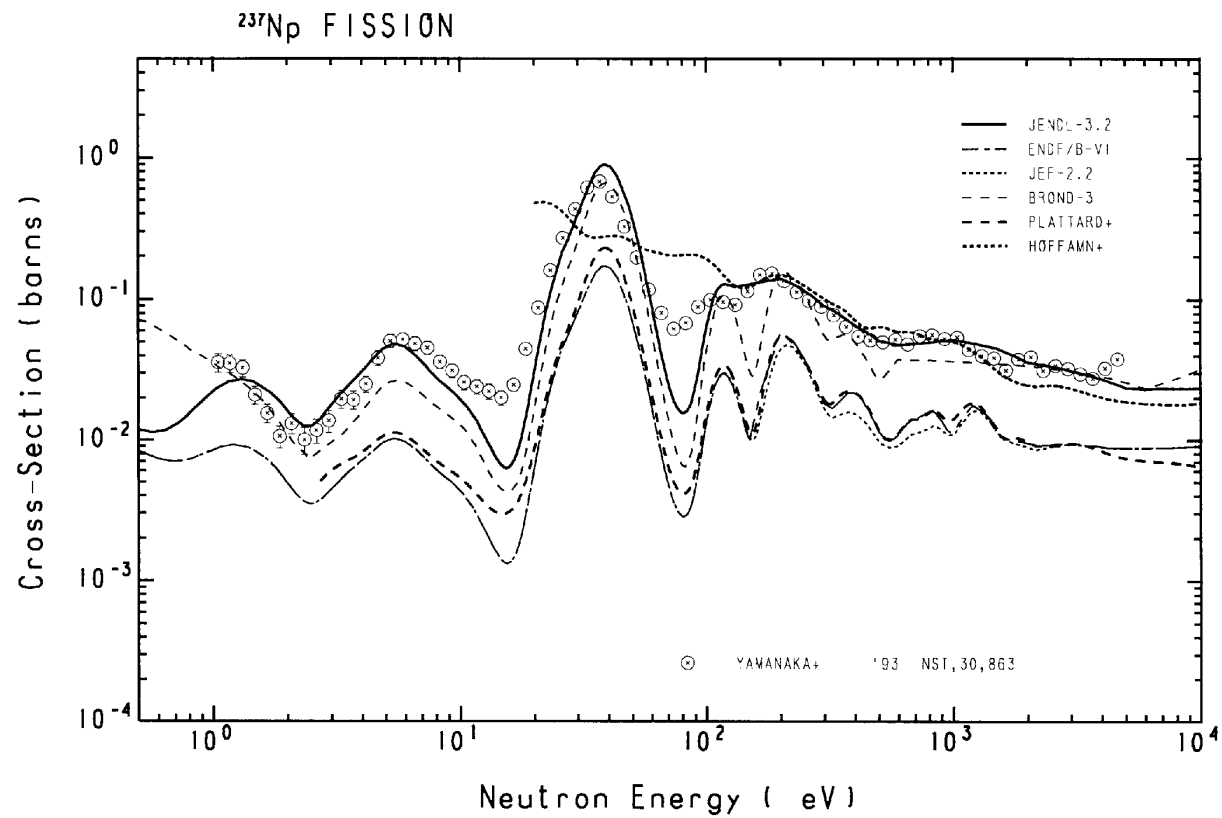


Figure 2.2. ^{237}Np fission cross-section

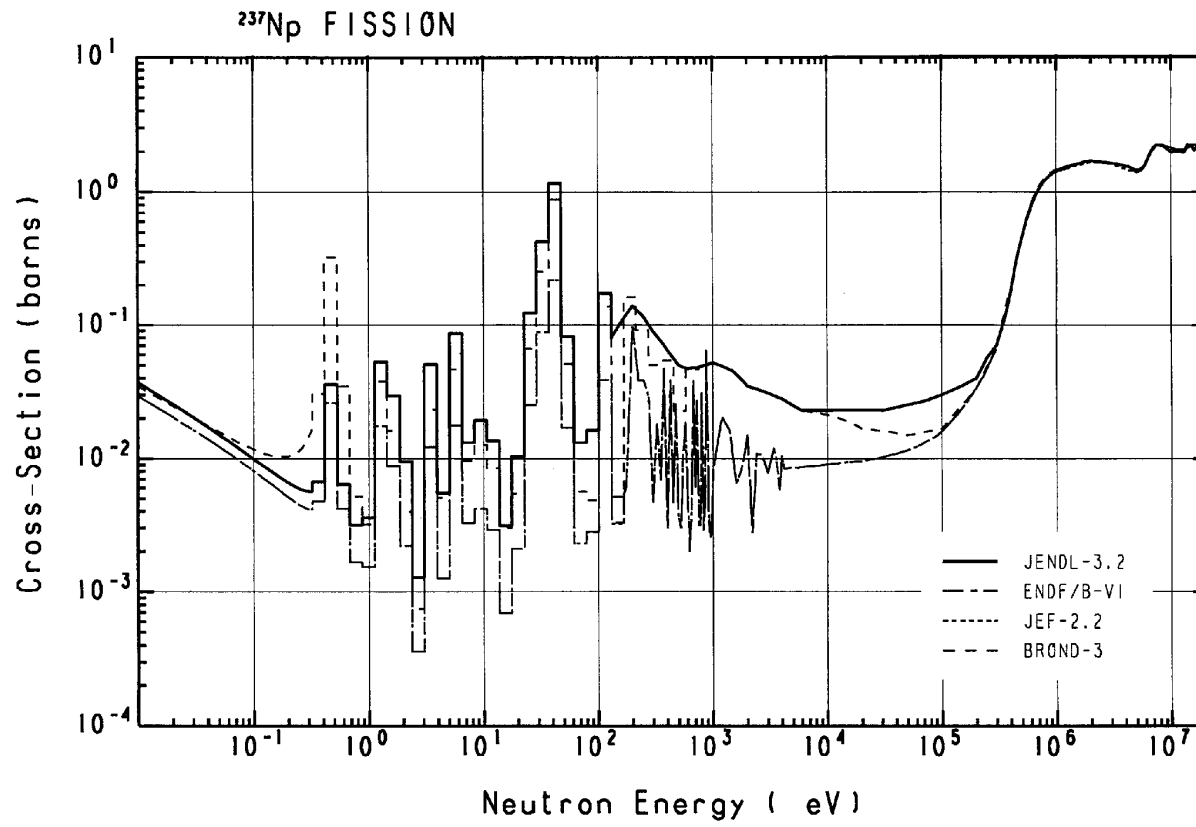


Figure 2.3. ^{237}Np fission cross-section (1 keV to 20 MeV).

Only the experimental data reported after 1970 are shown. The data of Hoffman, et al. and Plattard, et al. are excluded because their energy points are too many.

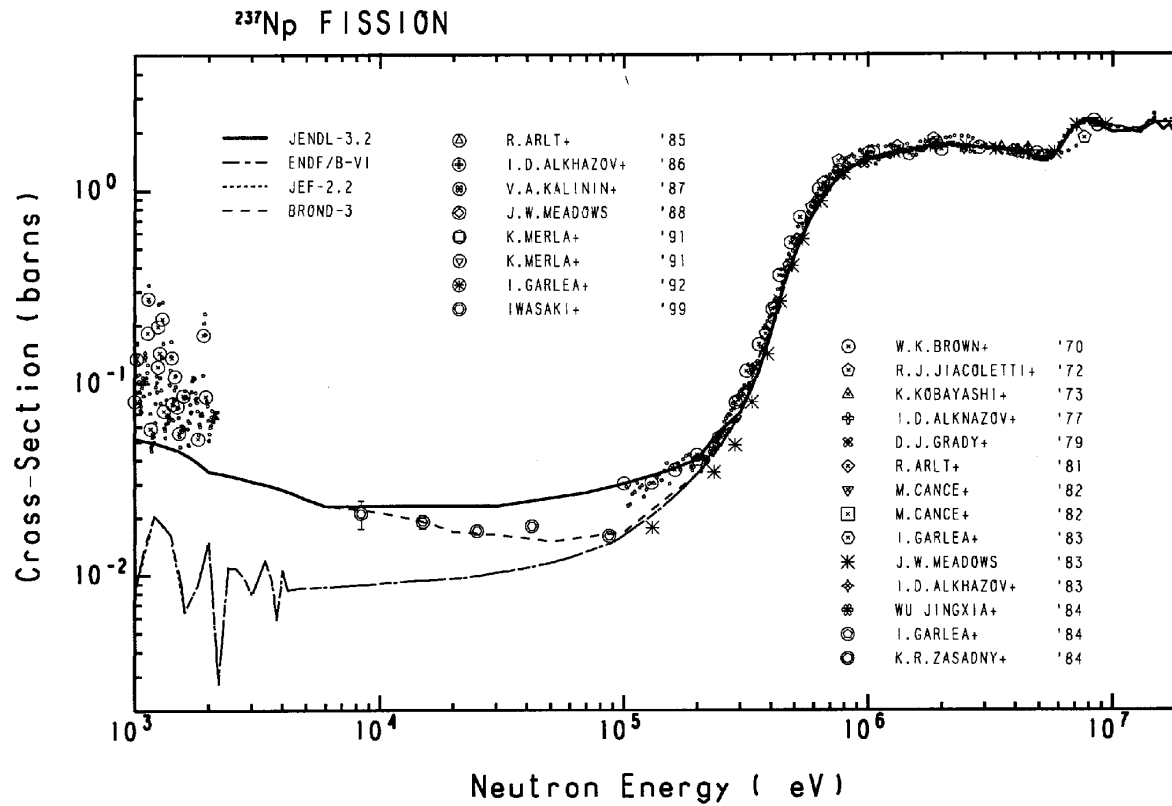


Figure 2.4. ^{237}Np capture cross-section

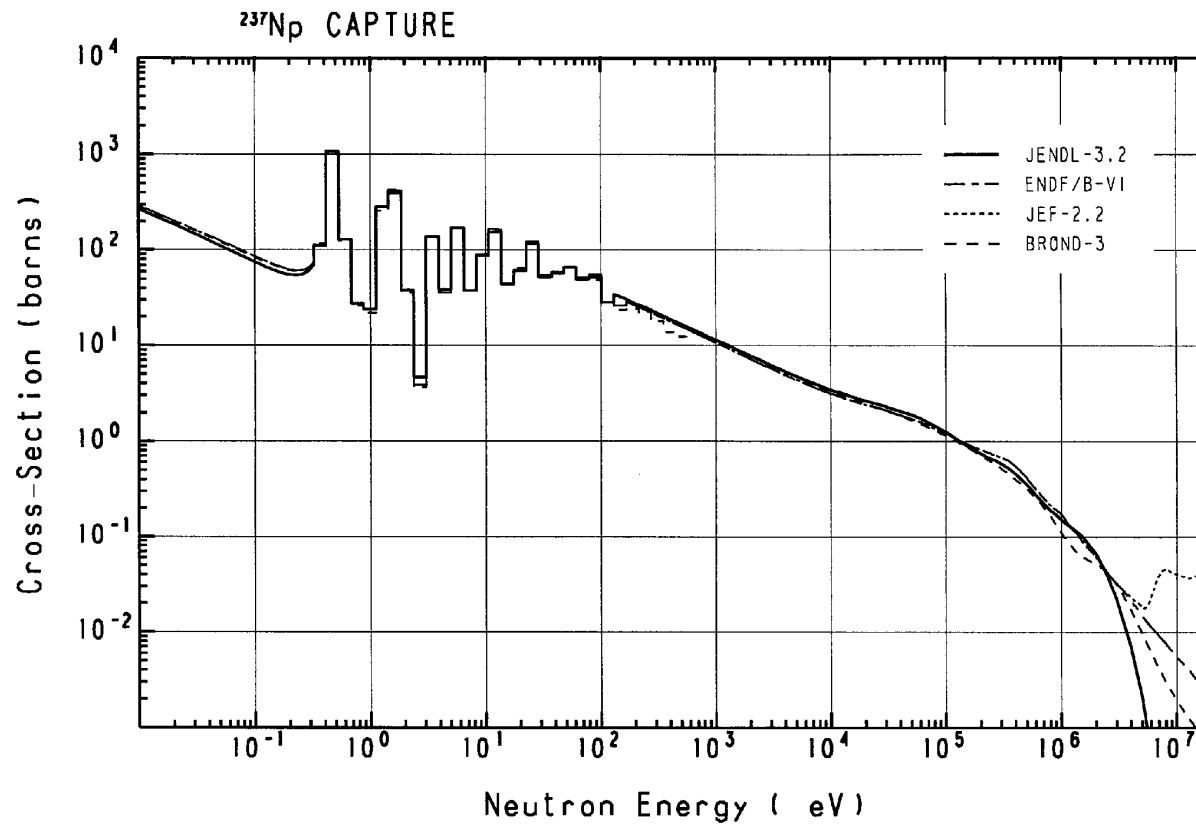


Figure 2.5. ^{237}Np capture cross-section.
The experimental data of Hoffman, et al. [24] are excluded.

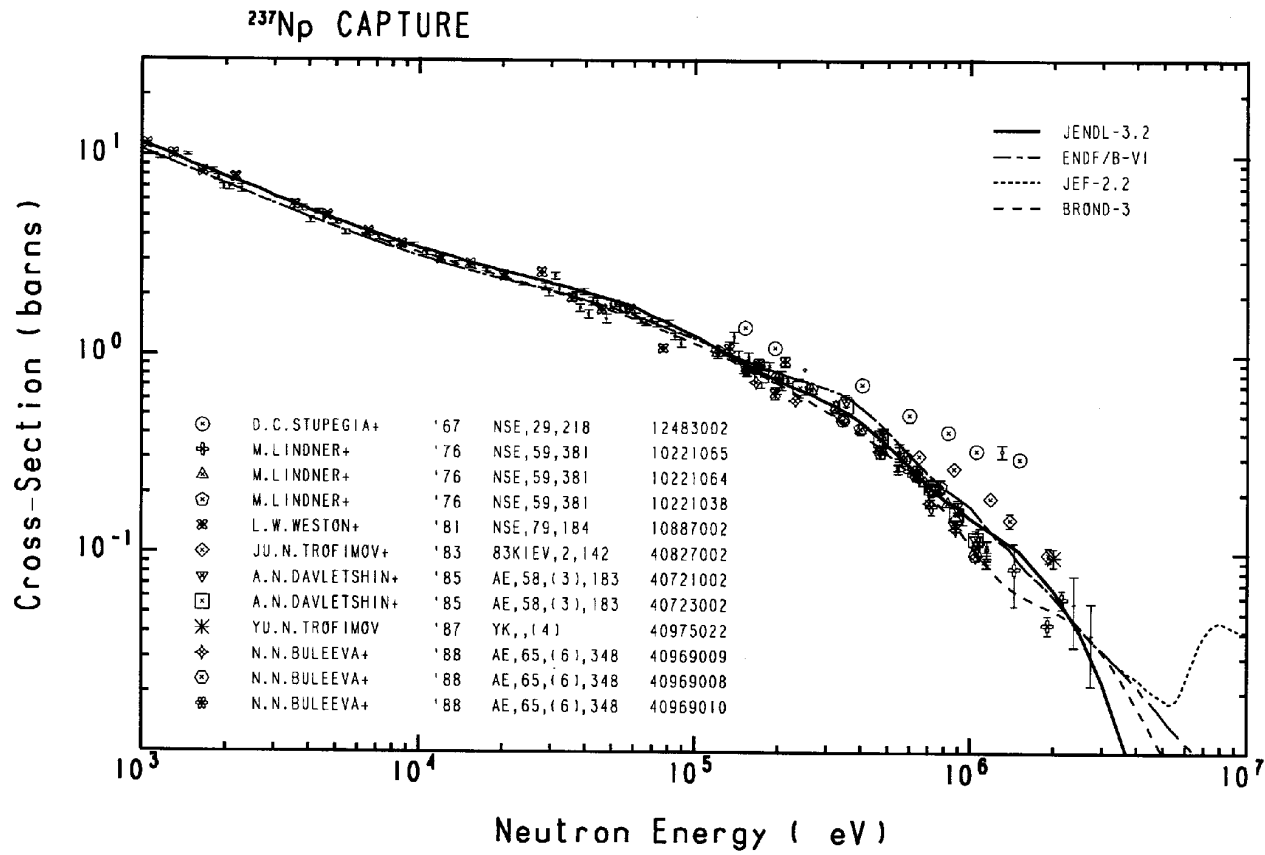


Figure 2.6. $^{237}\text{Np}(n,2n)$ cross-sections.
 The data for total $^{237}\text{Np}(n,2n)$ and $^{237}\text{Np}(n,2n)^{236m}\text{Np}$ cross-sections are shown.

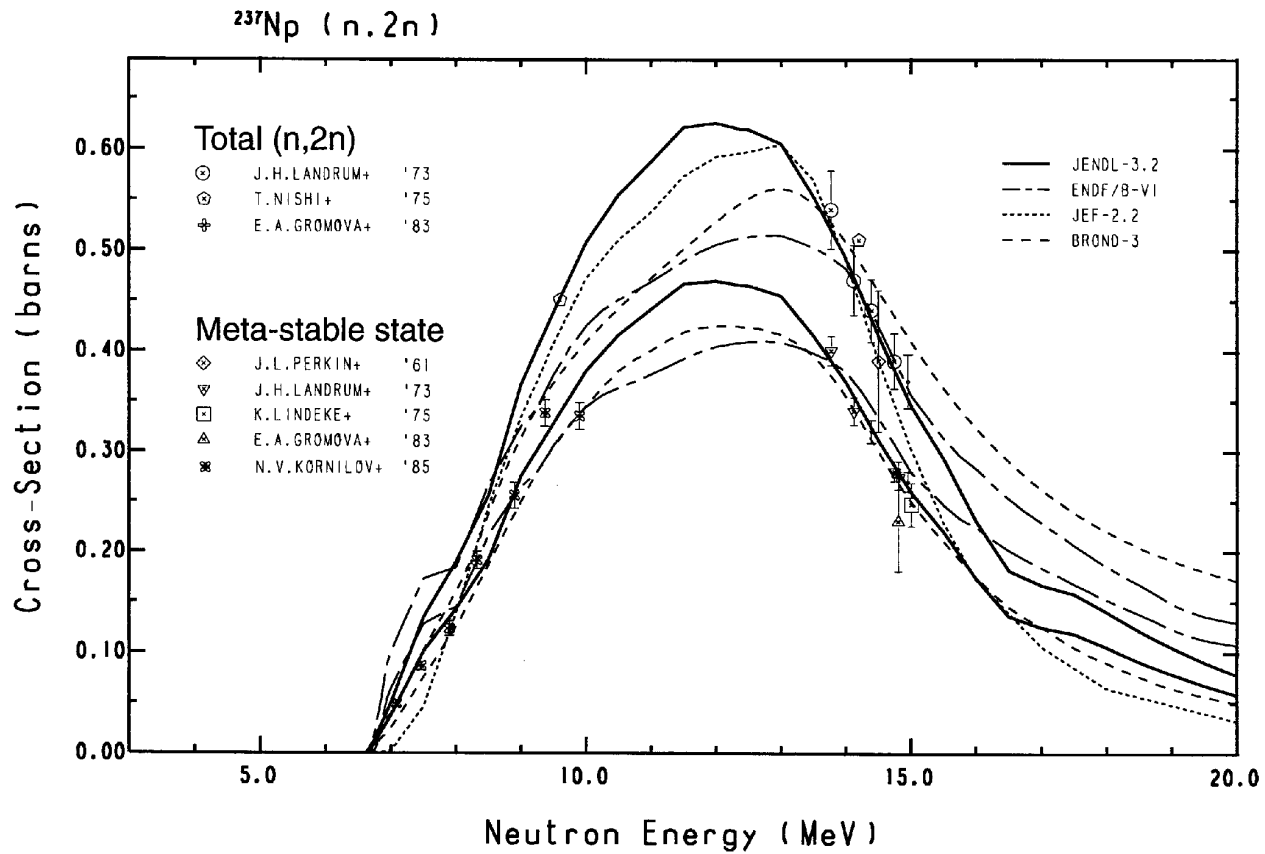


Figure 2.7. ^{237}Np (n,2n) and (n,3n) reaction cross-sections

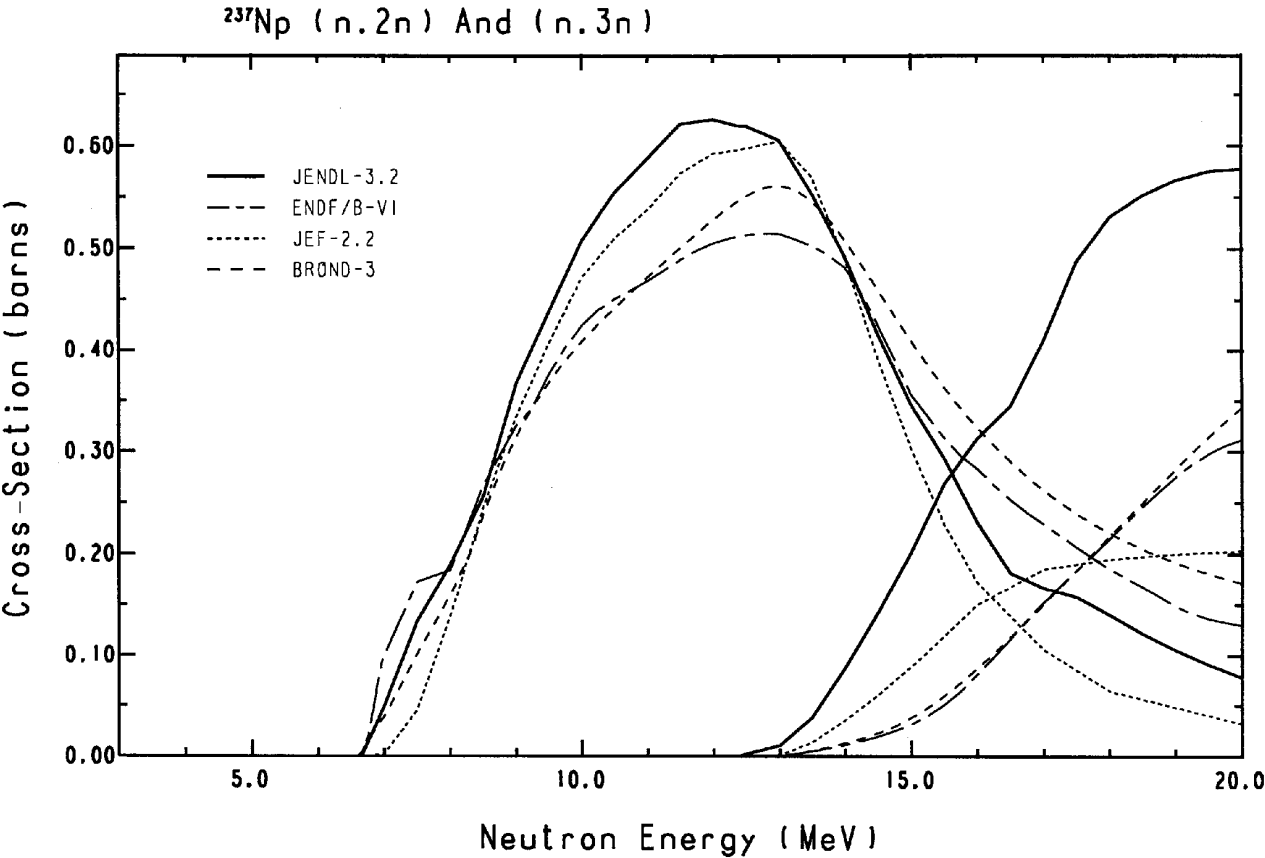


Figure 2.8. ^{237}Np total inelastic scattering cross-section

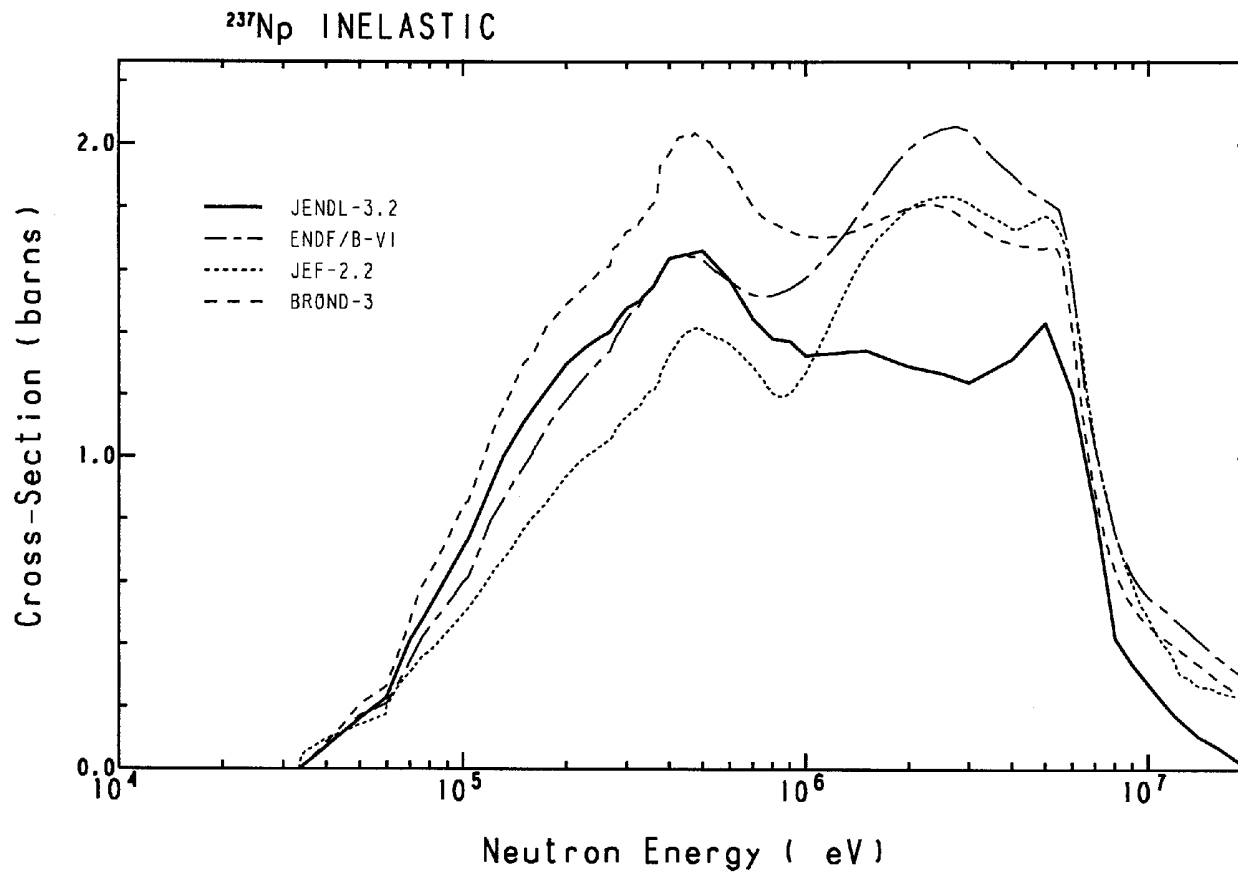


Figure 2.9. ^{237}Np elastic scattering cross-section

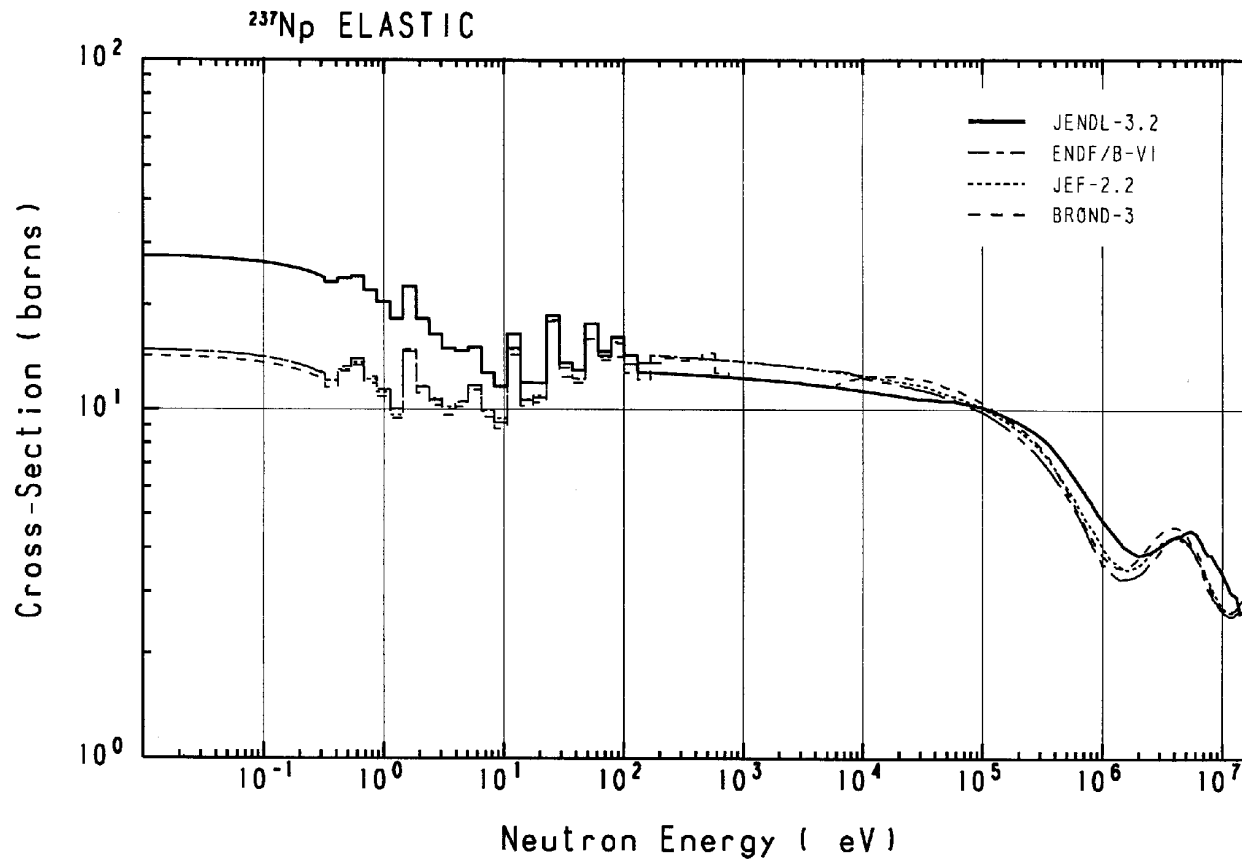


Figure 2.10. ^{237}Np total cross-section

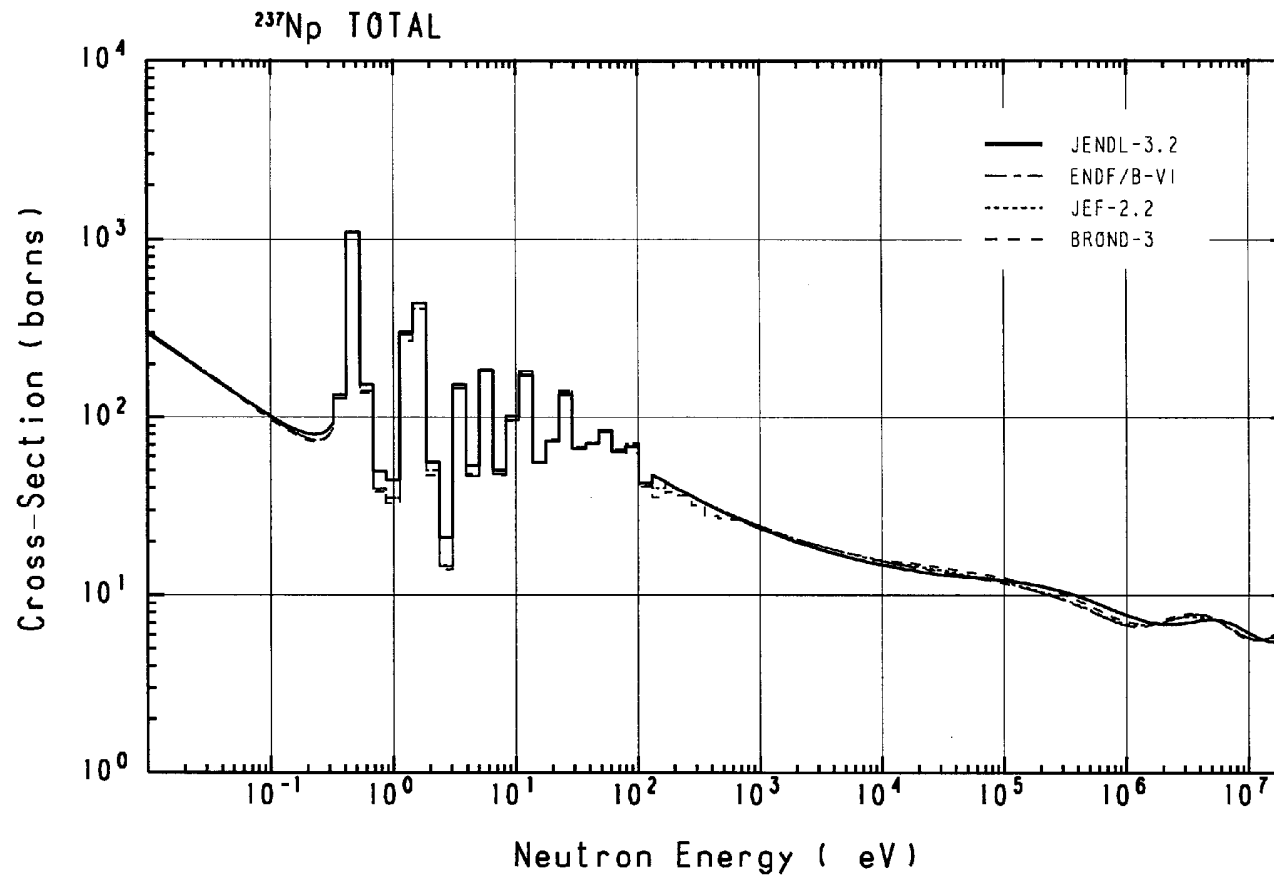


Figure 2.11. ^{241}Am fission cross-section

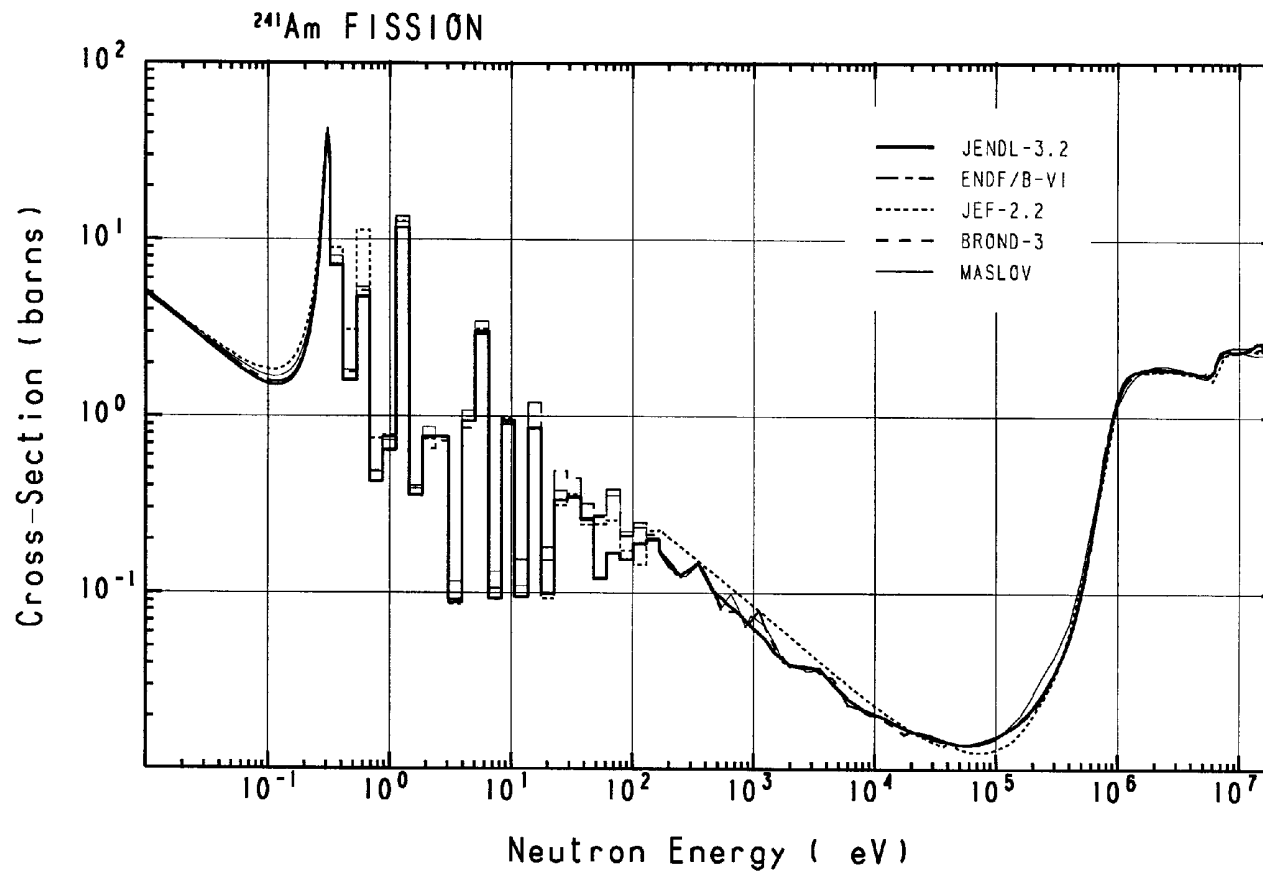


Figure 2.12(a). ^{241}Am fission cross-section
Since so many experimental data exist, the legend of them is not given.

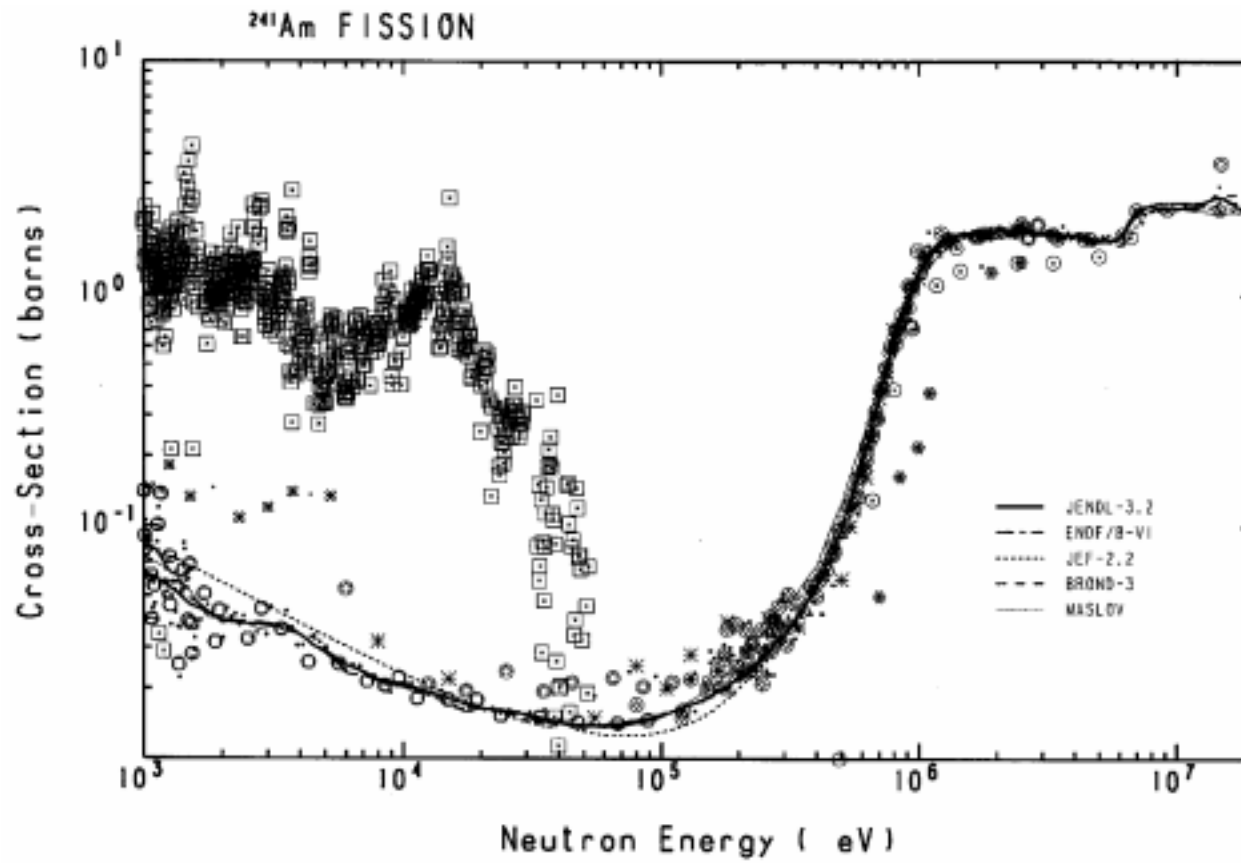


Figure 2.12(b). ^{241}Am fission cross-section

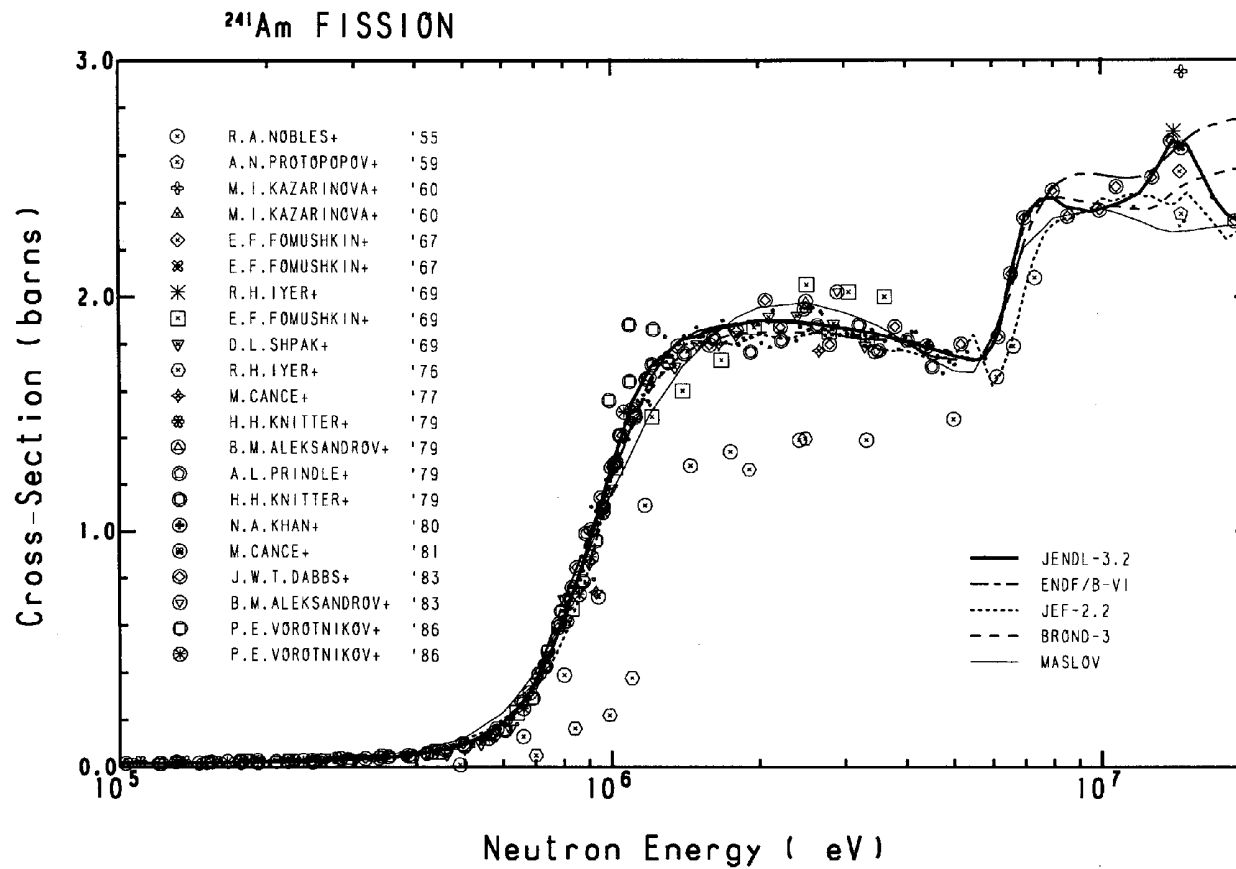


Figure 2.13. ^{241}Am fission cross-section
(comparison with Yamamoto et al. [32])

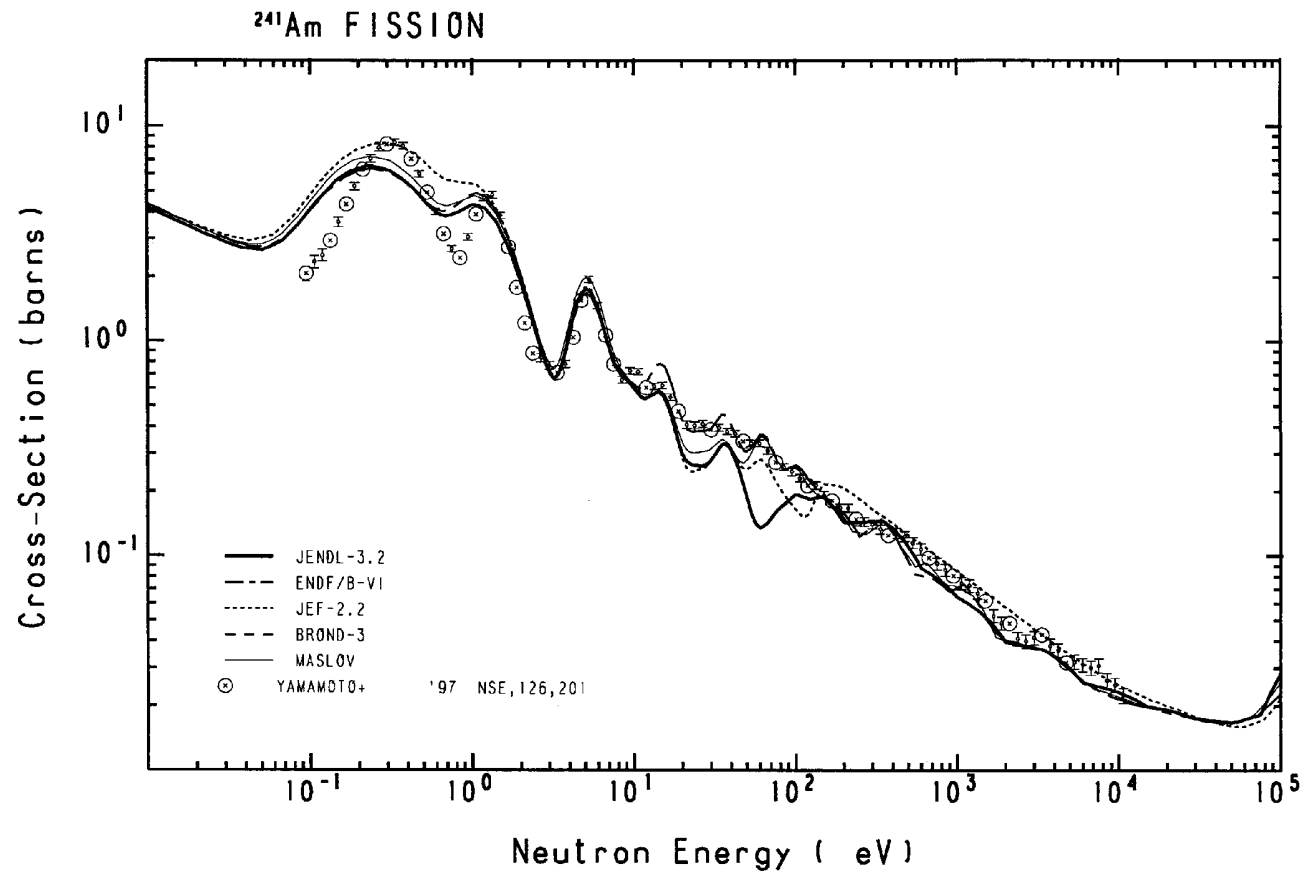


Figure 2.14. ^{241}Am total cross-section in the energy range from 0.01 to 1 eV

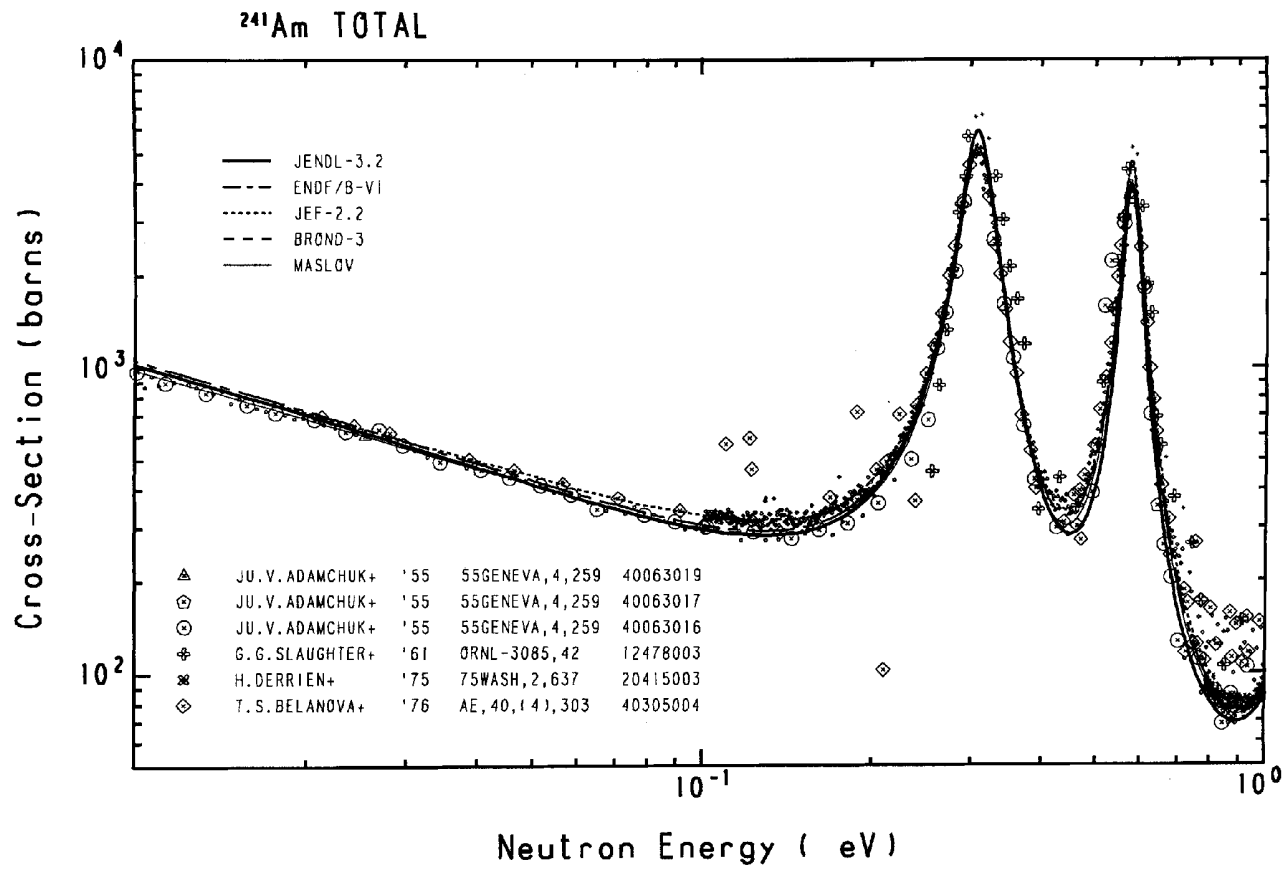


Figure 2.15. ^{241}Am capture cross-section

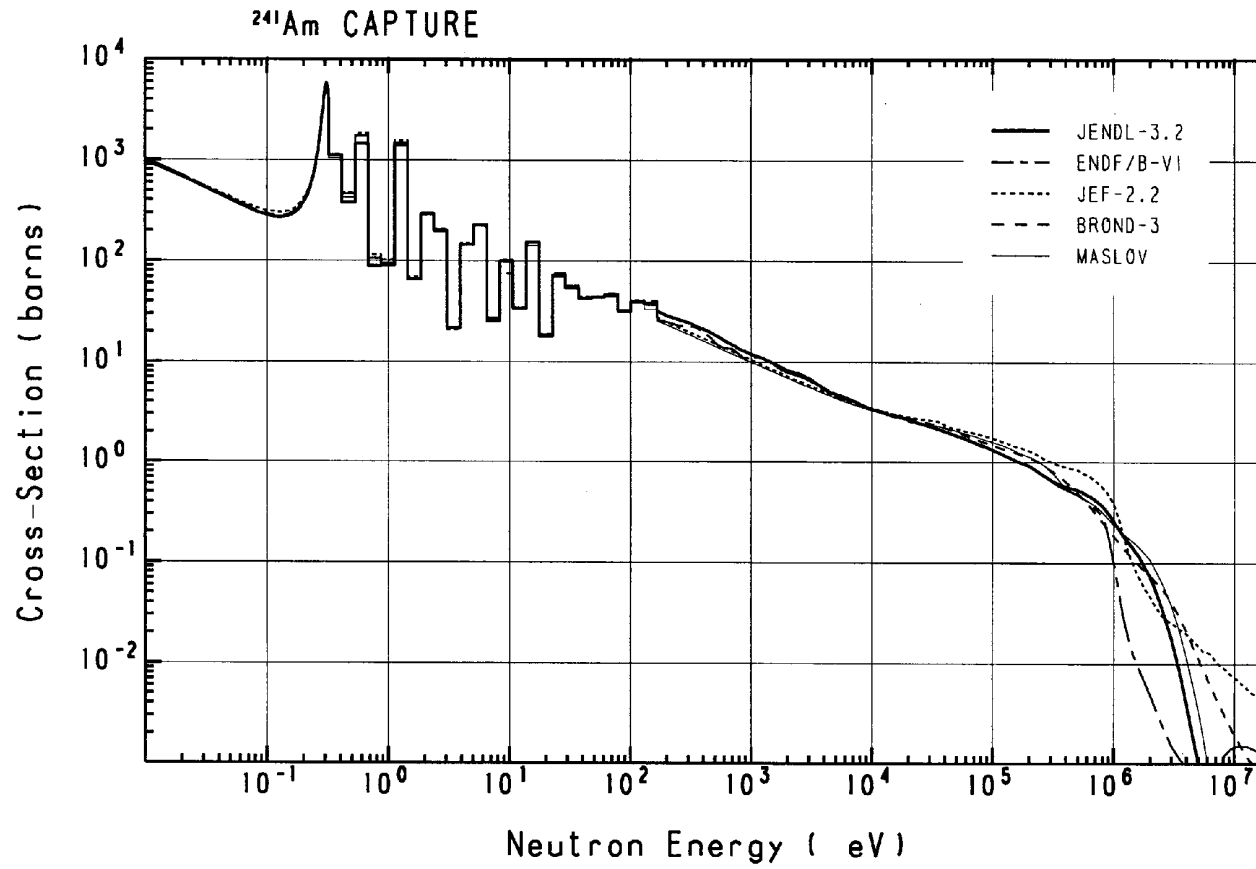


Figure 2.16. ^{241}Am capture cross-section

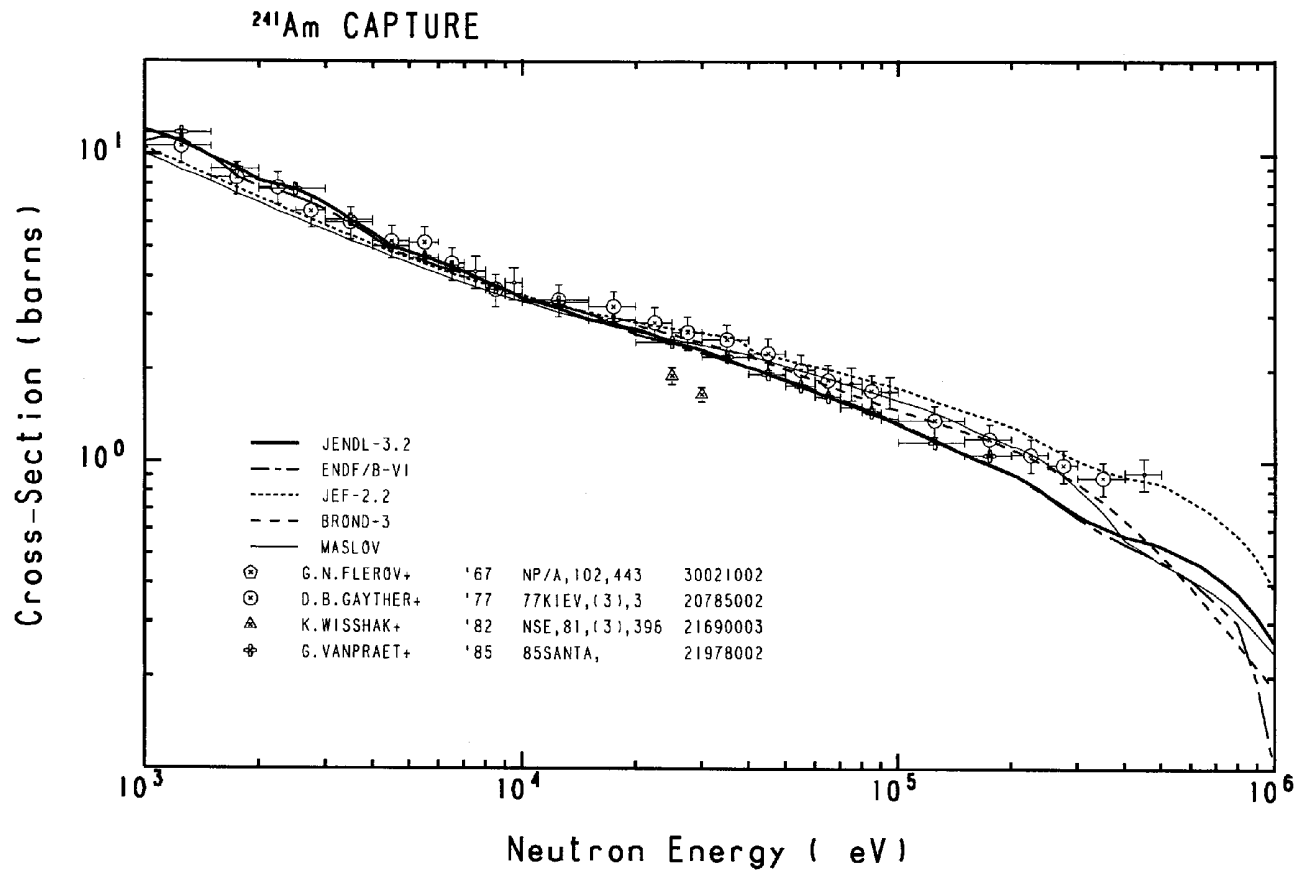


Figure 2.17. Isomeric ratio of $^{241}\text{Am}(n,\gamma)^{242g}\text{Am}$ and total $^{241}\text{Am}(n,\gamma)$ cross-sections

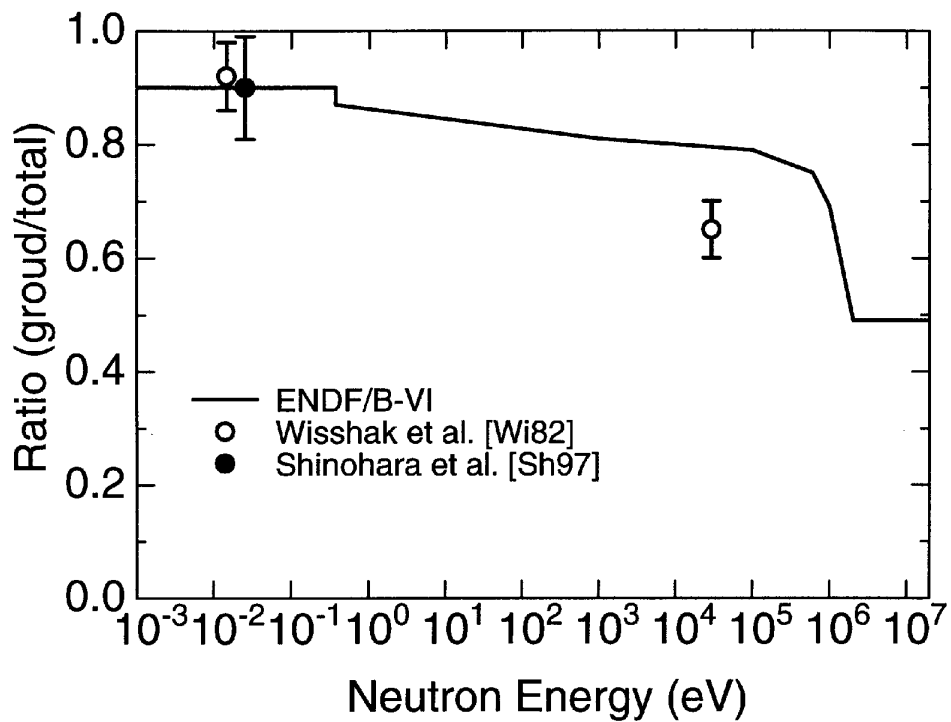


Figure 2.18. ^{241}Am (n,2n) and (n,3n) reaction cross-sections

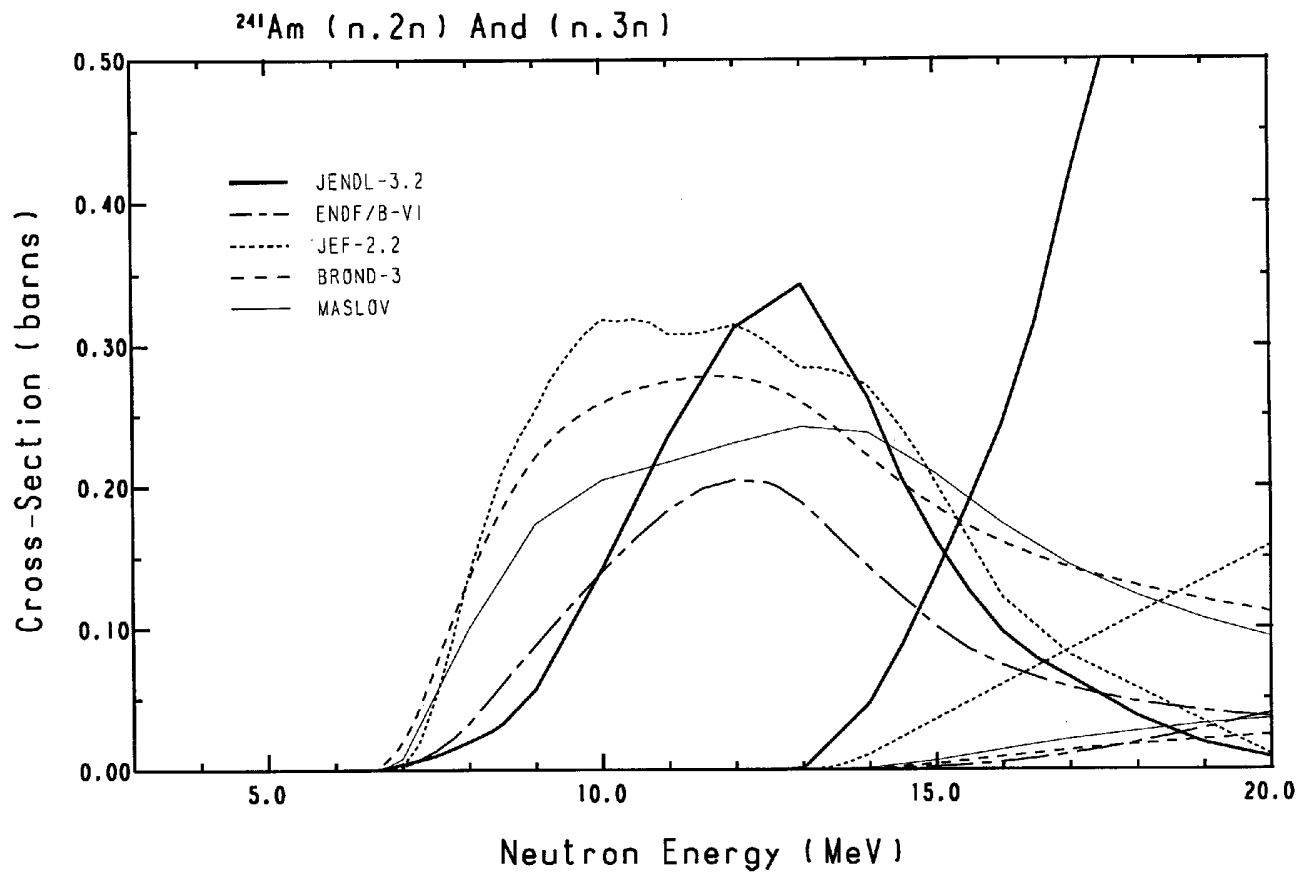


Figure 2.19. ^{241}Am total inelastic scattering cross-section

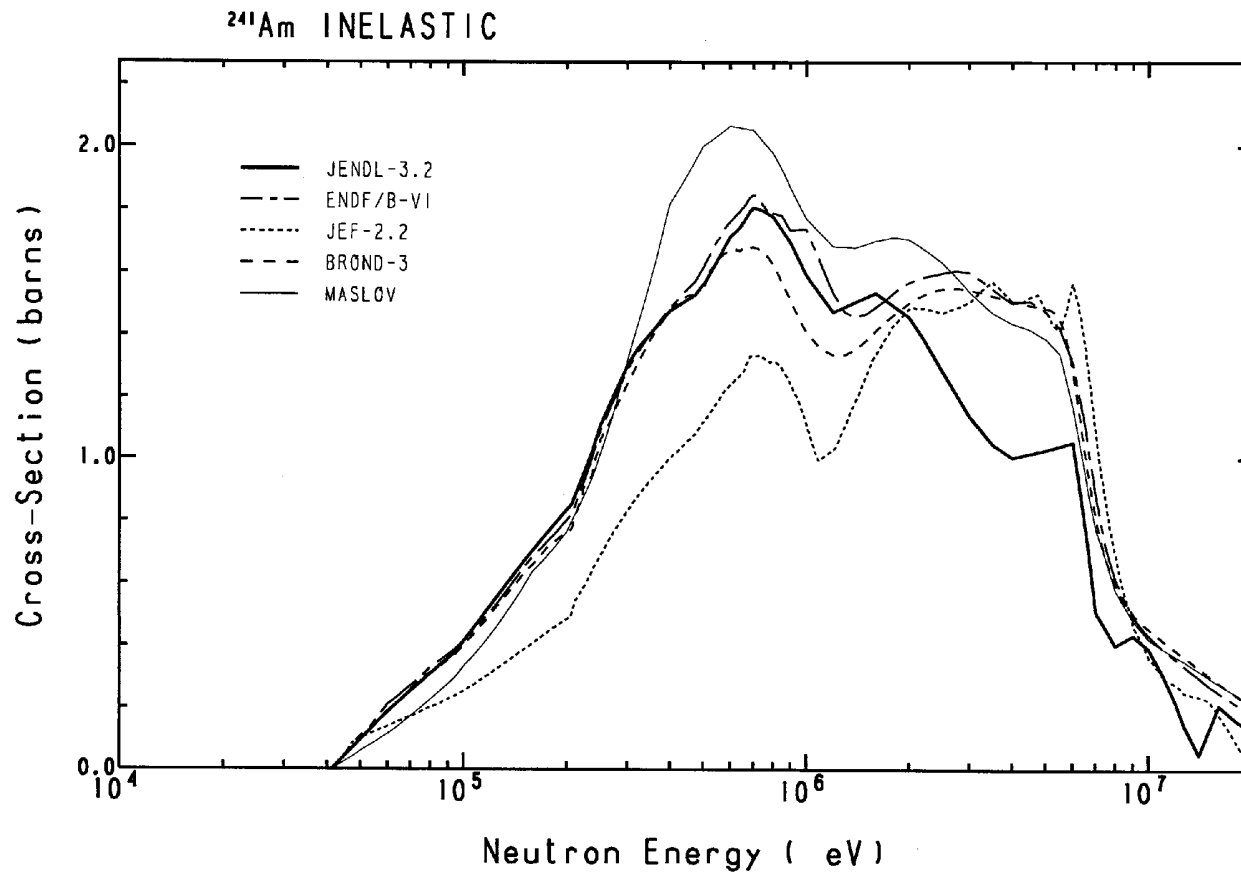


Figure 2.20. ^{241}Am elastic scattering cross-section

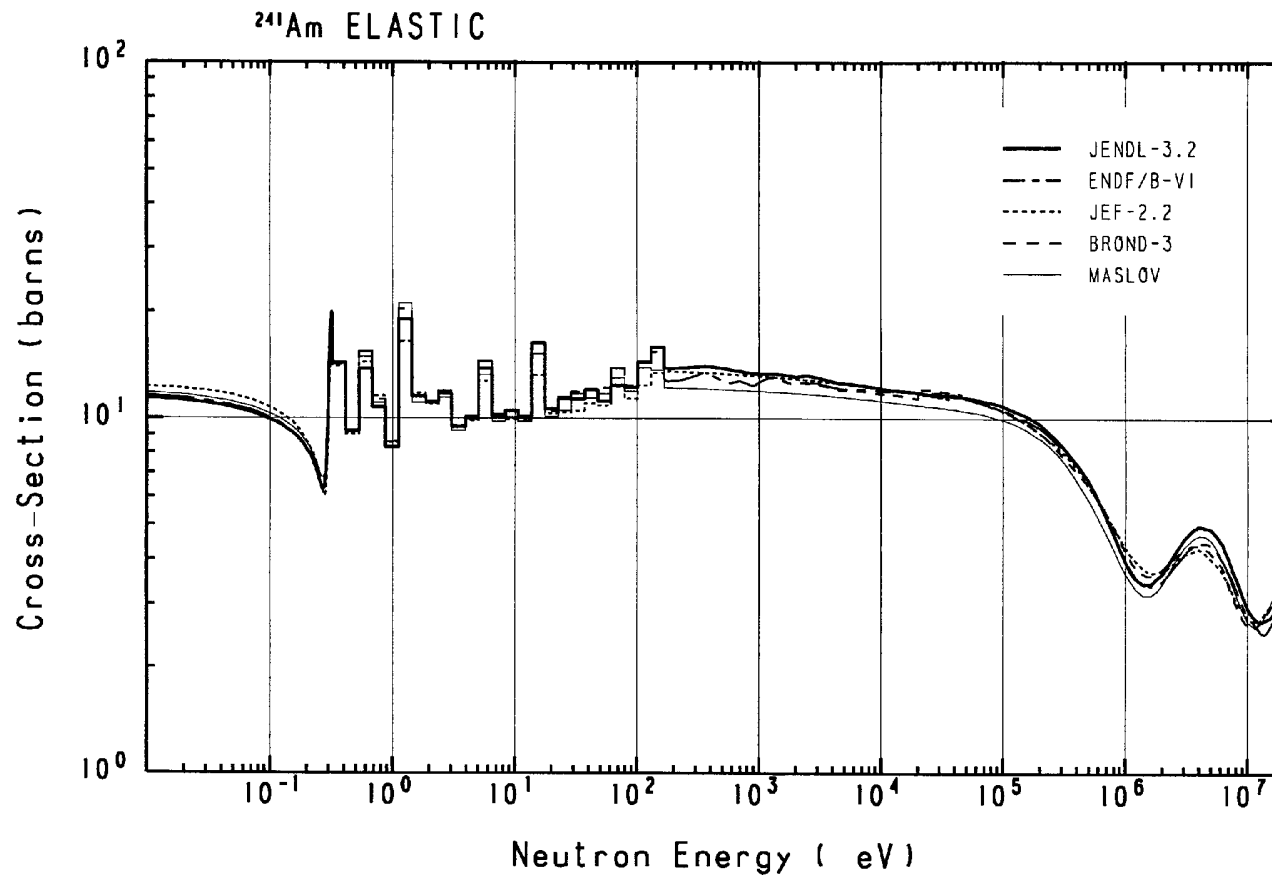


Figure 2.21. ^{241}Am total cross-section

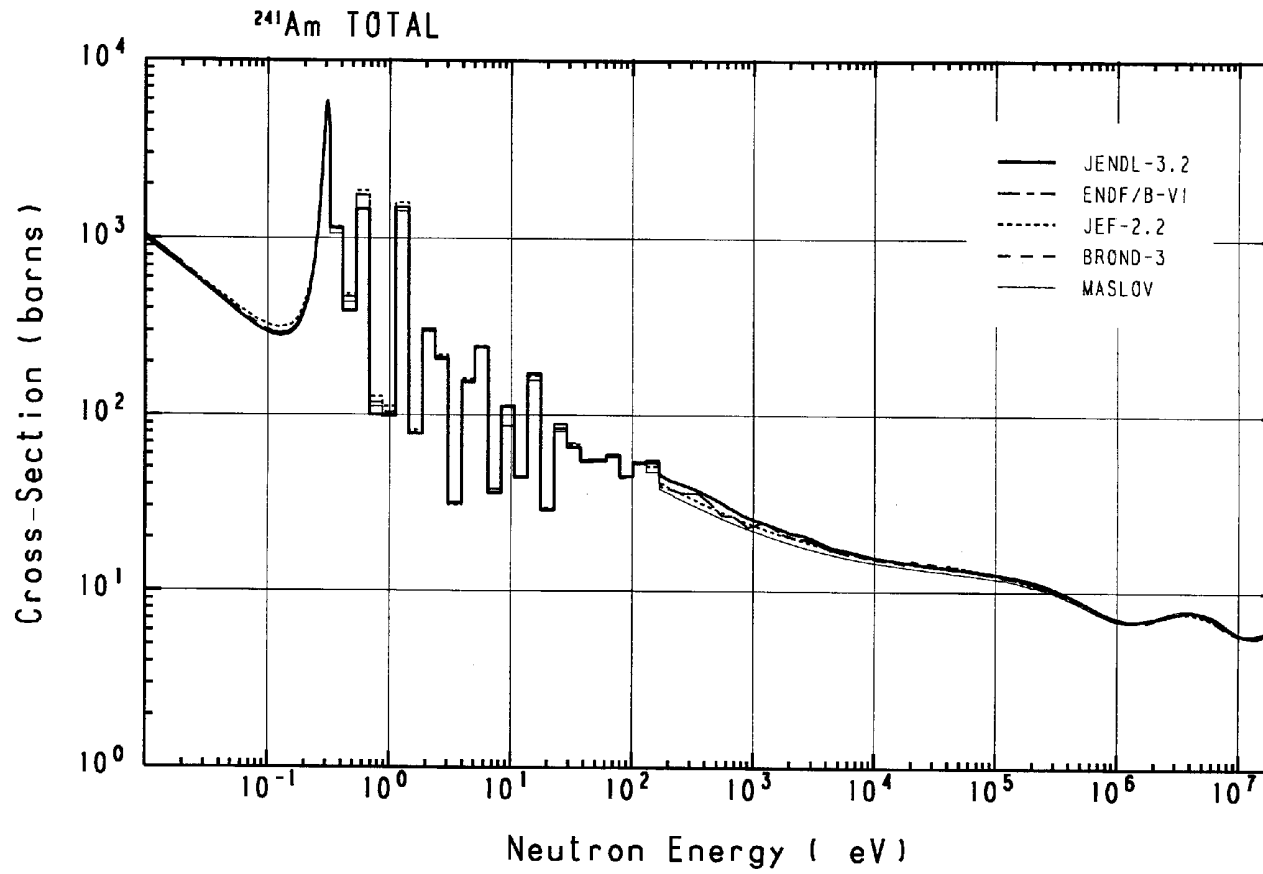


Figure 2.22. ²⁴³Am fission cross-section

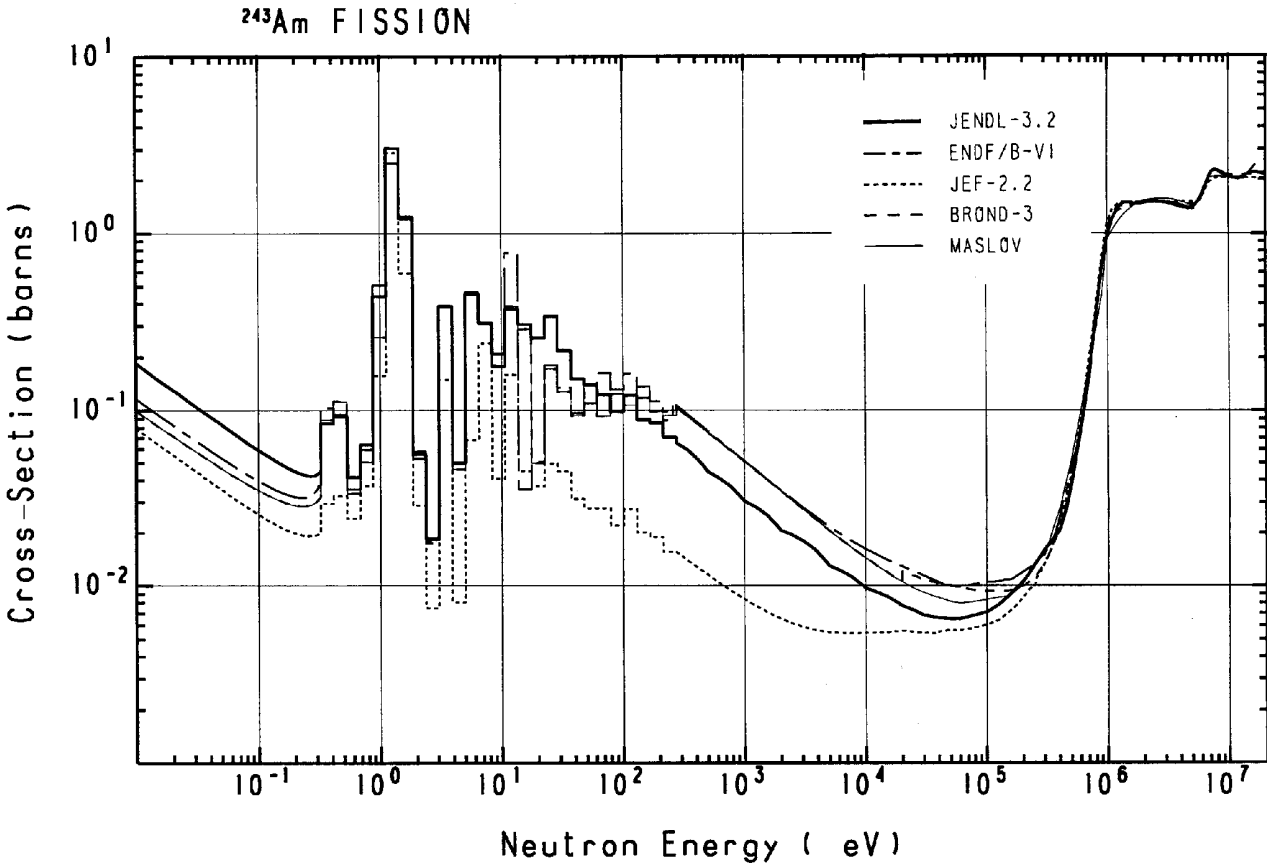


Figure 2.23. ^{243}Am fission cross-section (comparison with Kobayashi, et al. [46])

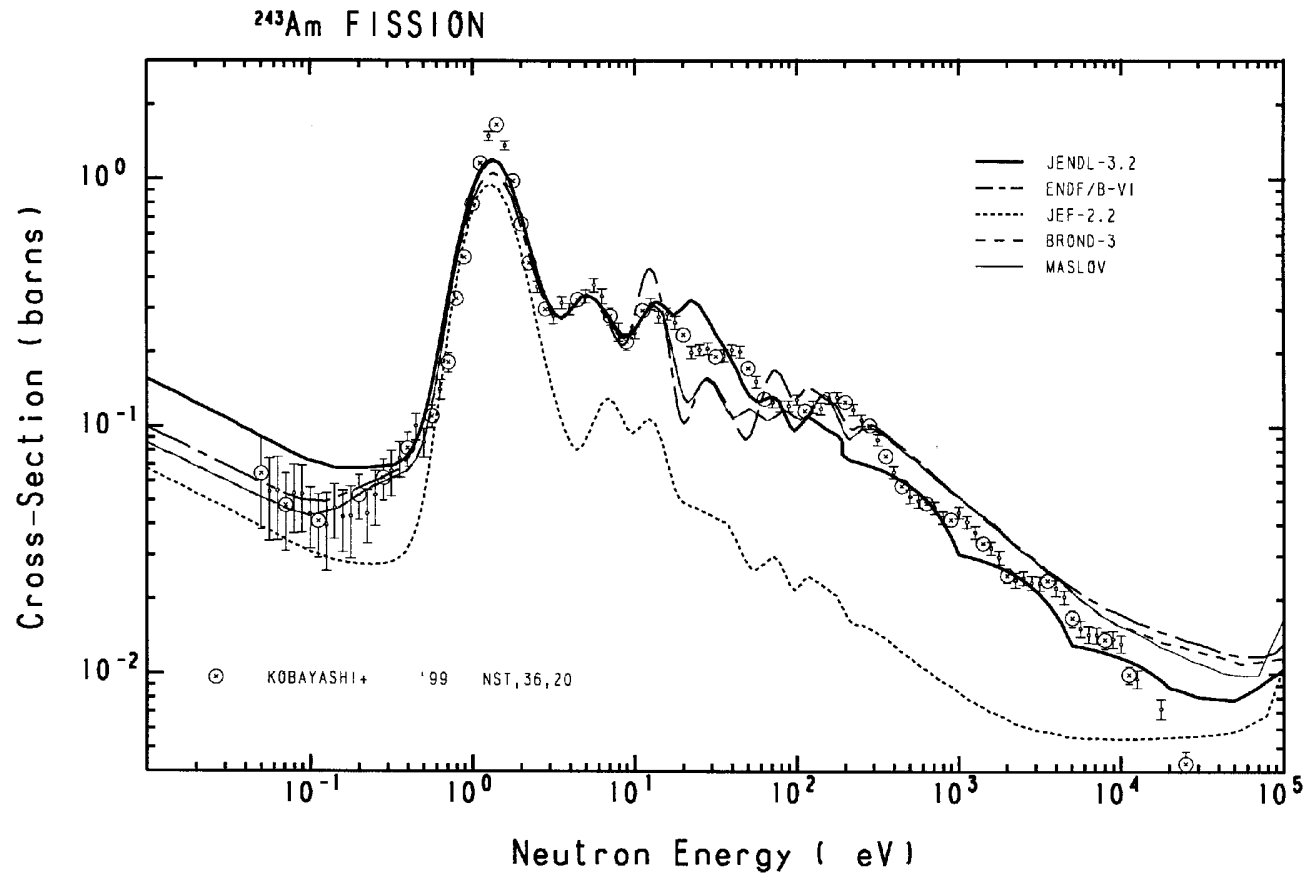


Figure 2.24(a). ^{243}Am fission cross-section

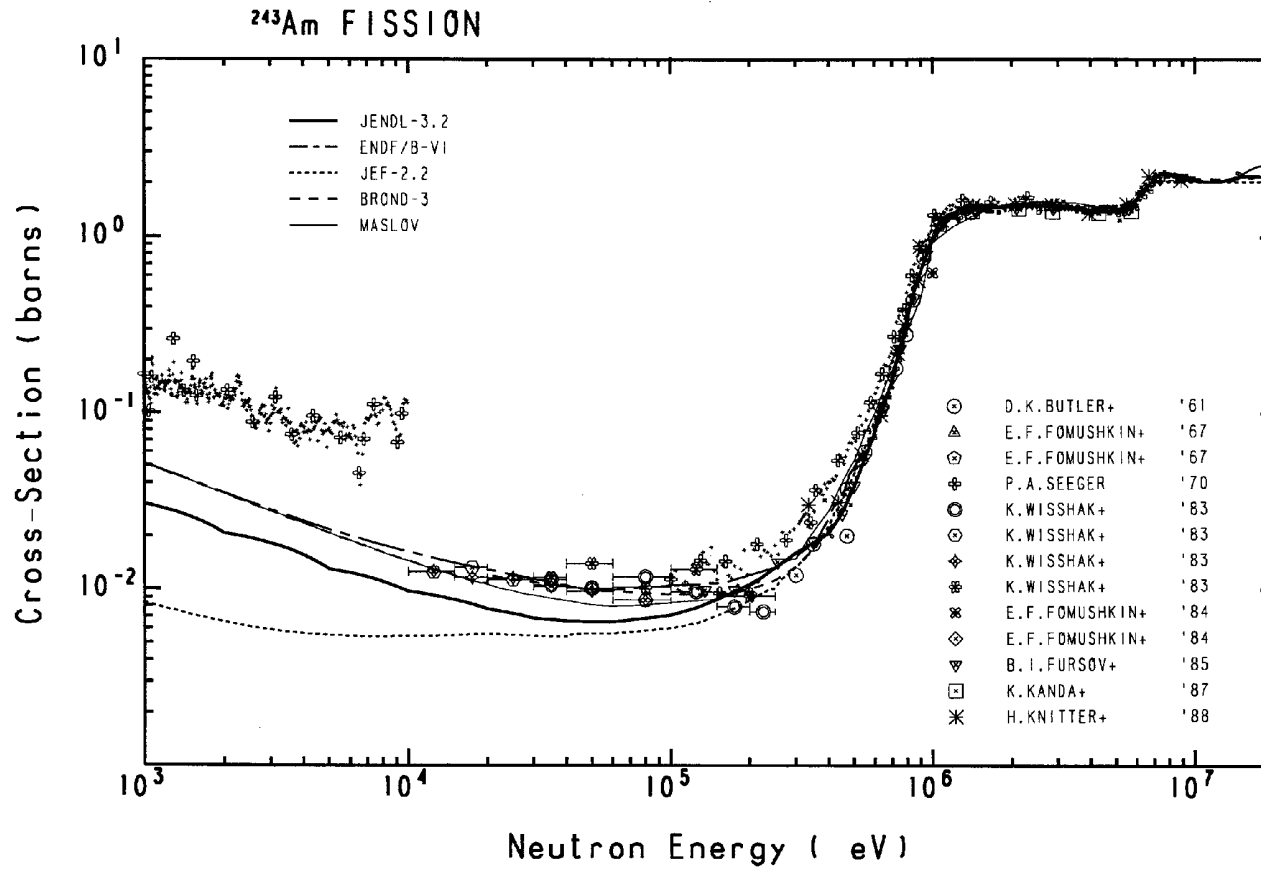


Figure 2.24(b). ²⁴³Am fission cross-section

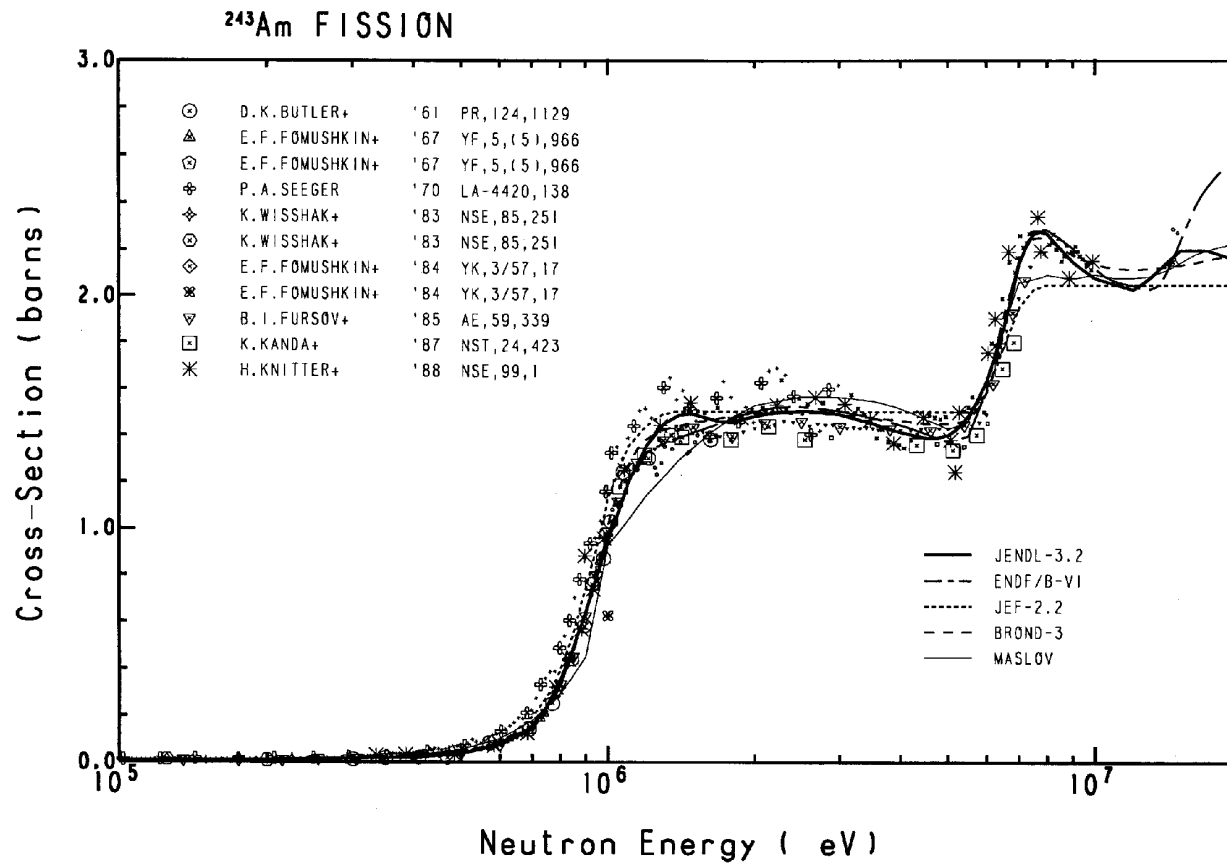


Figure 2.25. ^{243}Am capture cross-section

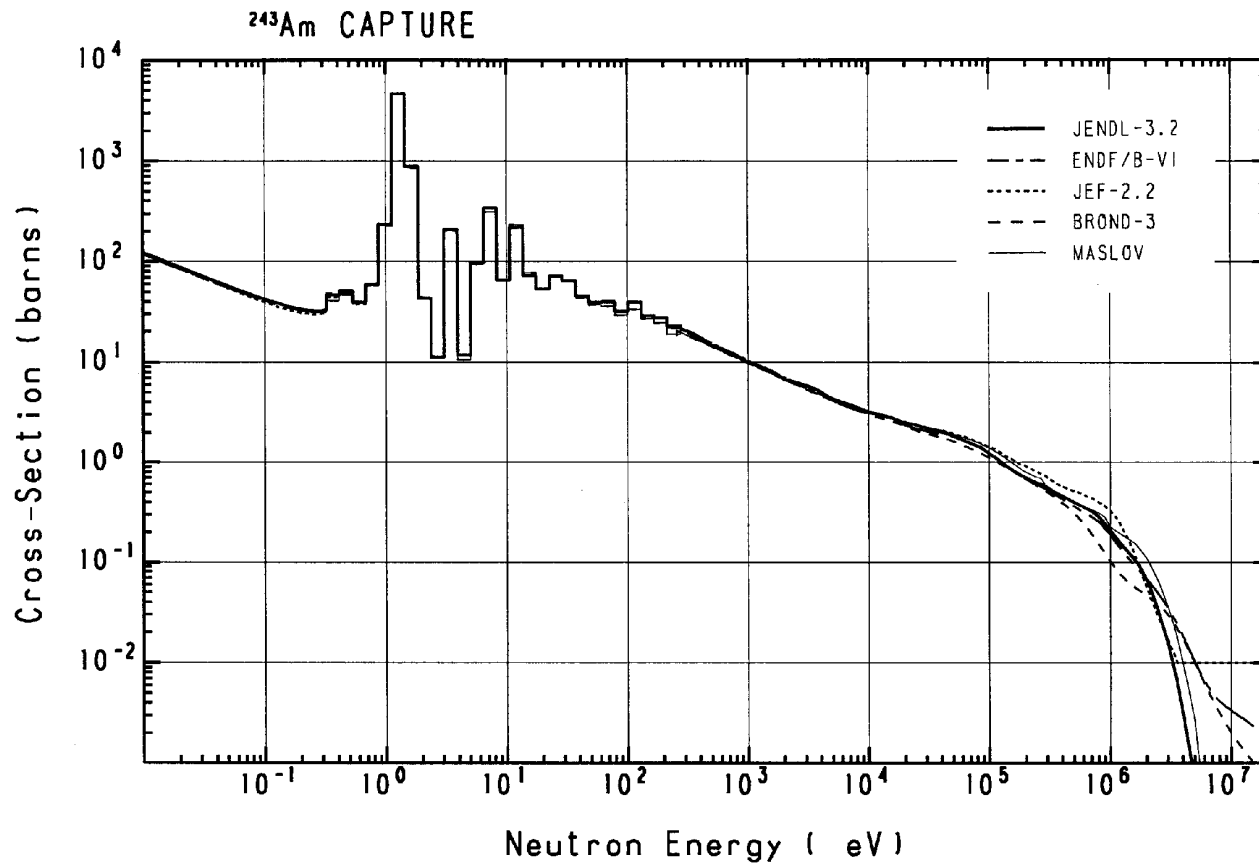


Figure 2.26. ^{243}Am capture cross-section
 Averaged values of the evaluated data are shown below 275 eV

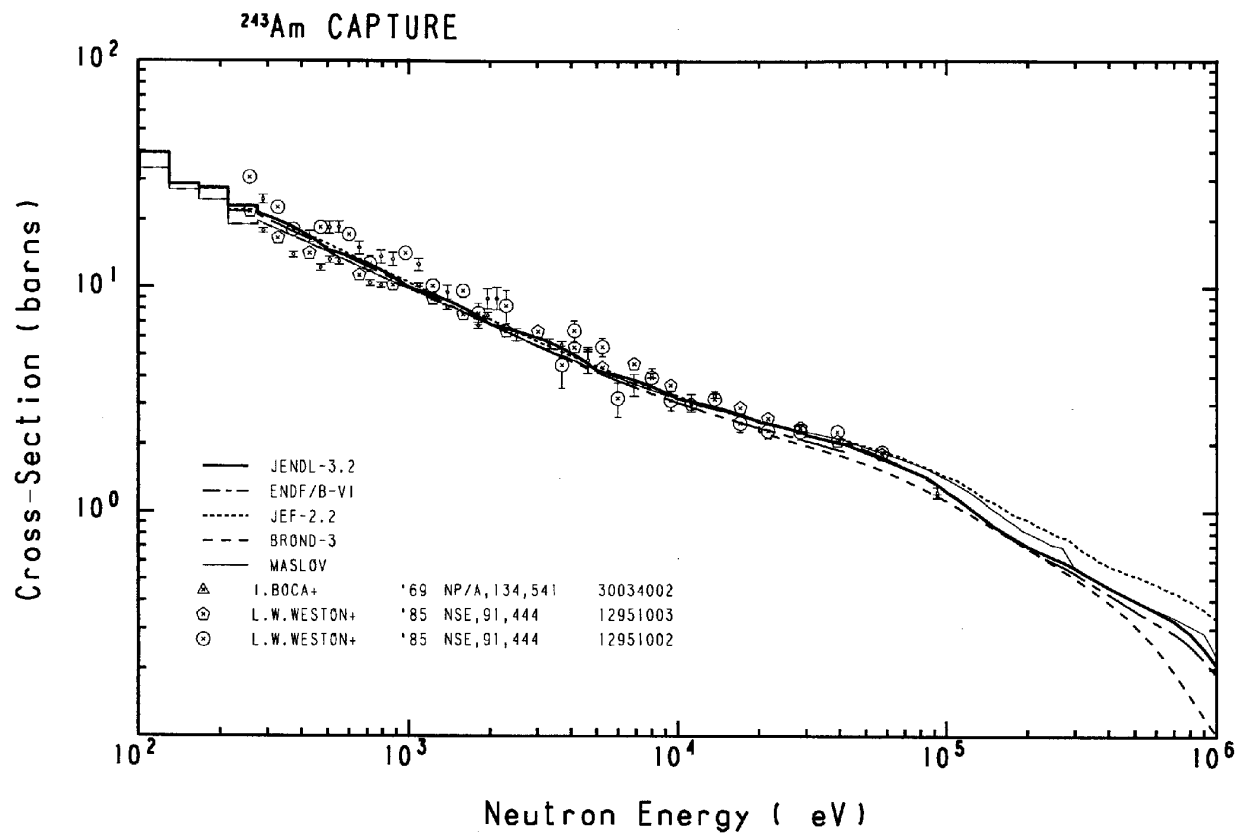


Figure 2.27. $^{243}\text{Am}(n,2n)$ and $(n,3n)$ reaction cross-sections

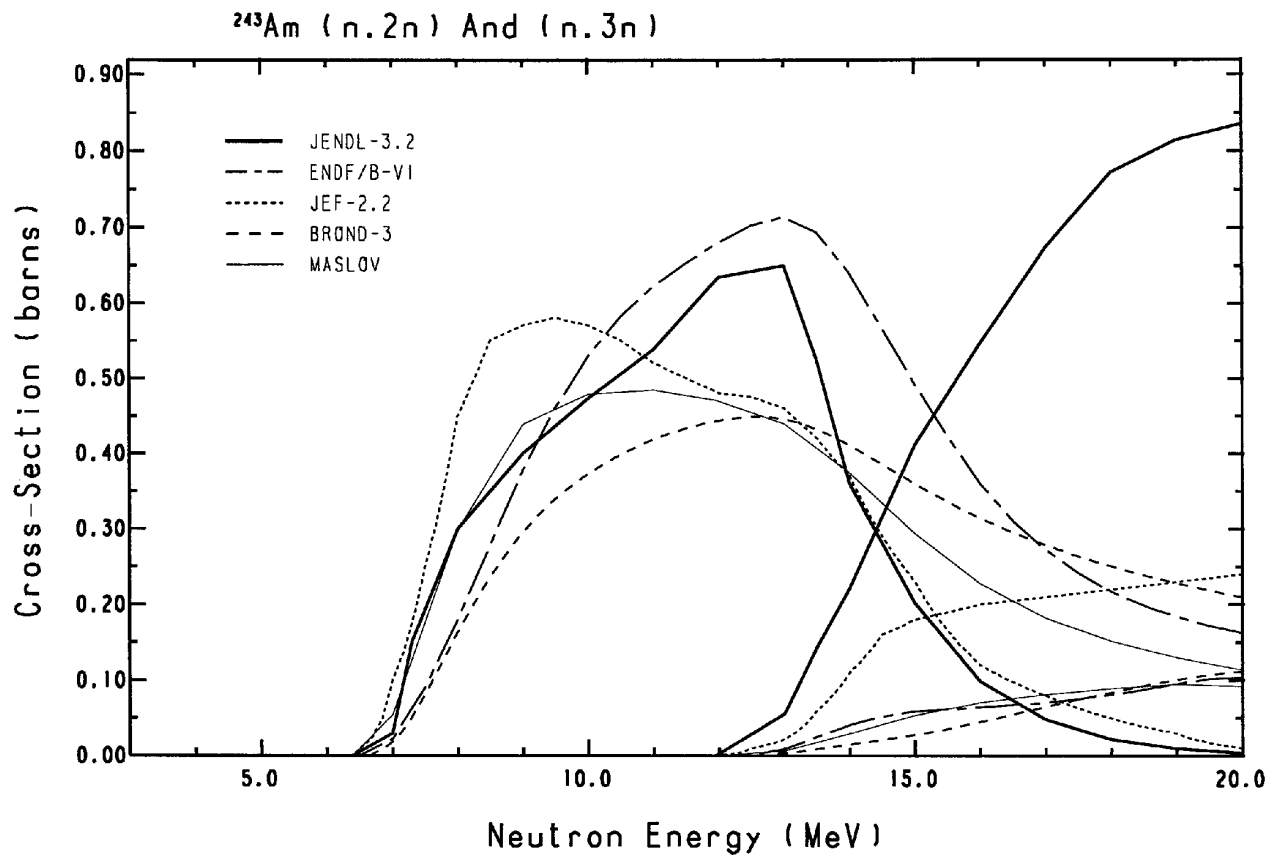


Figure 2.28. ^{243}Am total inelastic scattering cross-section

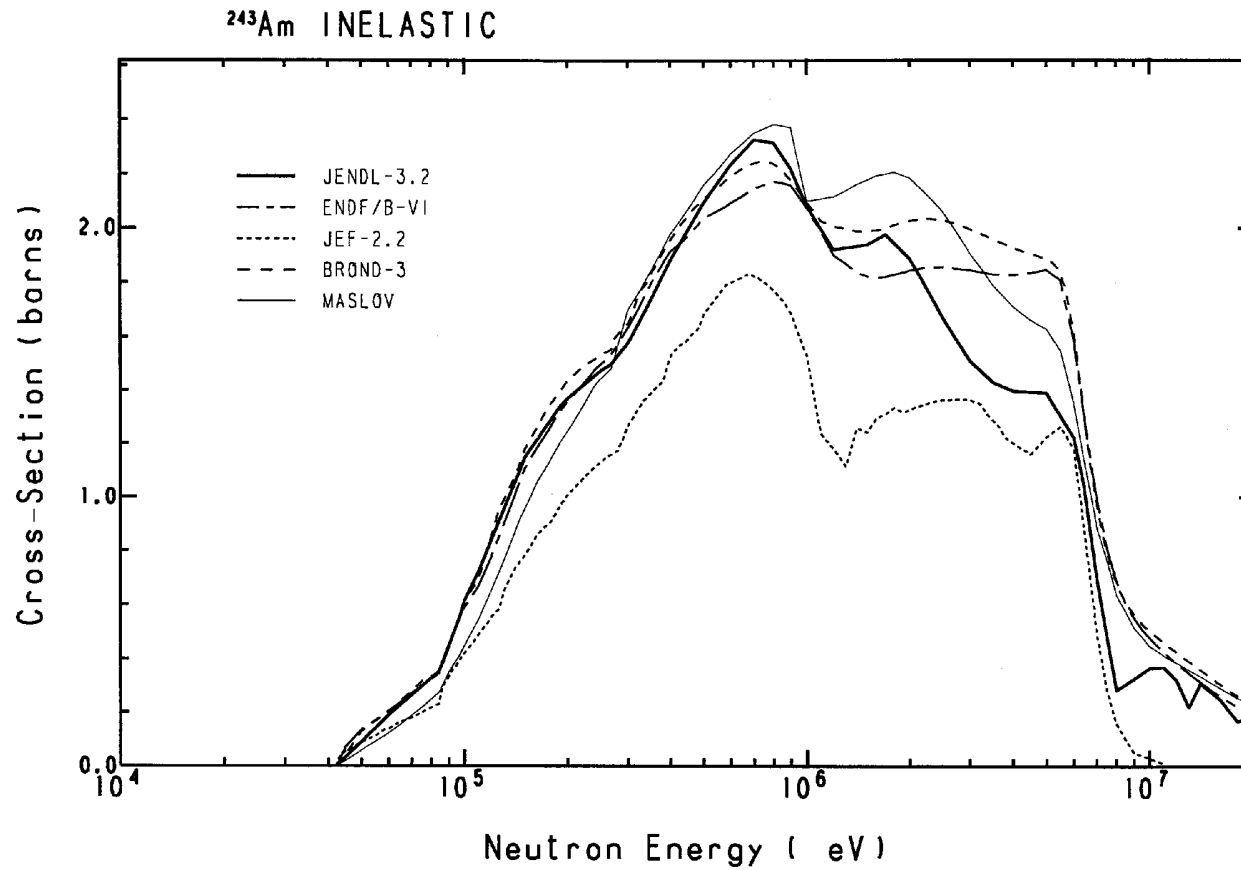


Figure 2.29. ^{243}Am elastic scattering cross-section

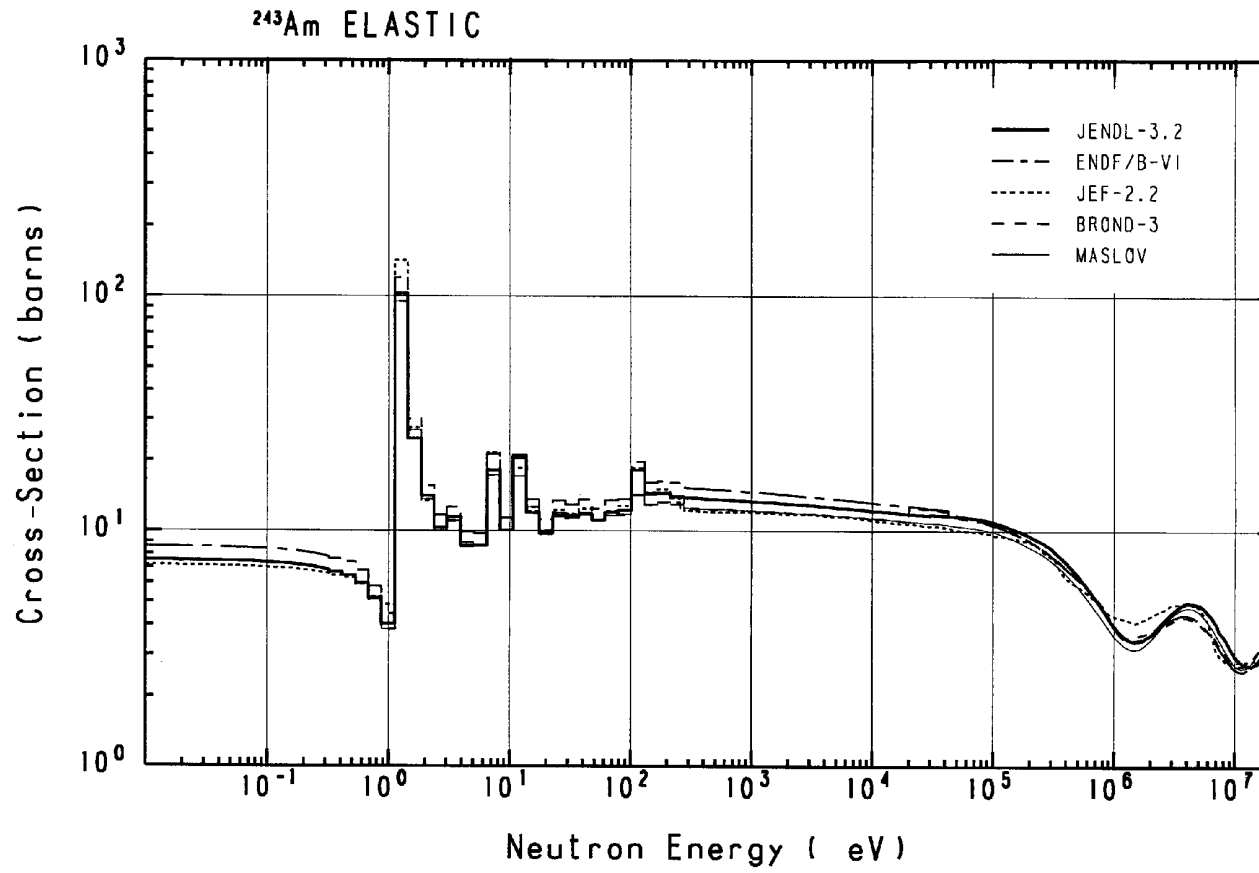


Figure 2.30. ^{243}Am total cross-section

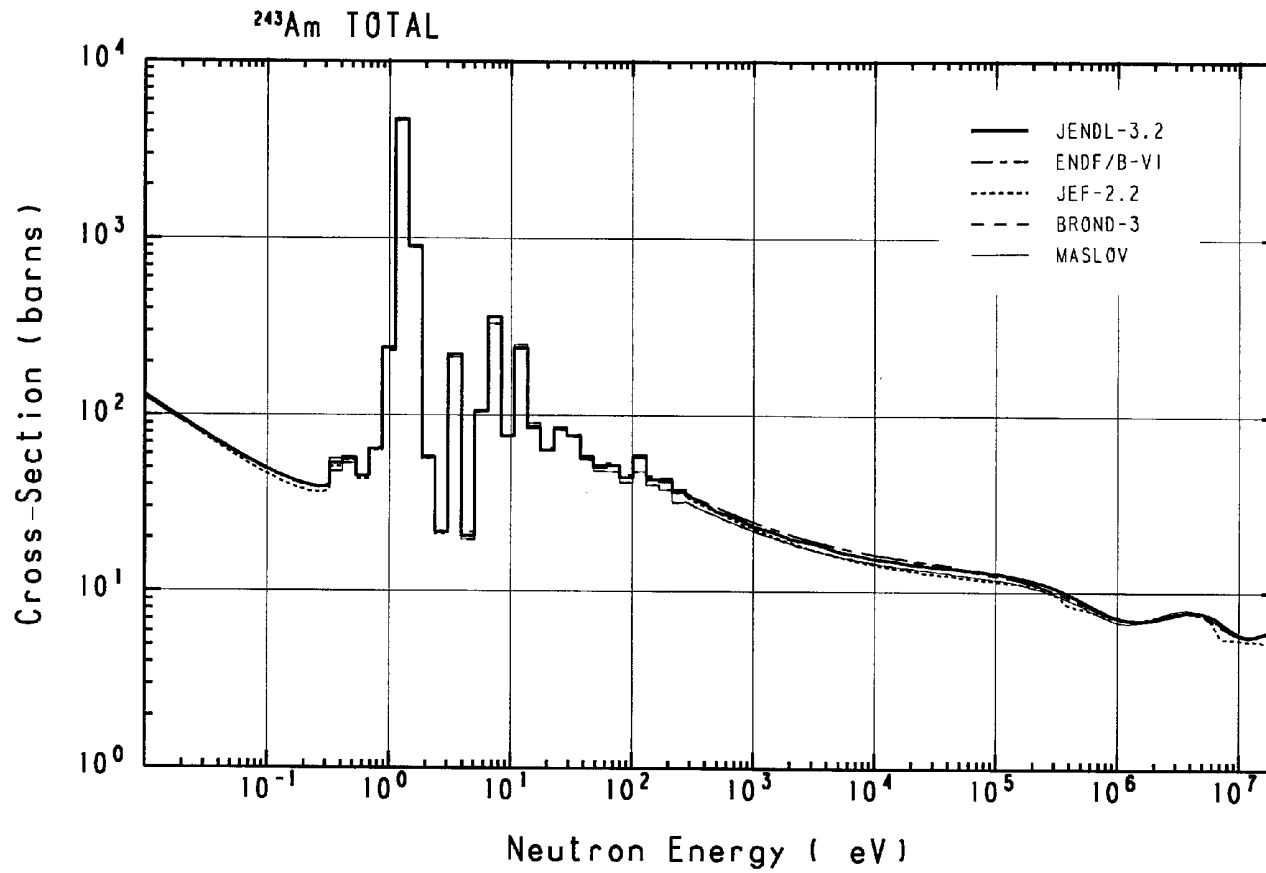


Figure 2.31. ^{242}Cm fission cross-section

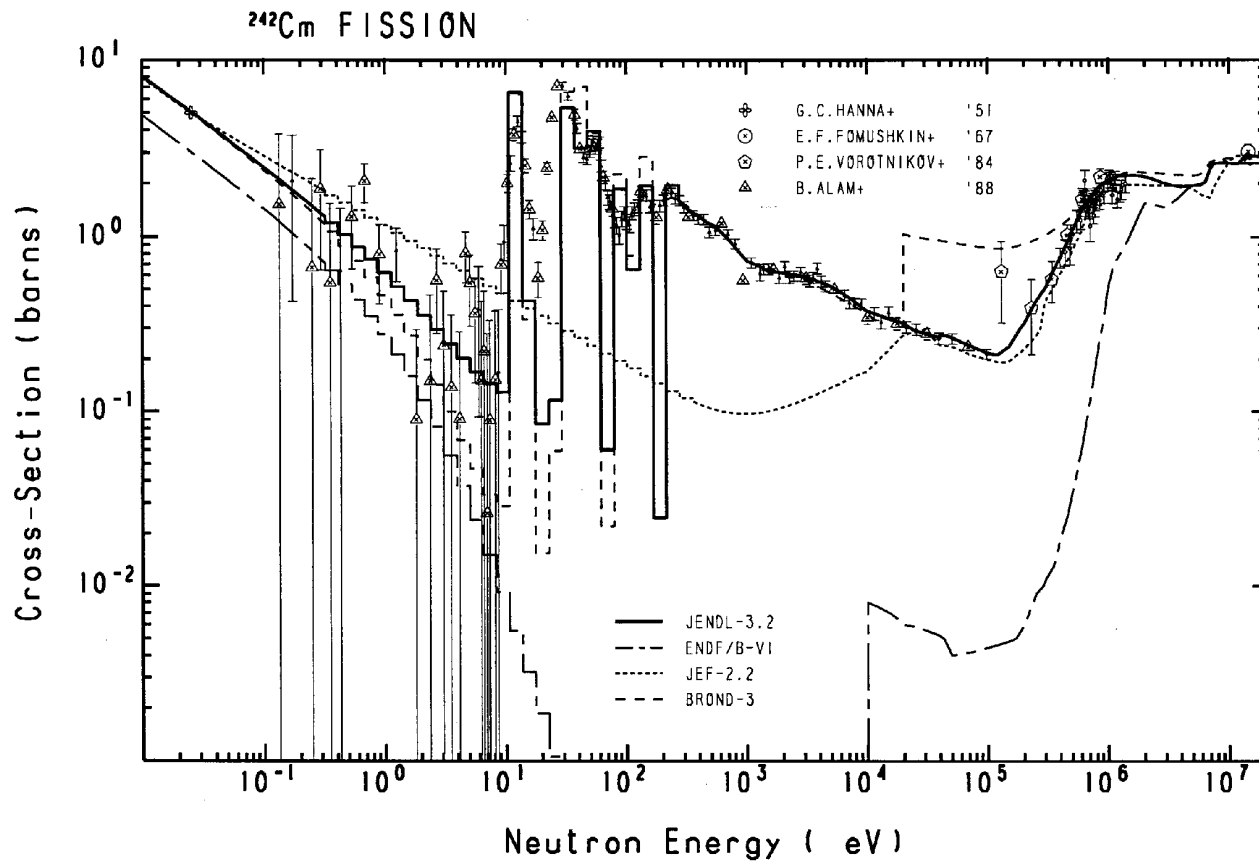


Figure 2.32. ^{242}Cm capture cross-section

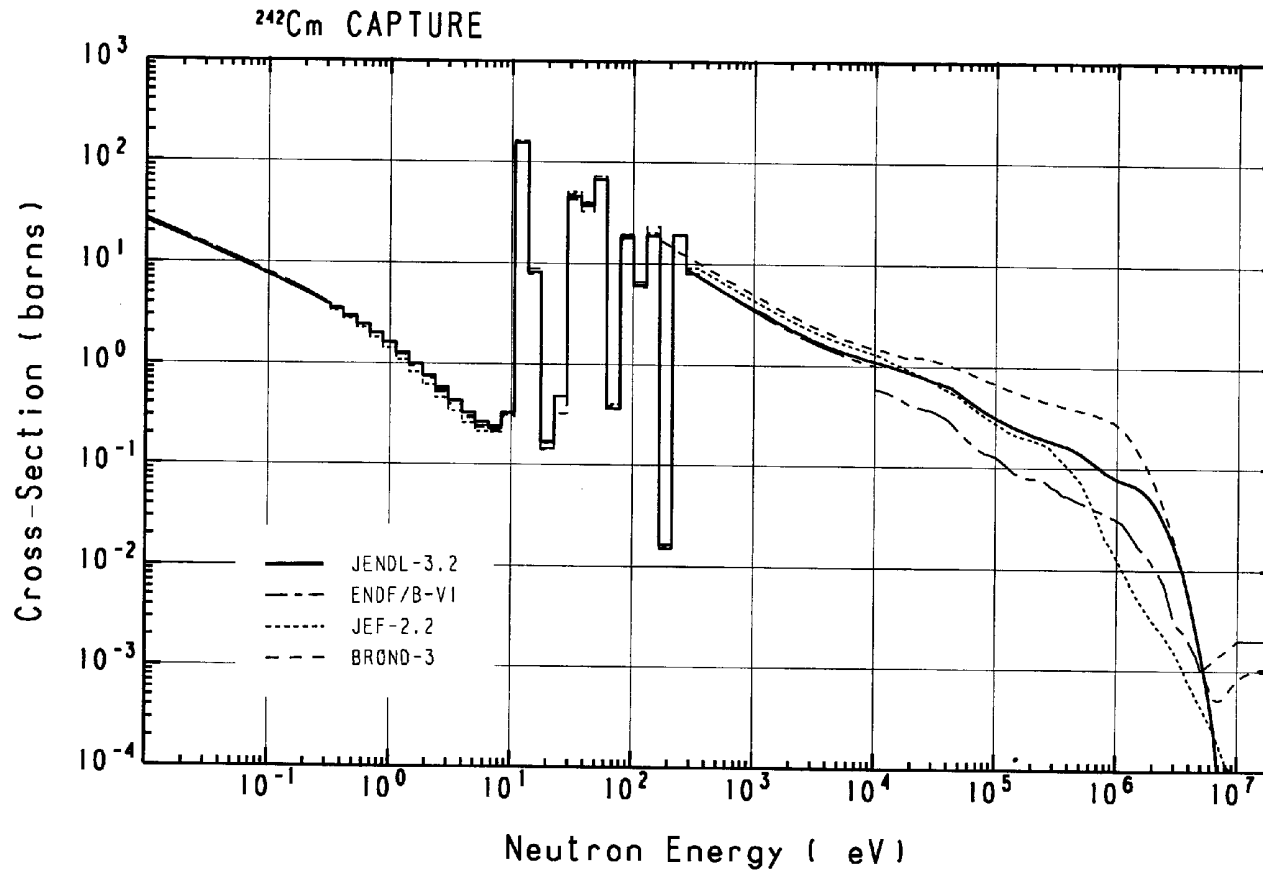


Figure 2.33. $^{242}\text{Cm}(n,2n)$ and $(n,3n)$ reaction cross-sections

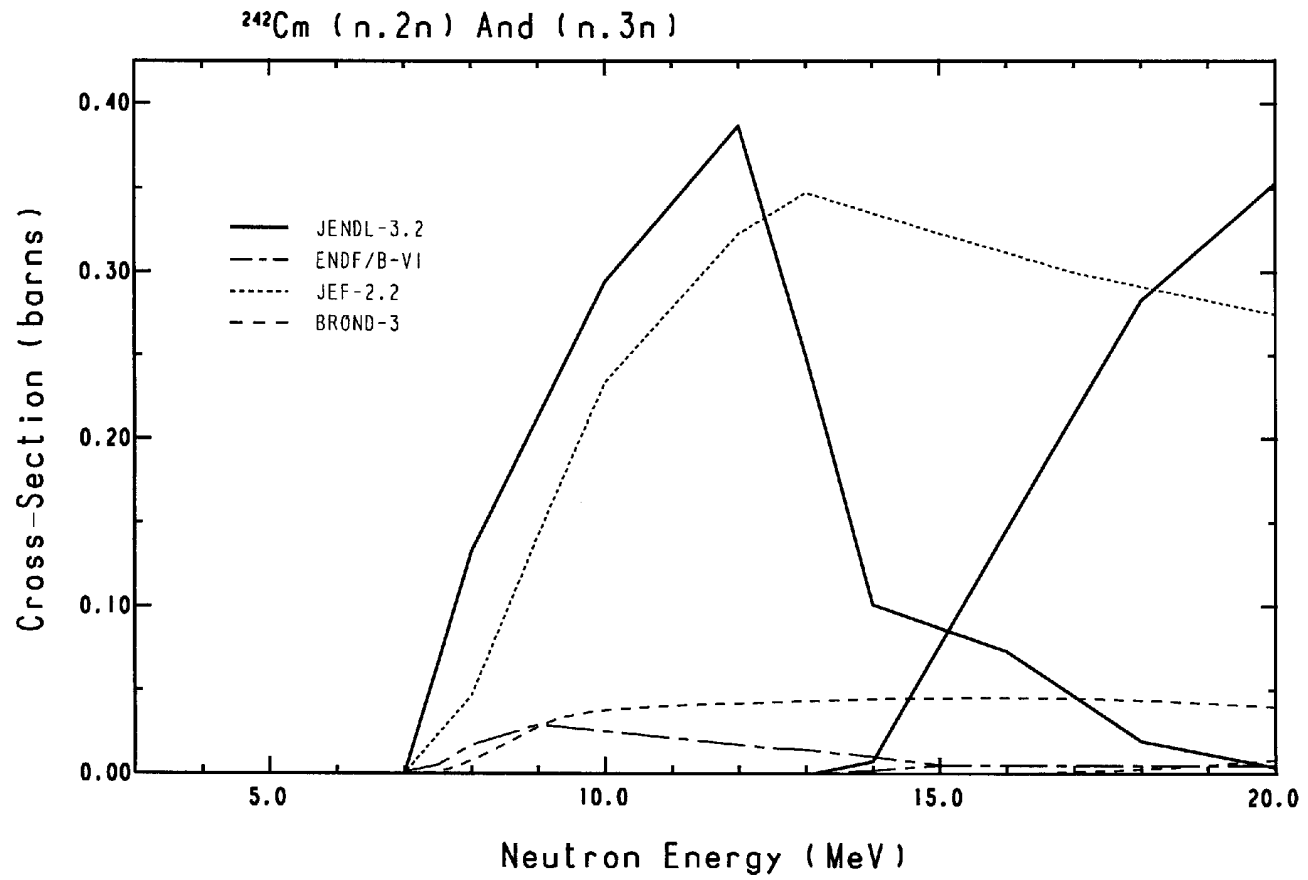


Figure 2.34. ^{242}Cm total inelastic scattering cross-section

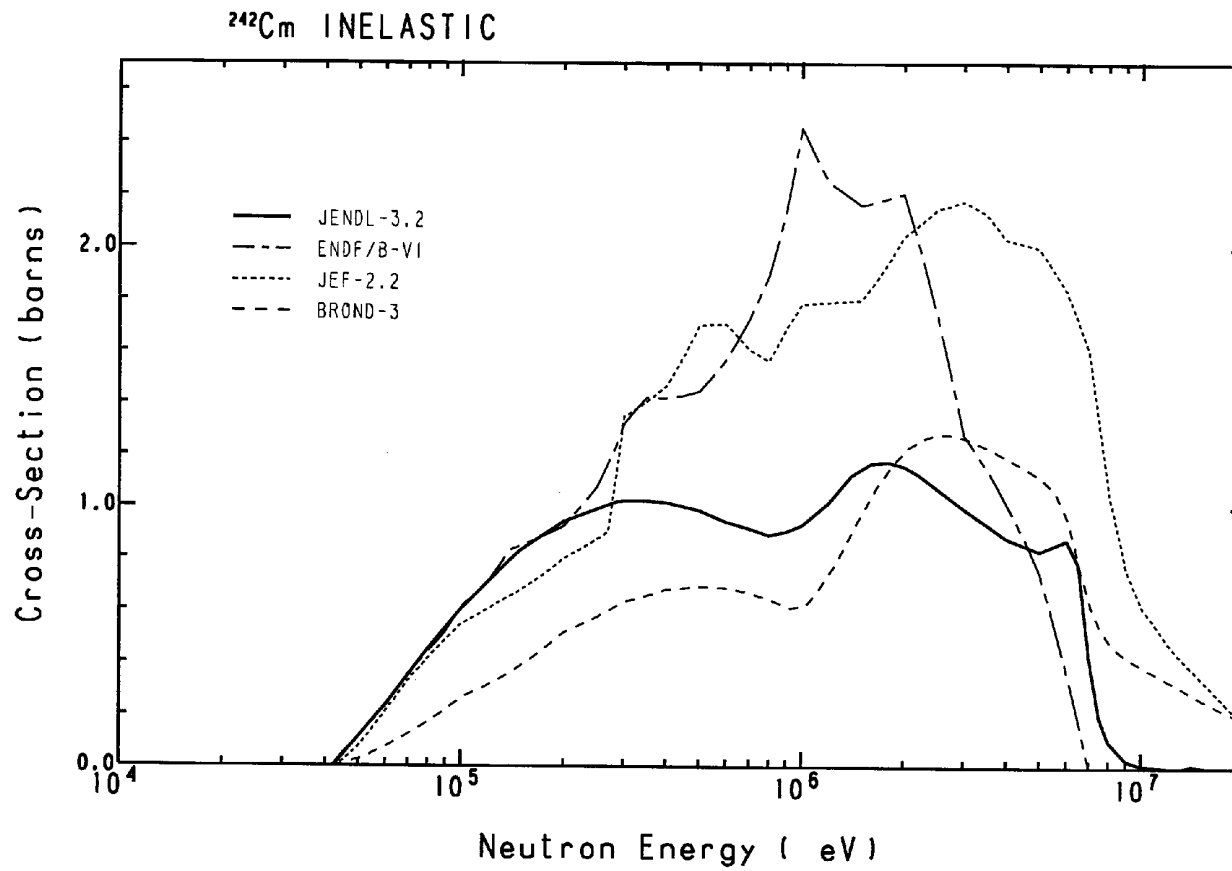


Figure 2.35. ^{242}Cm elastic scattering cross-section

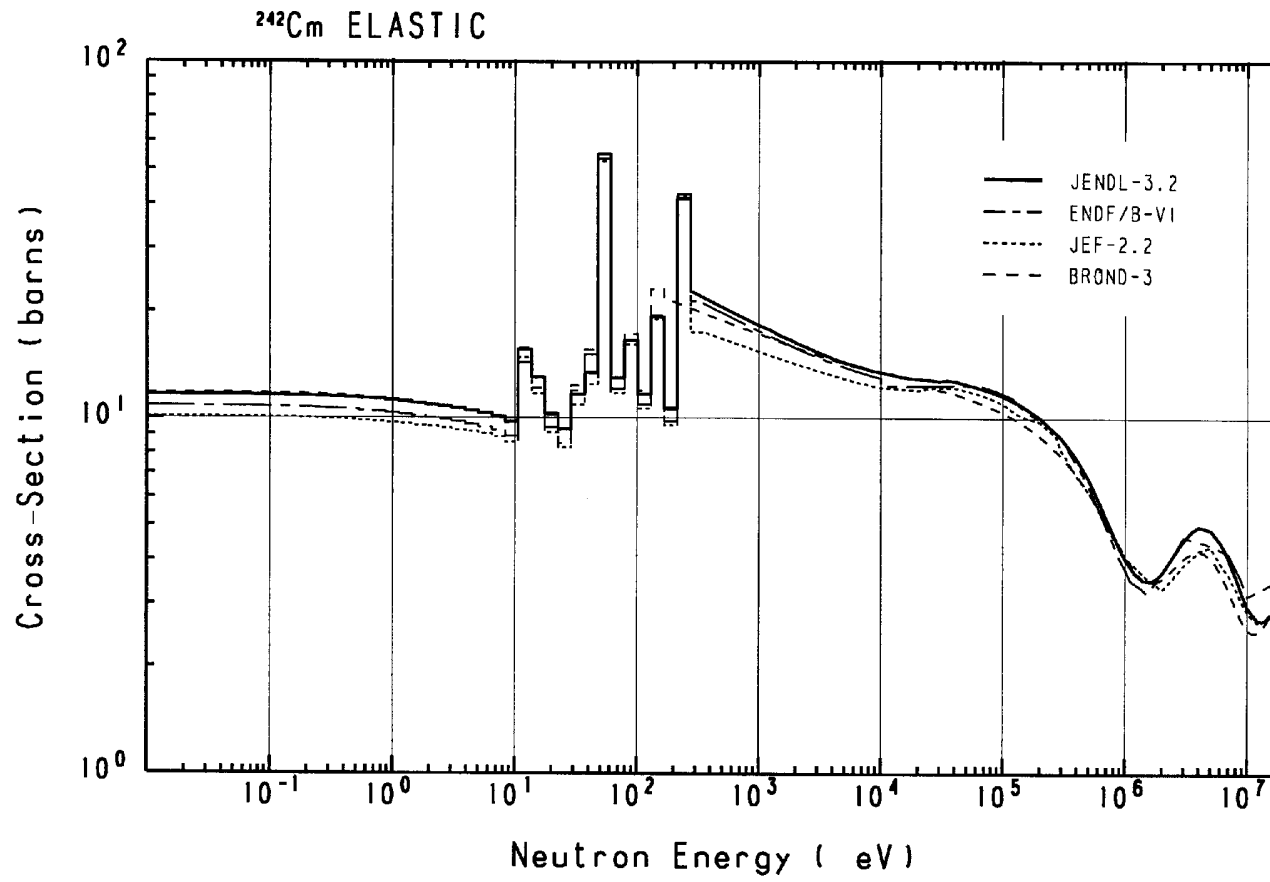


Figure 2.36. ^{242}Cm total cross-section

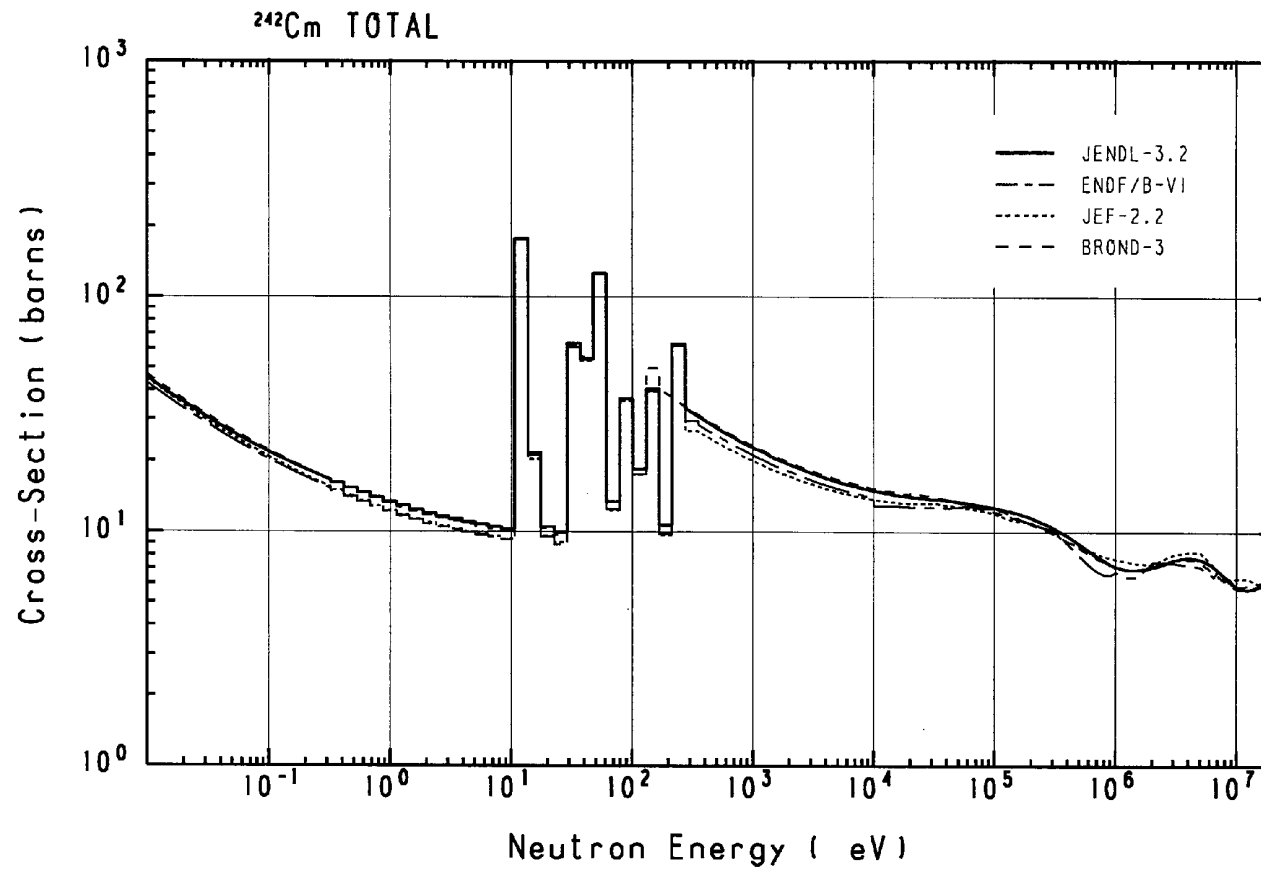


Figure 2.37. ^{243}Cm fission cross-section

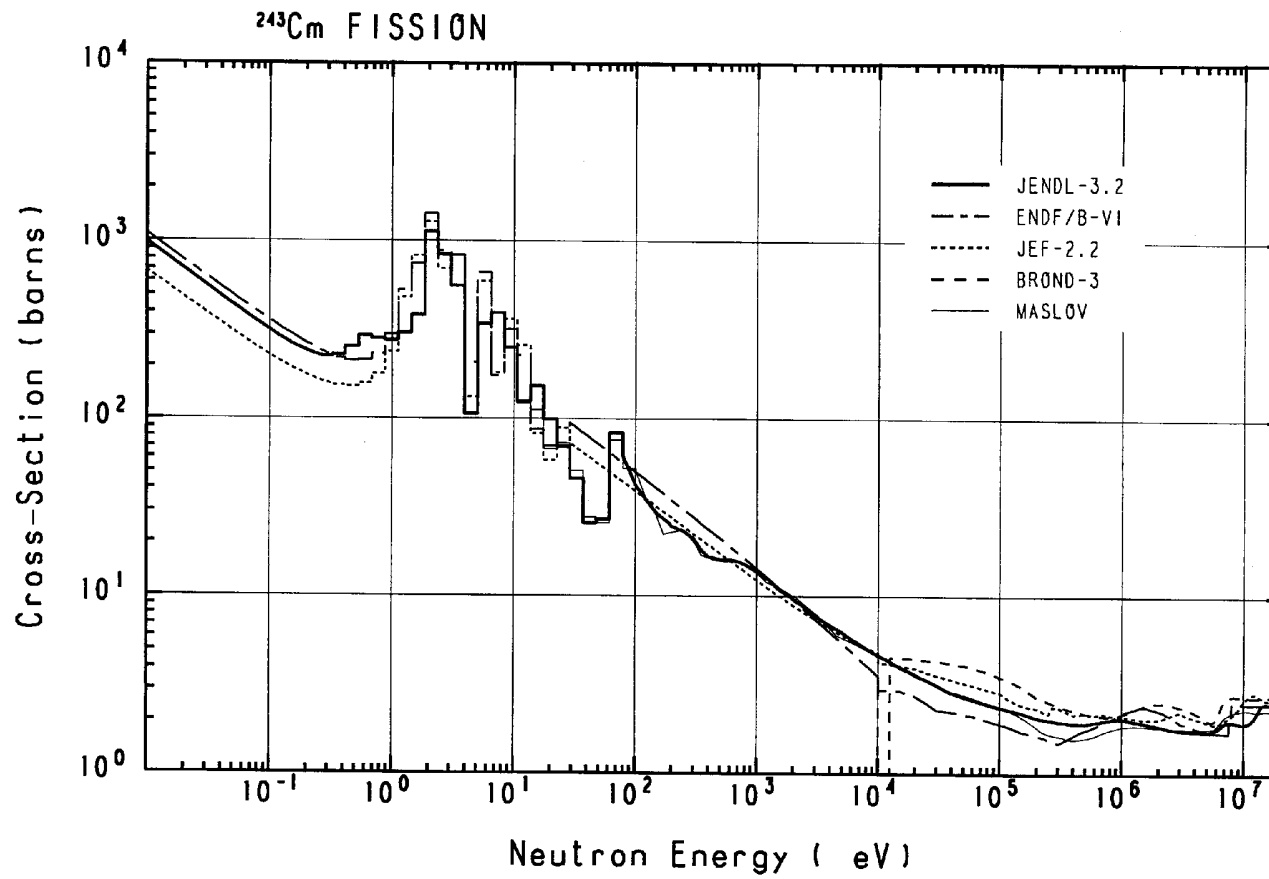


Figure 2.38. ^{243}Cm fission cross-section

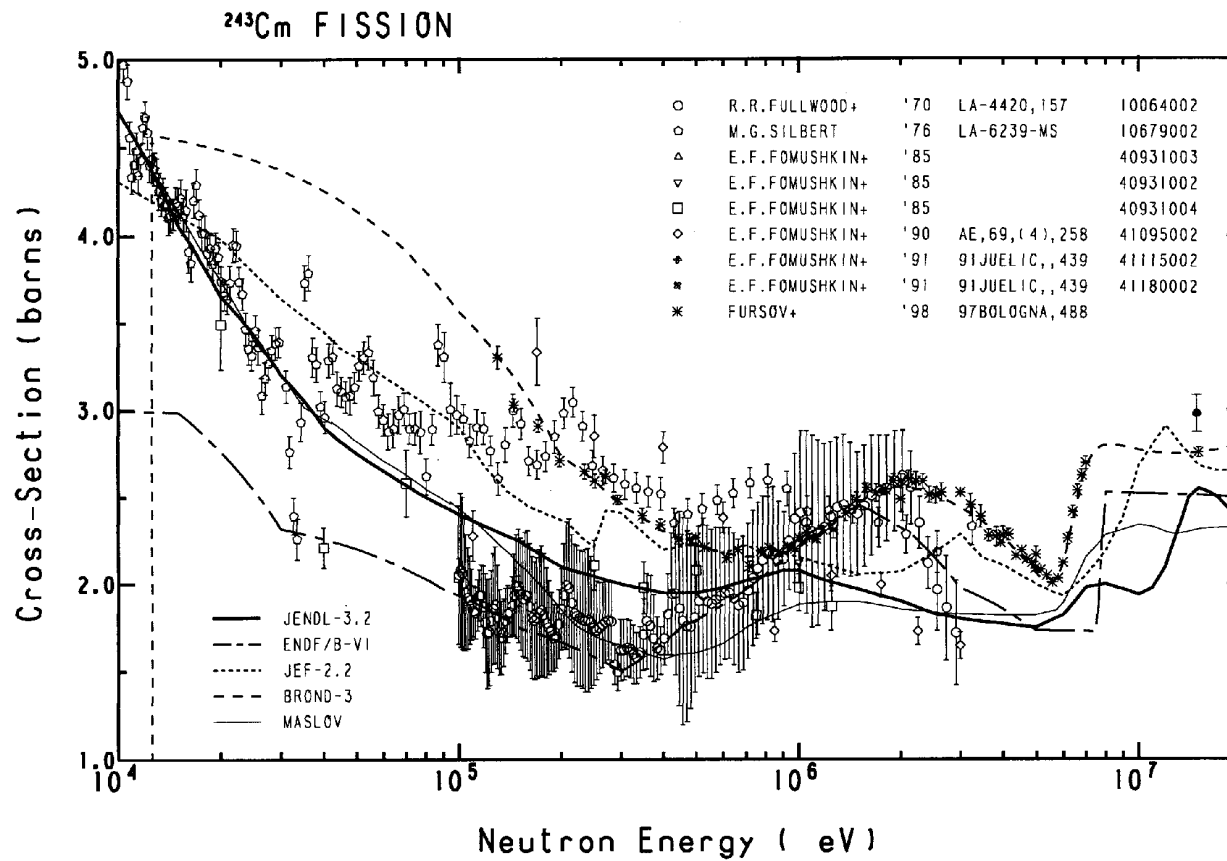


Figure 2.39. ^{243}Cm capture cross-section

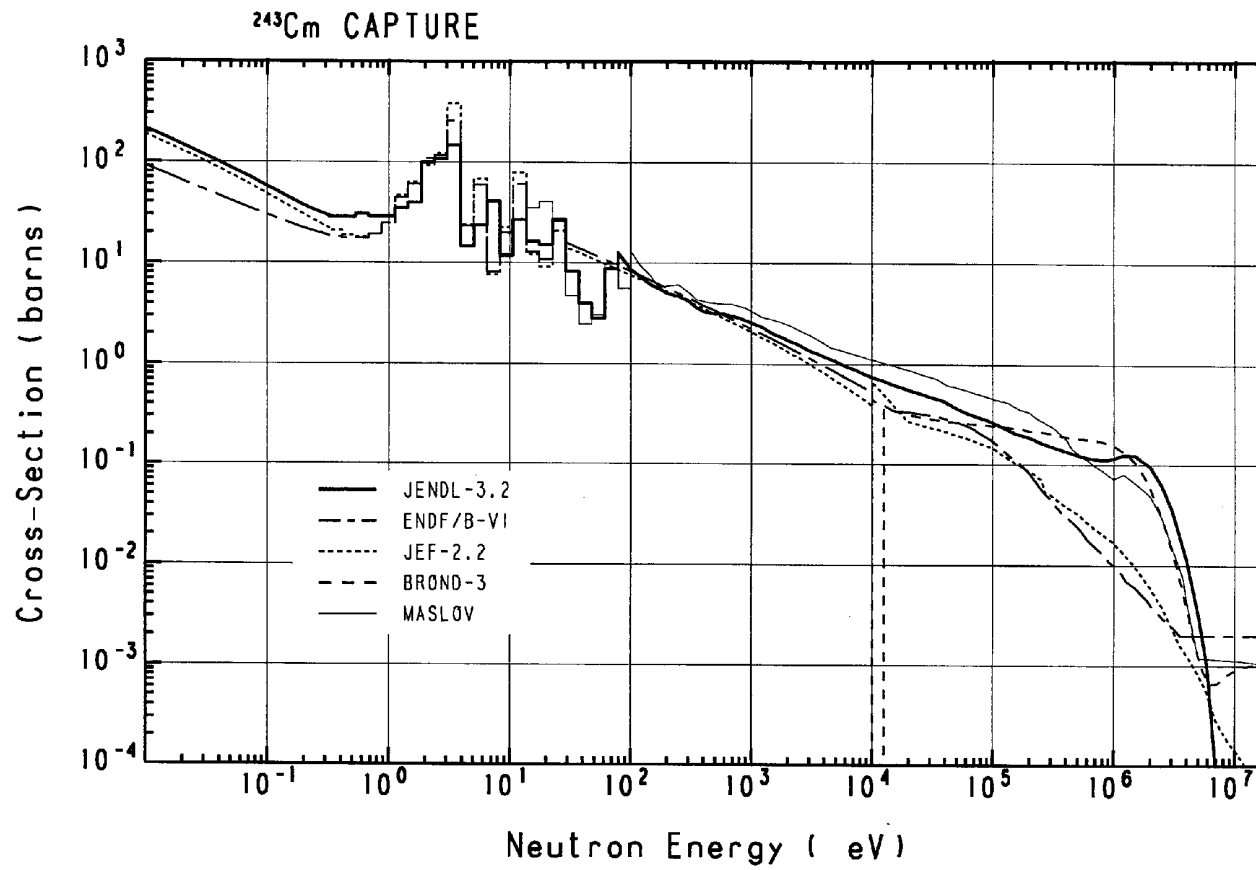


Figure 2.40. $^{243}\text{Cm}(n,2n)$ and $(n,3n)$ reaction cross-sections

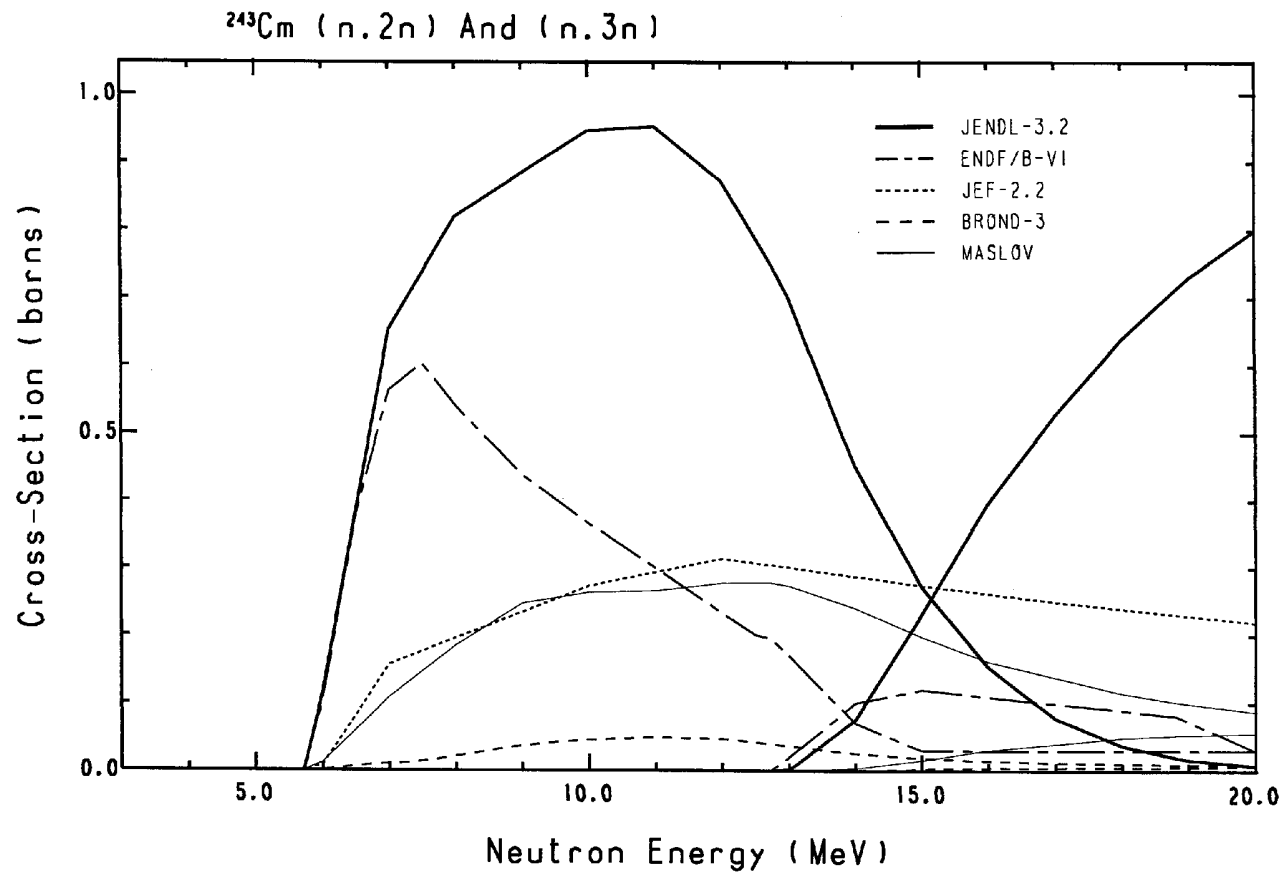


Figure 2.41. ^{243}Cm total inelastic scattering

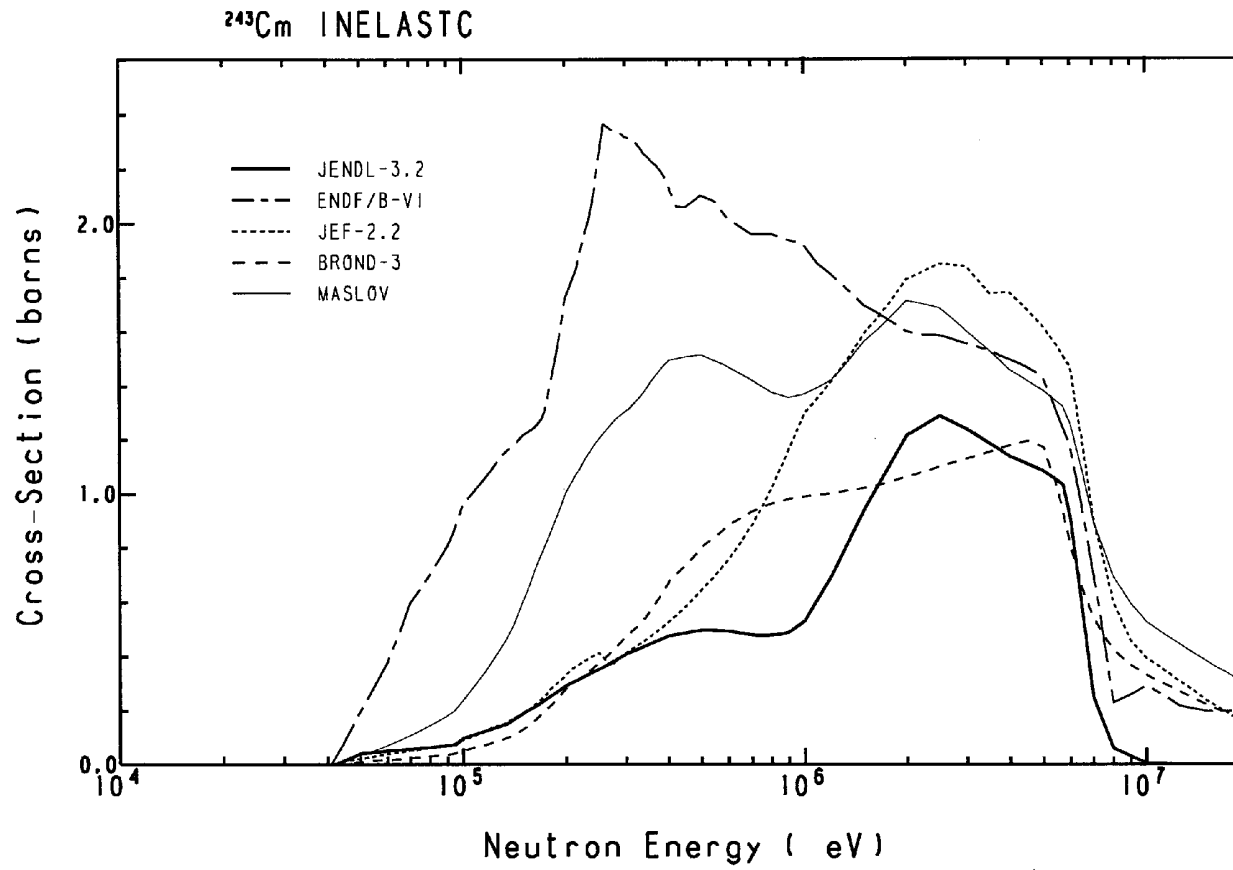


Figure 2.42. ^{243}Cm elastic scattering cross-section

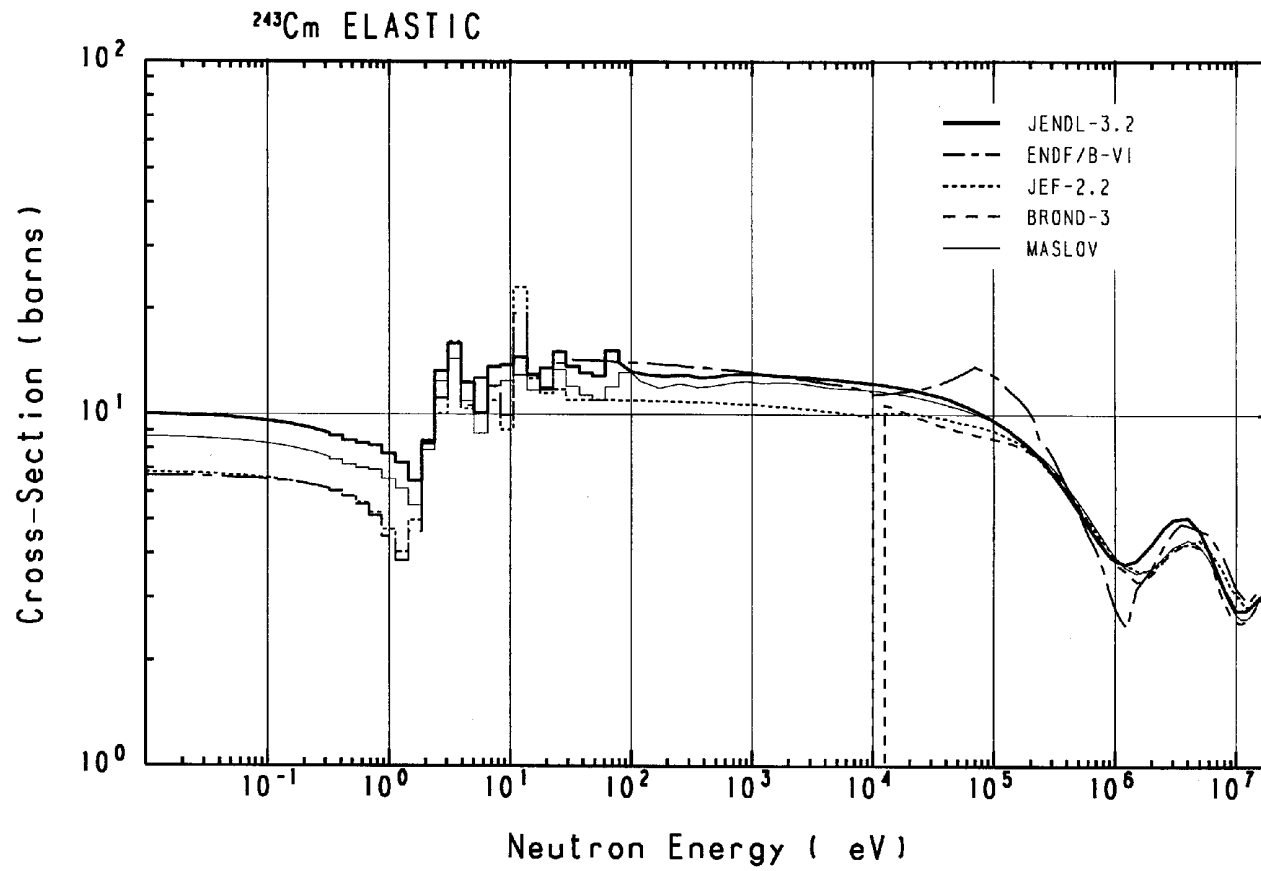


Figure 2.43. ^{243}Cm total cross-section

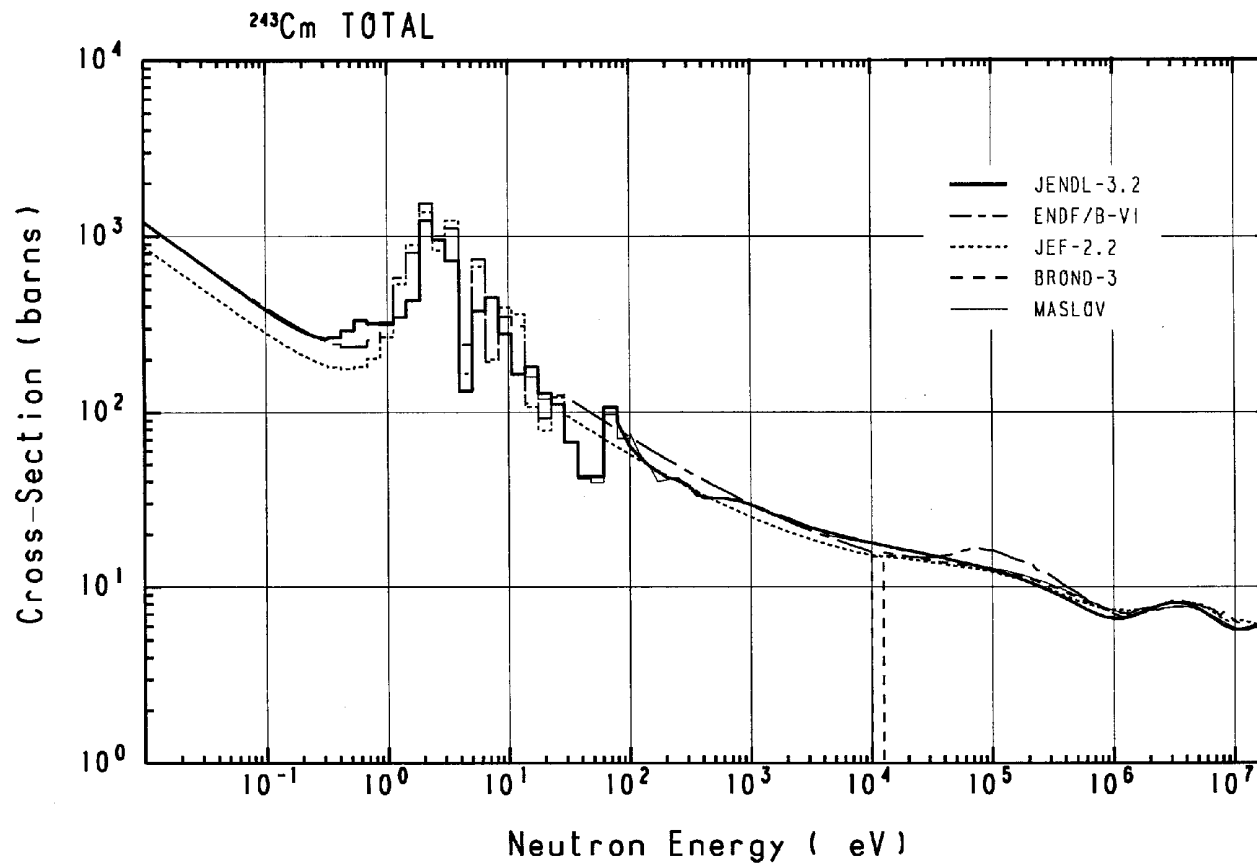


Figure 2.44. ^{244}Cm fission cross-section

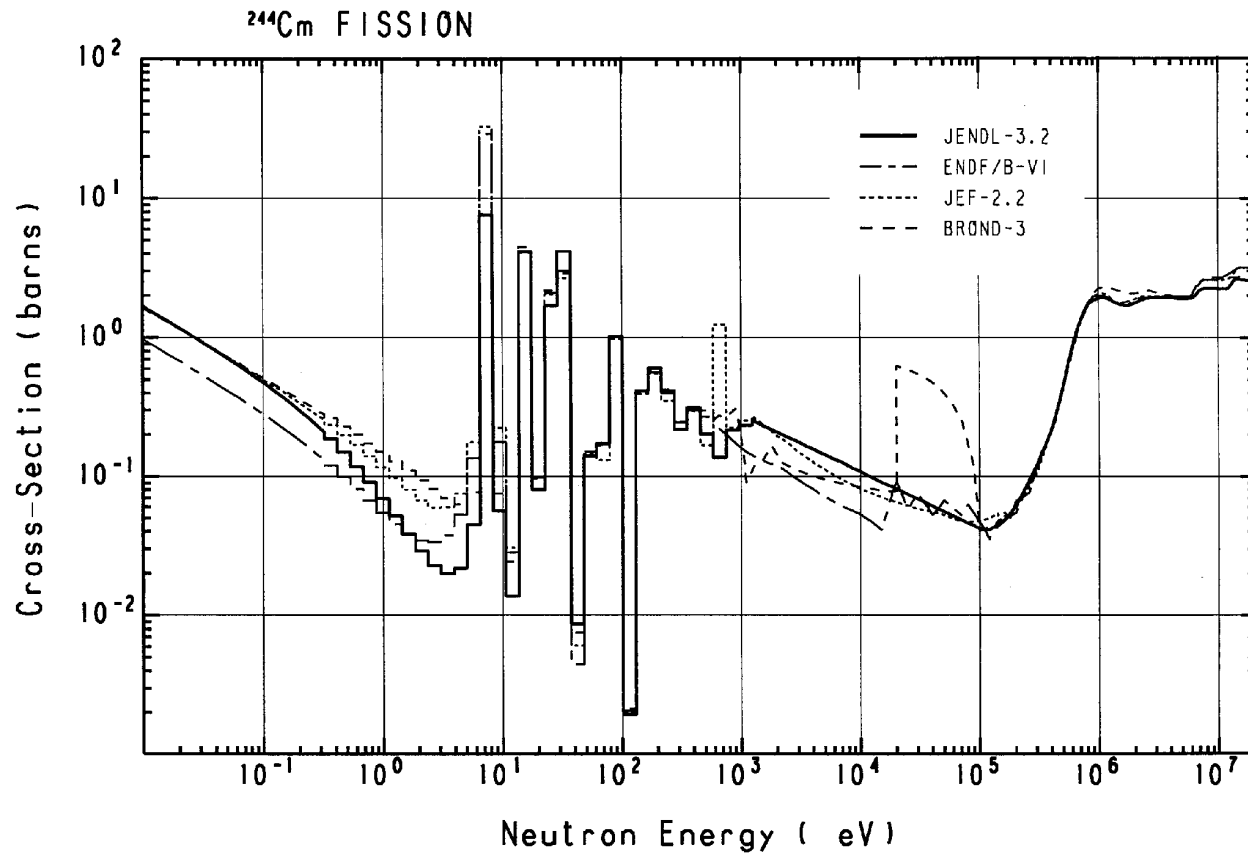


Figure 2.45(a). ^{244}Cm fission cross-section

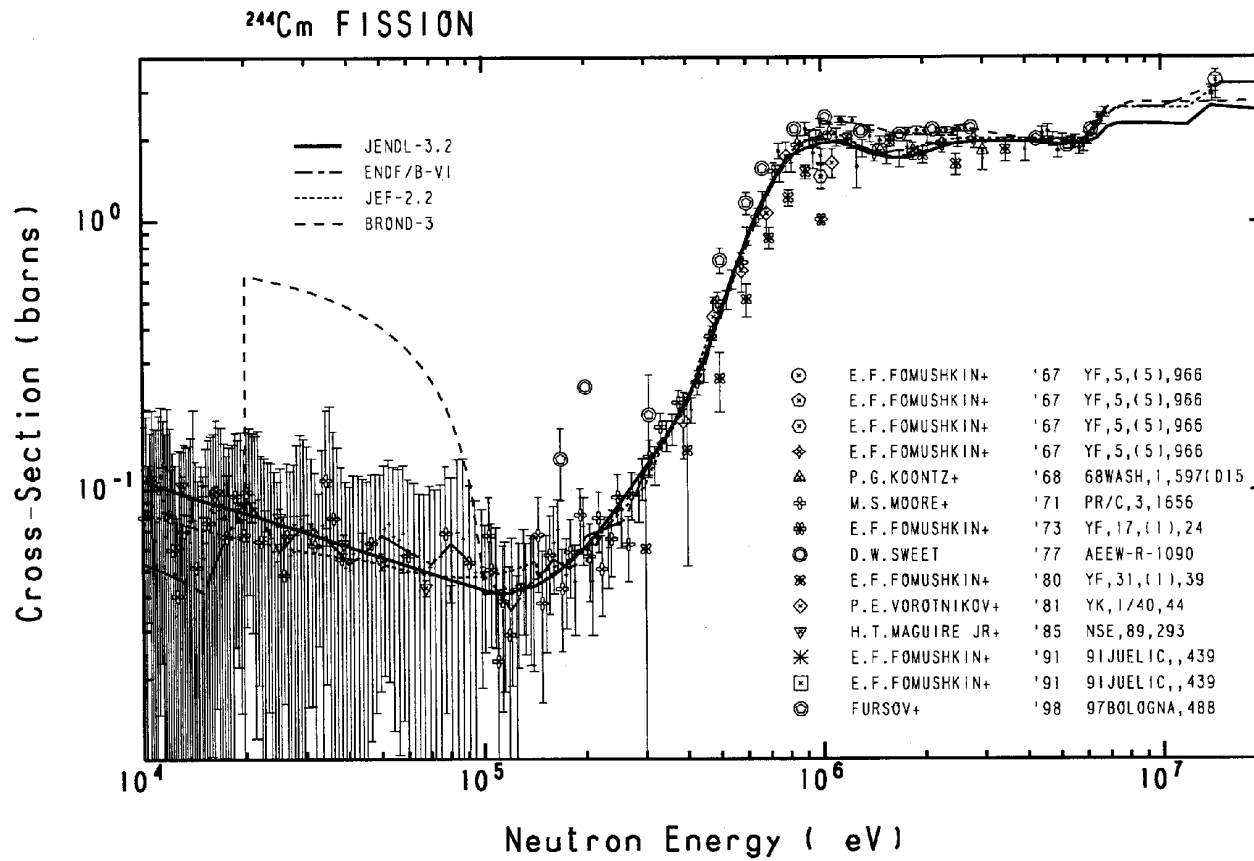


Figure 2.45(b). ^{244}Cm fission cross-section

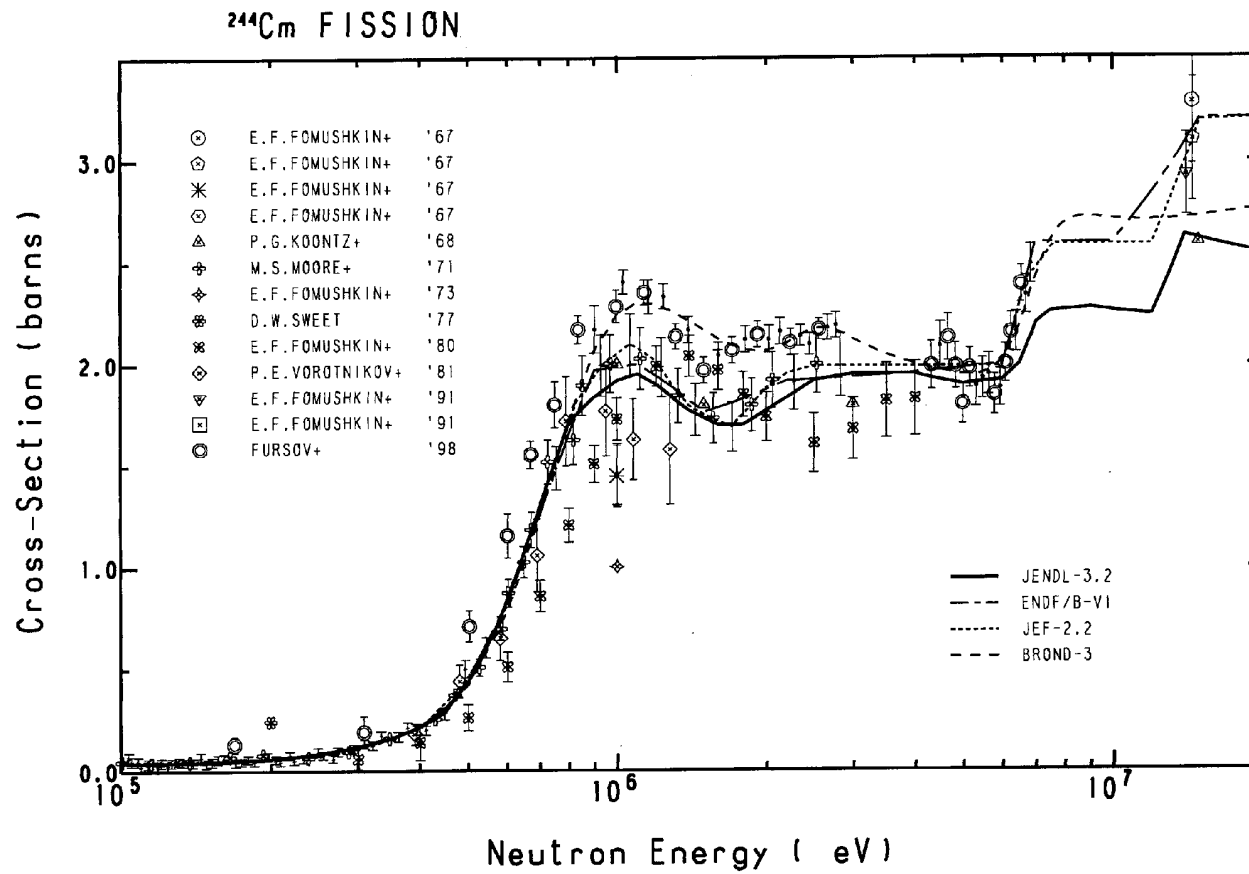


Figure 2.46. ^{244}Cm capture cross-section

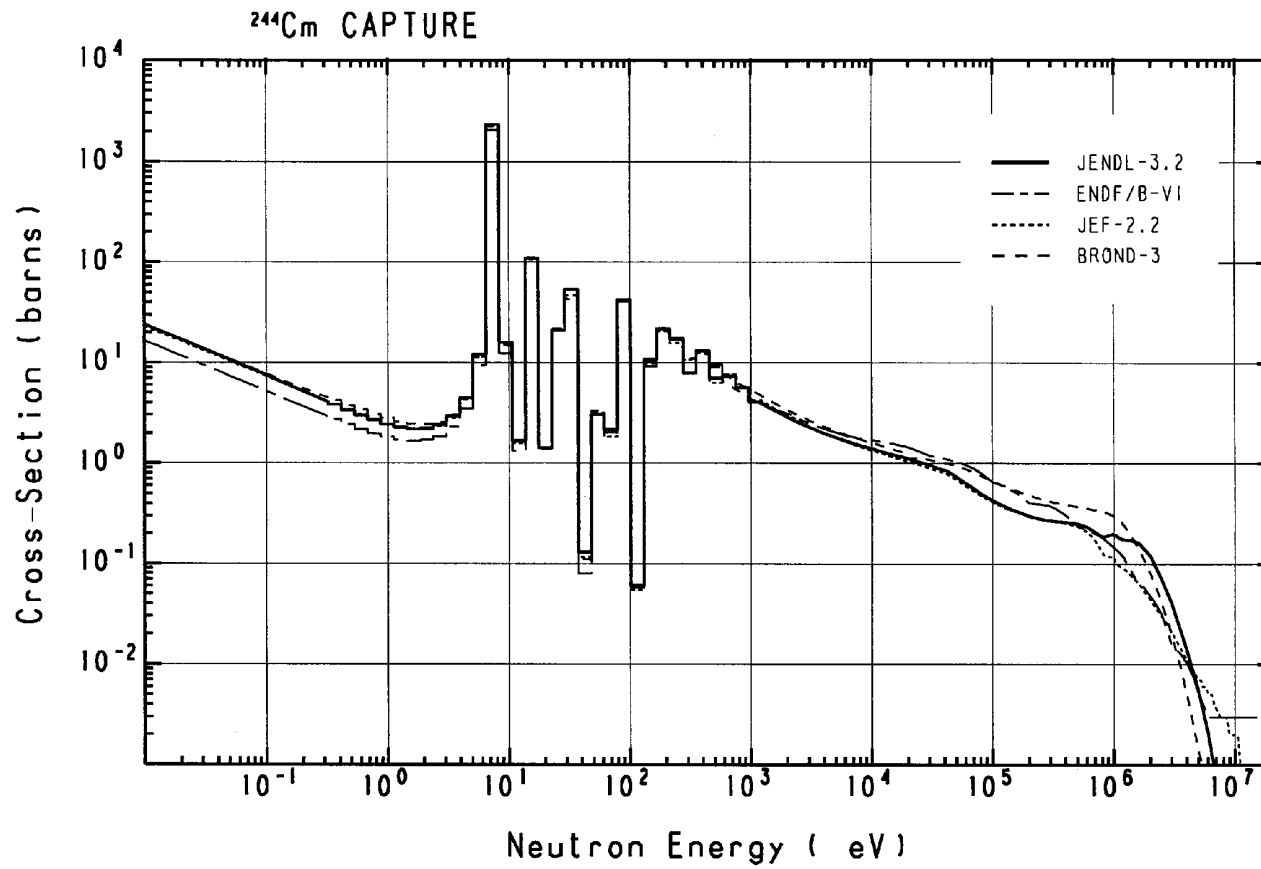


Figure 2.47. ²⁴⁴Cm capture cross-section

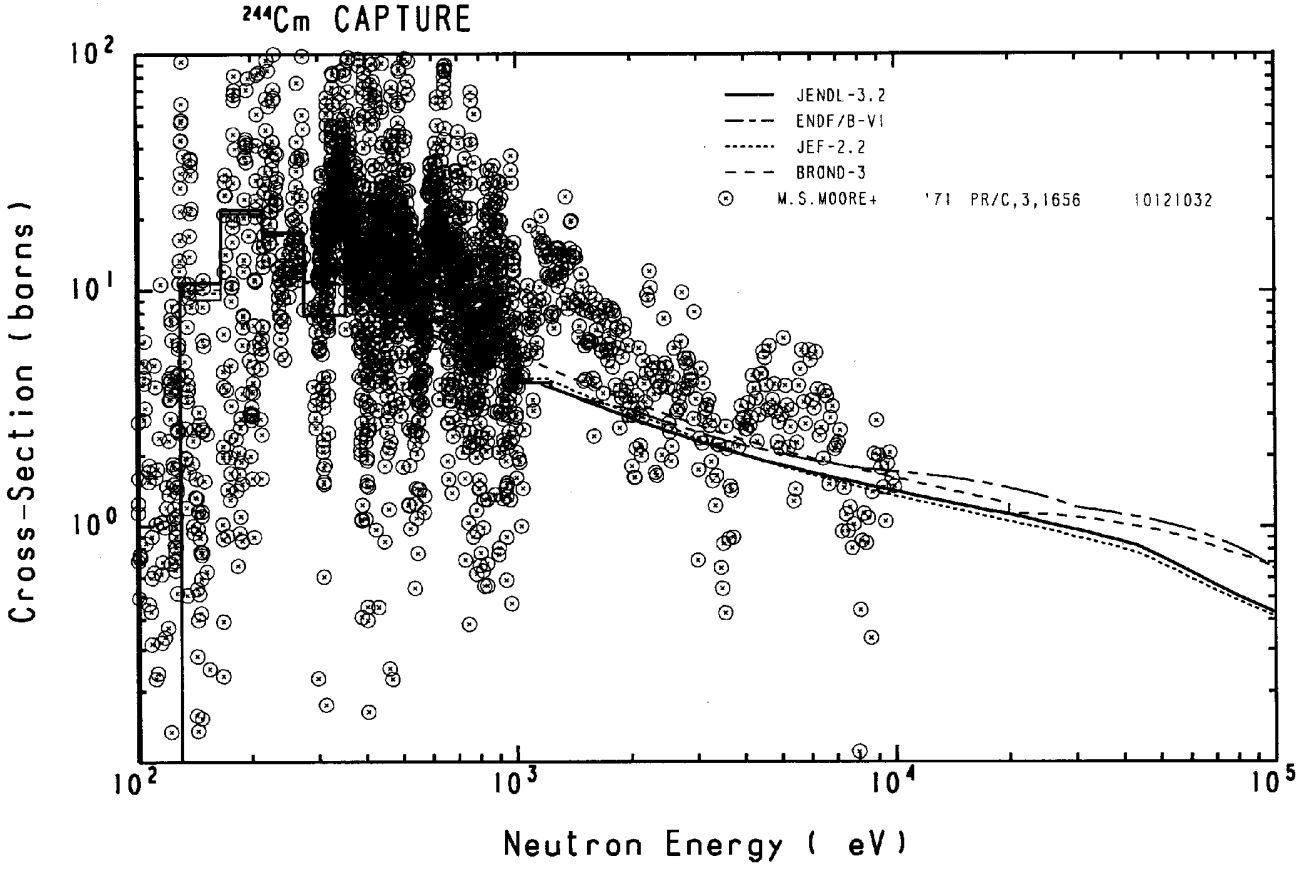


Figure 2.48. $^{244}\text{Cm}(n,2n)$ and $(n,3n)$ reaction cross-sections

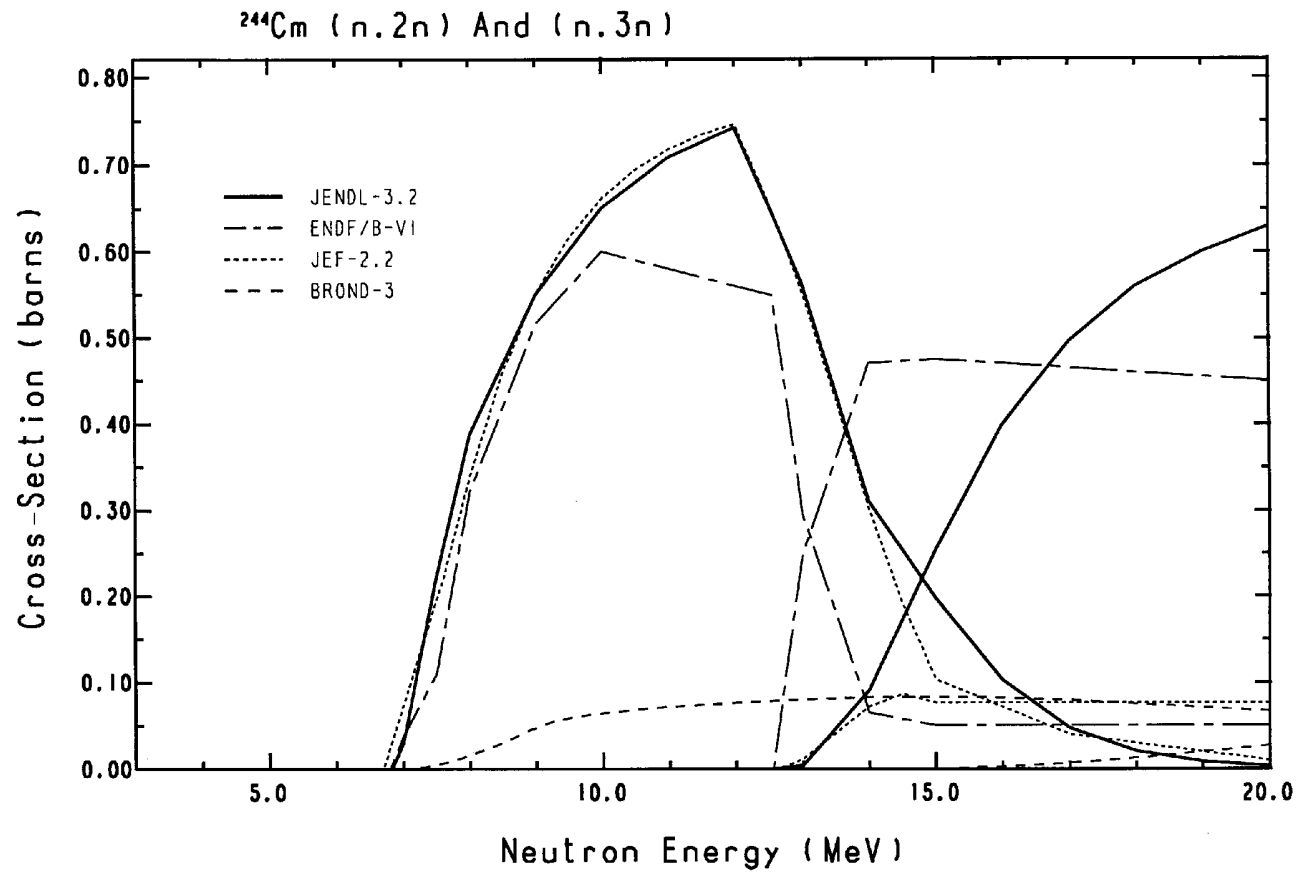


Figure 2.49. ^{244}Cm total inelastic scattering cross-section

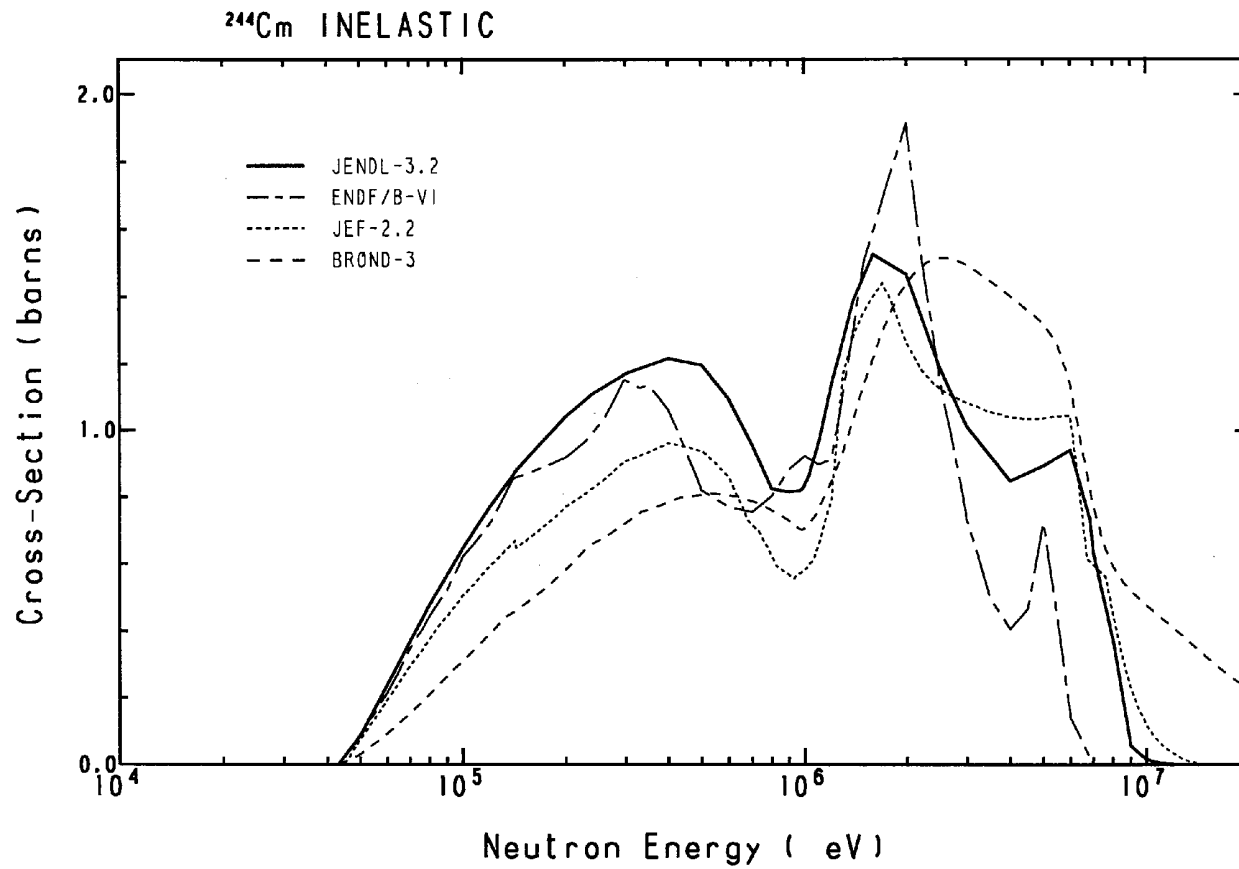


Figure 2.50. ^{244}Cm elastic scattering cross-section

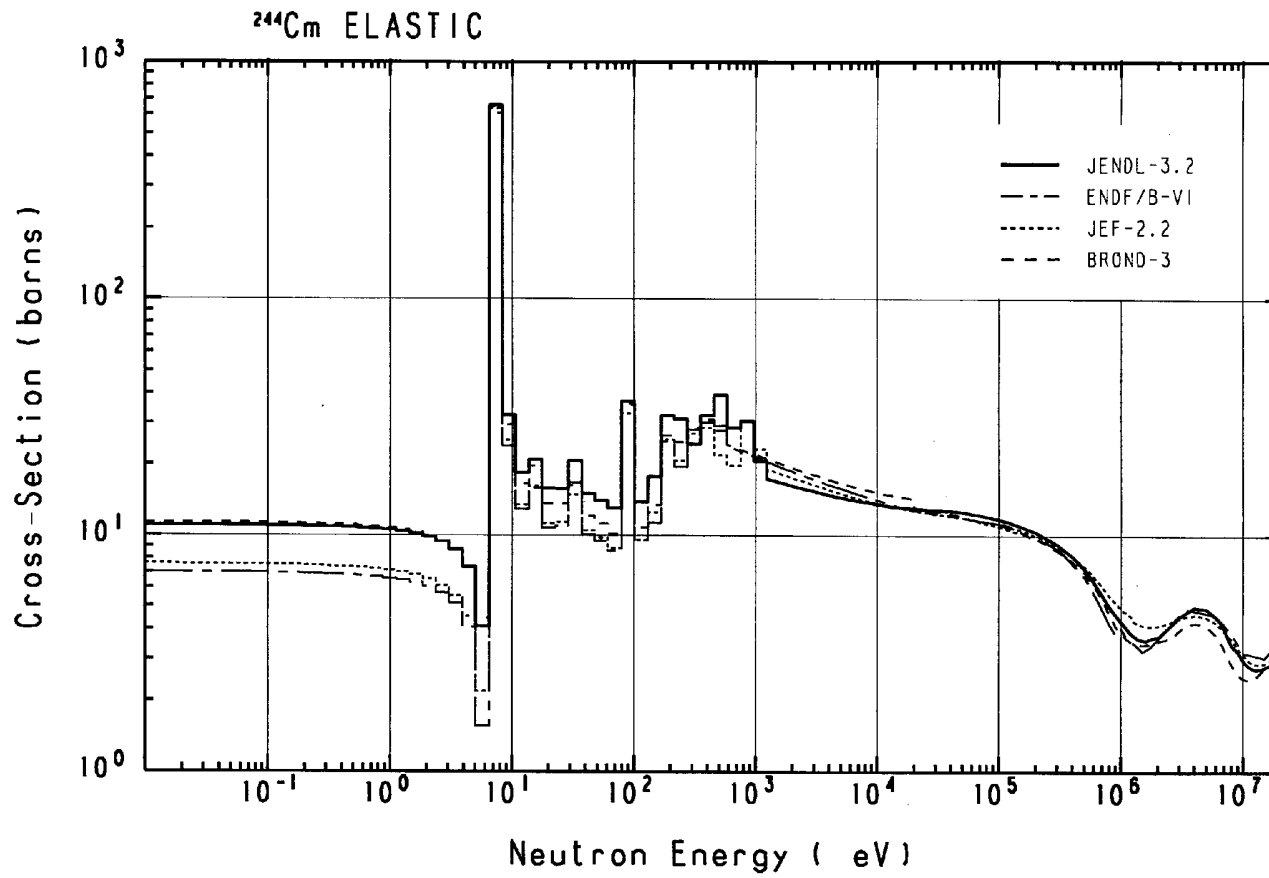


Figure 2.51. ^{244}Cm total cross-section

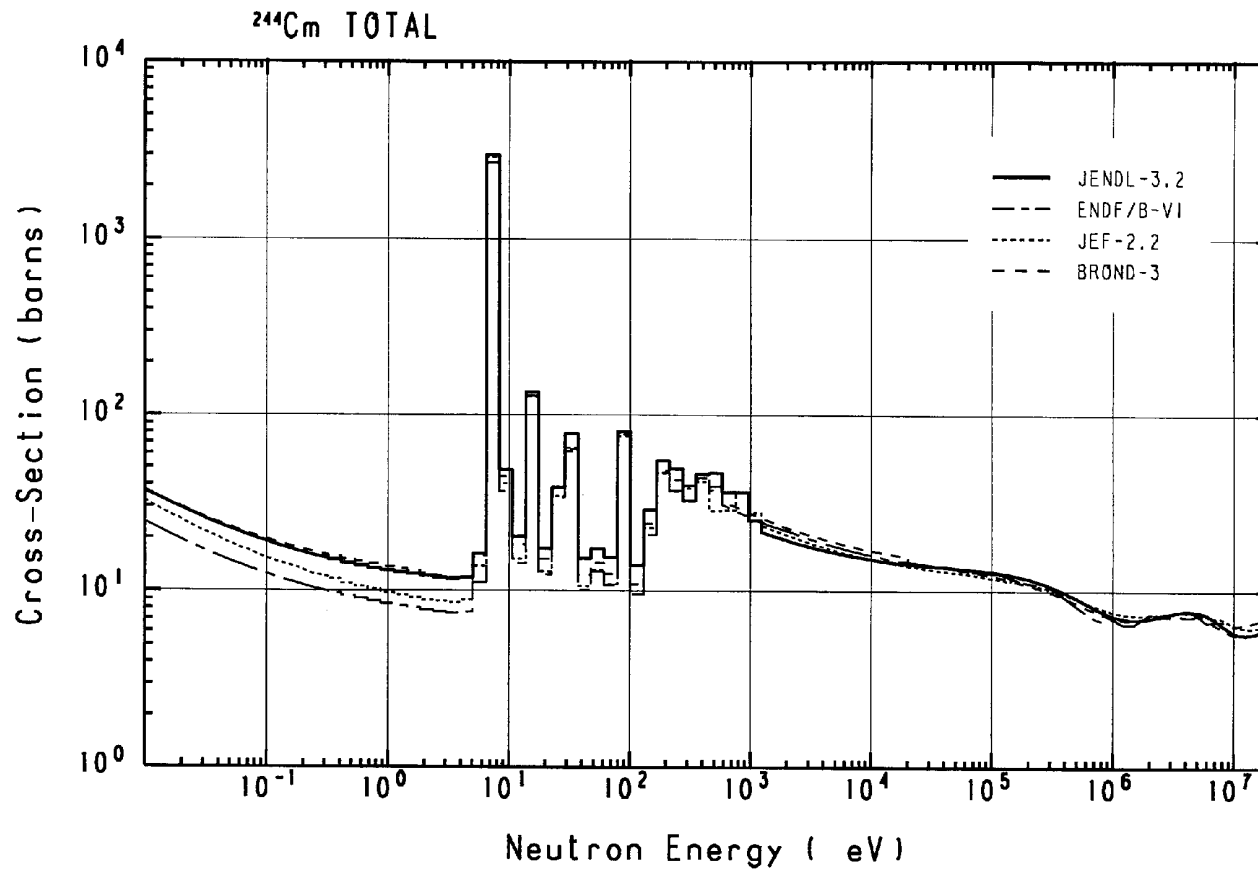


Figure 2.52. ^{245}Cm fission cross-section

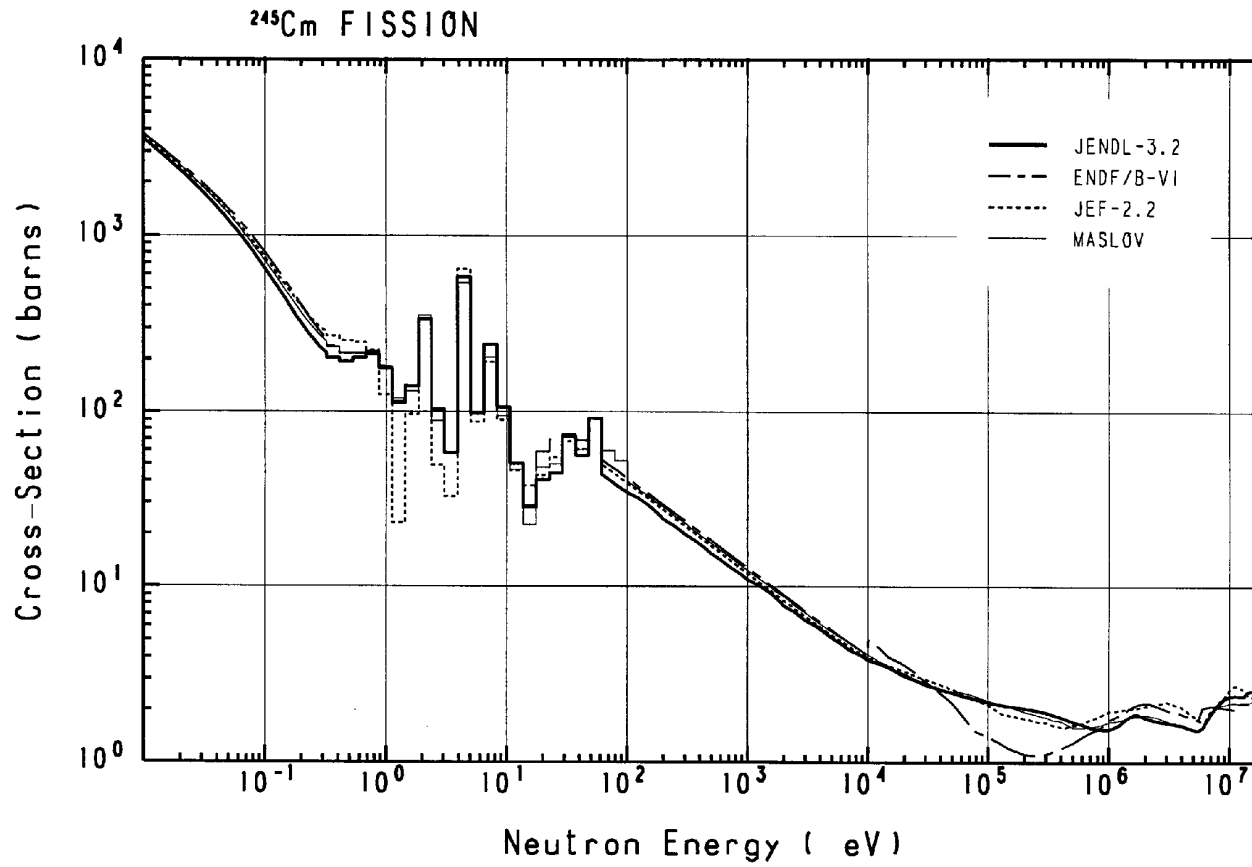


Figure 2.53. ^{245}Cm fission cross-section

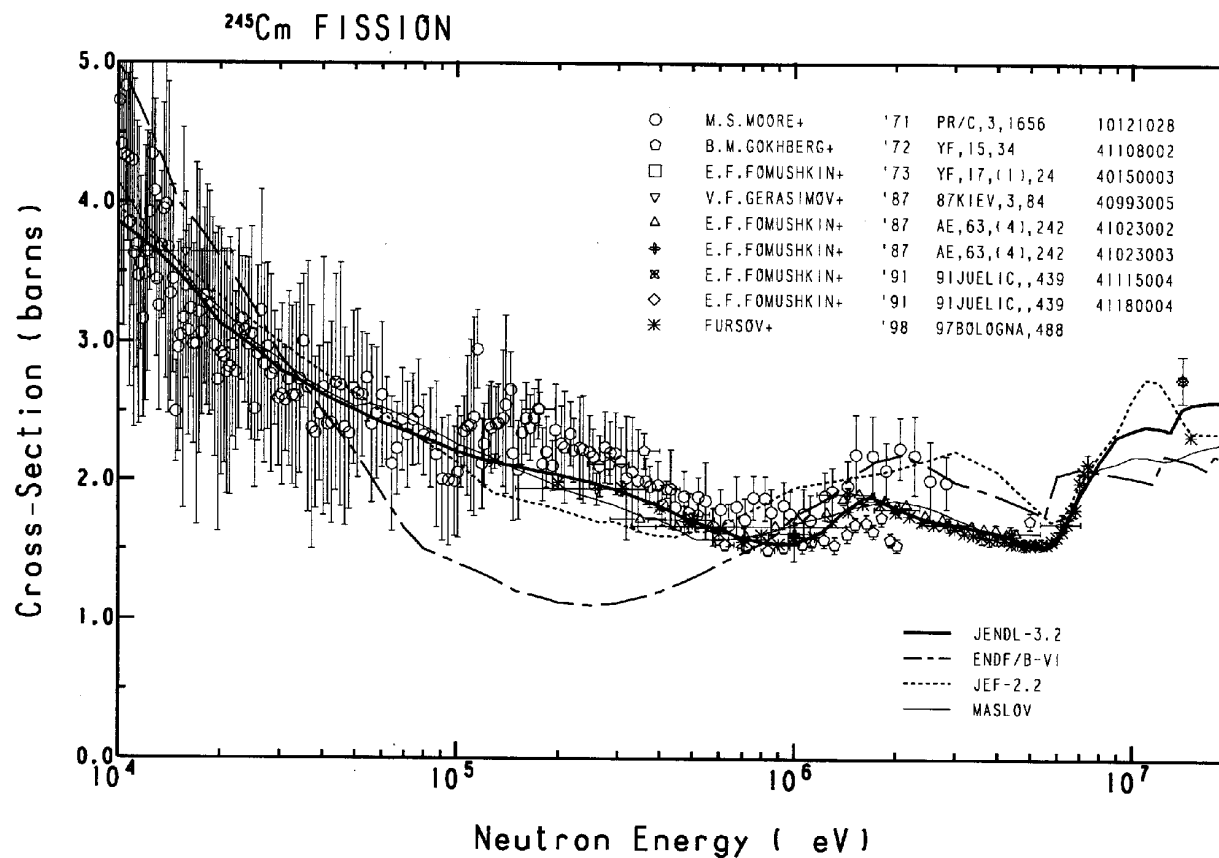


Figure 2.54. ^{245}Cm capture cross-section

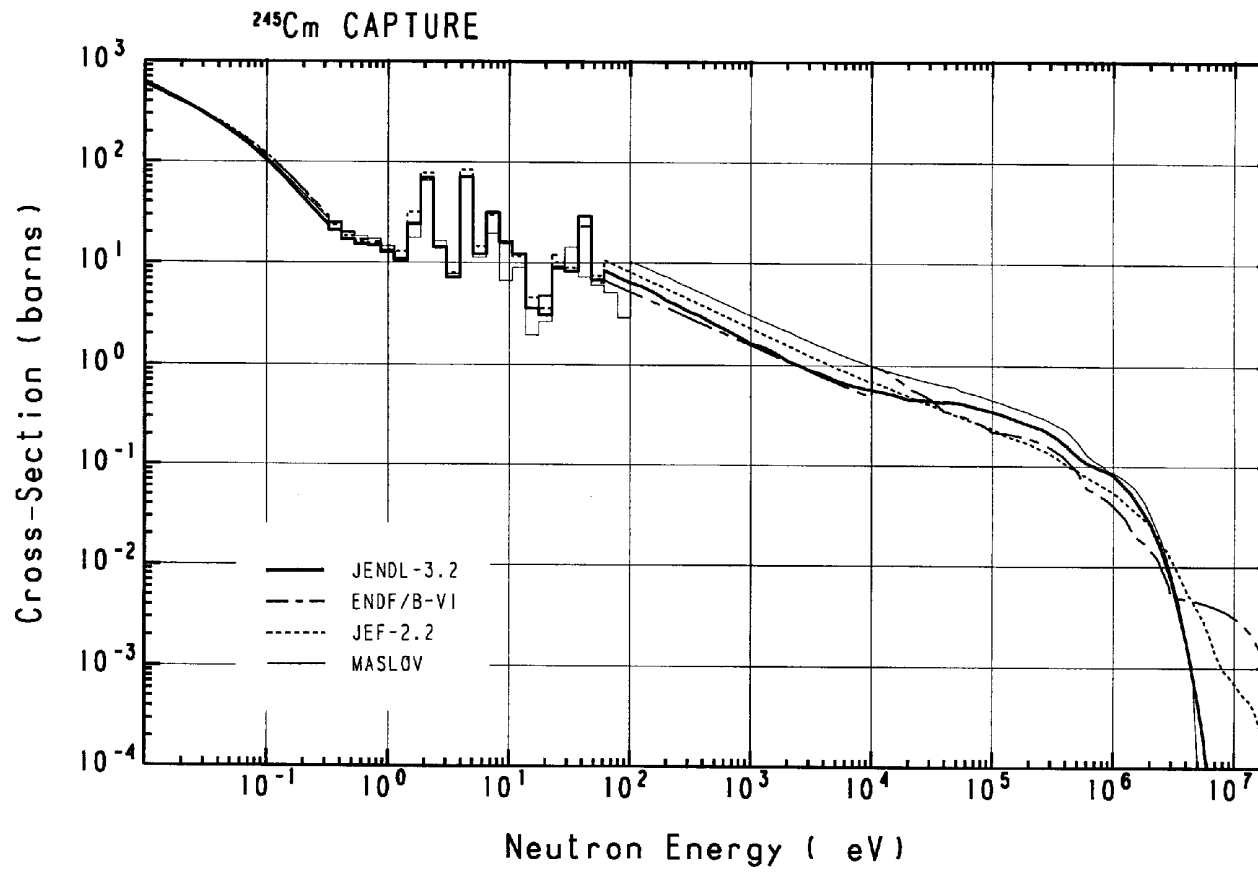


Figure 2.55. $^{245}\text{Cm}(n,2n)$ and $(n,3n)$ reaction cross-sections

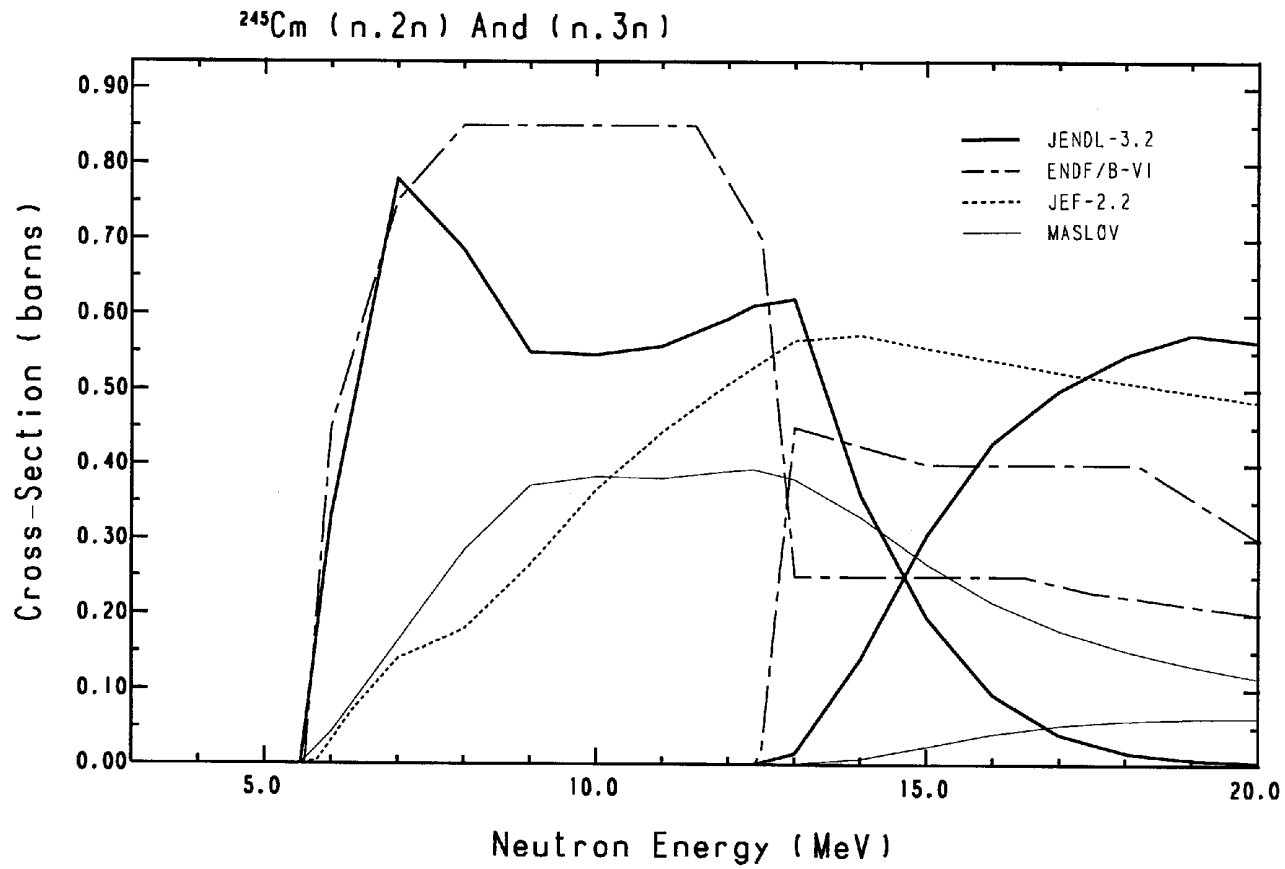


Figure 2.56. ^{245}Cm total inelastic scattering

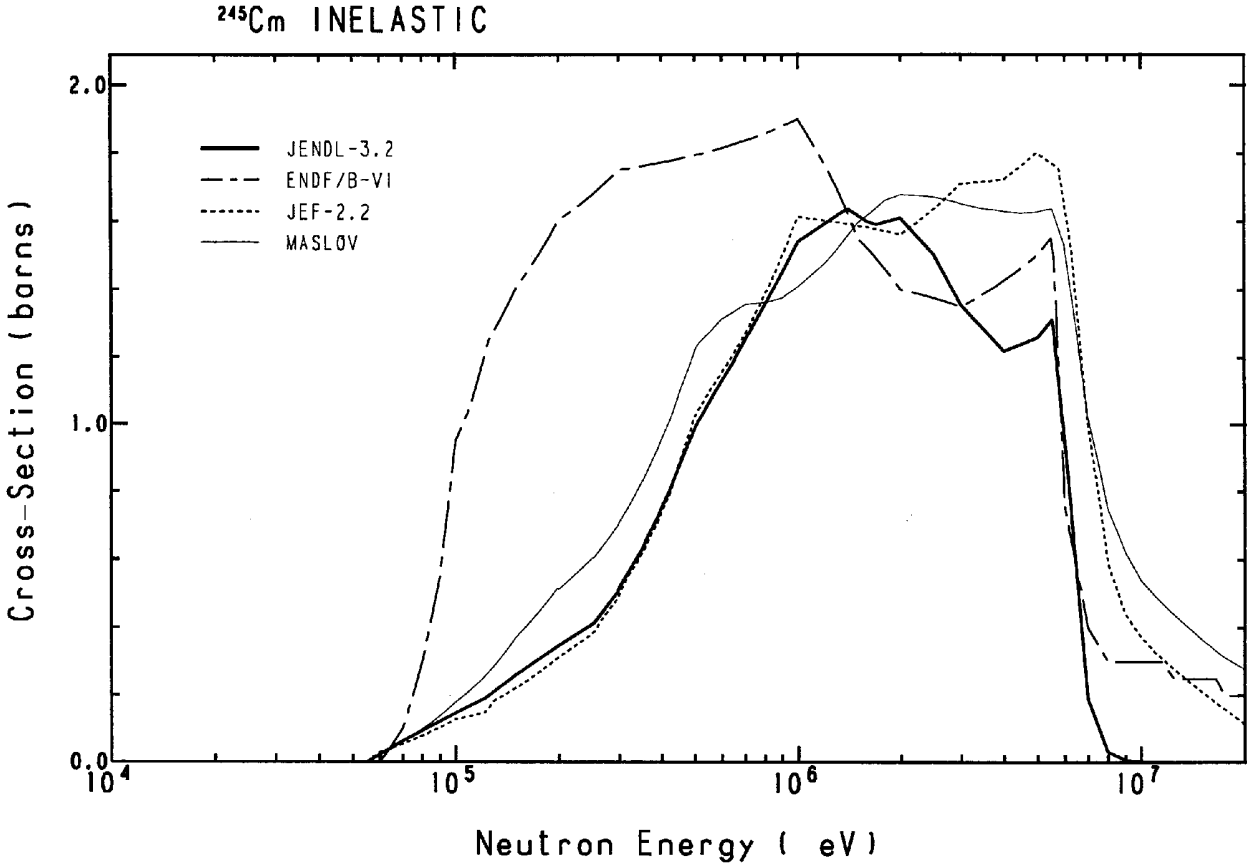


Figure 2.57. ^{245}Cm elastic scattering cross-section

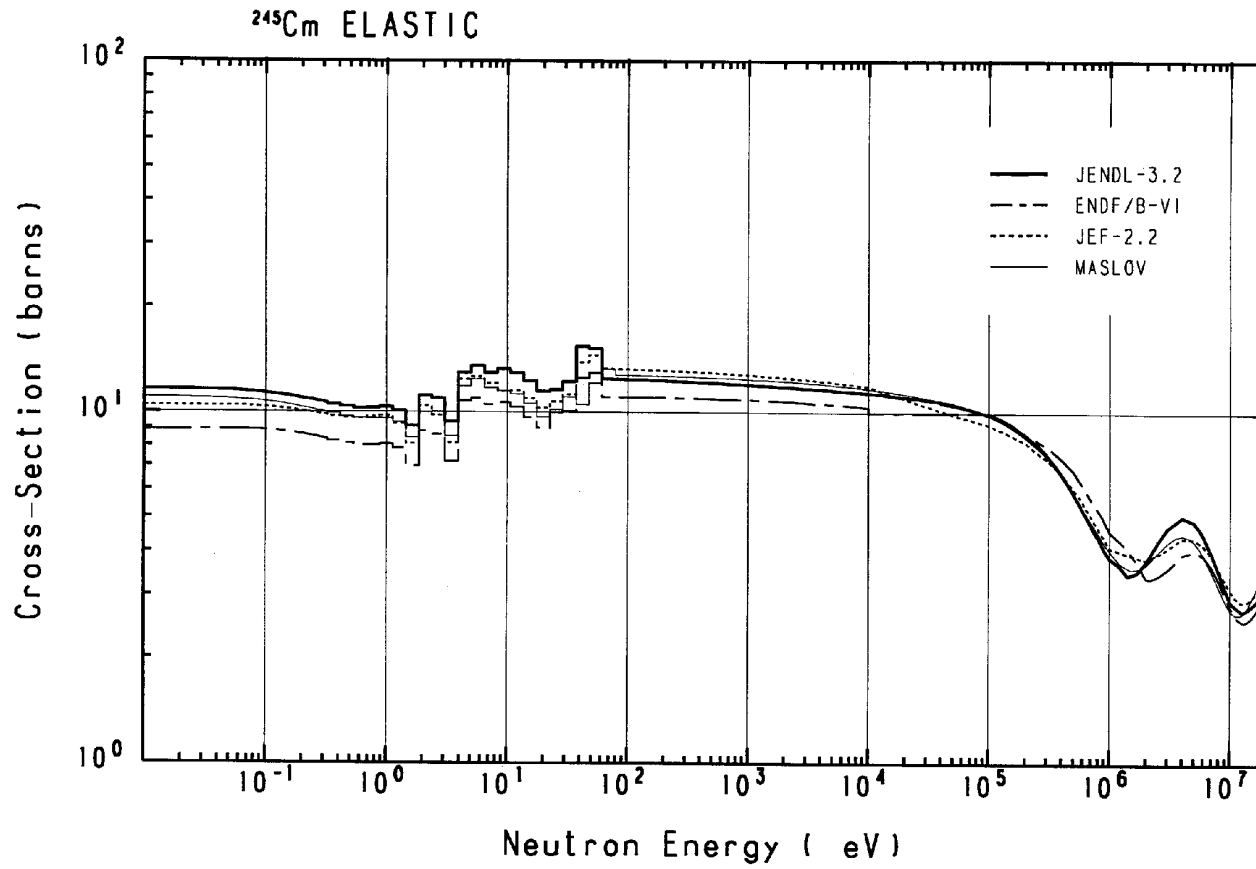


Figure 2.58. ^{245}Cm total cross-section

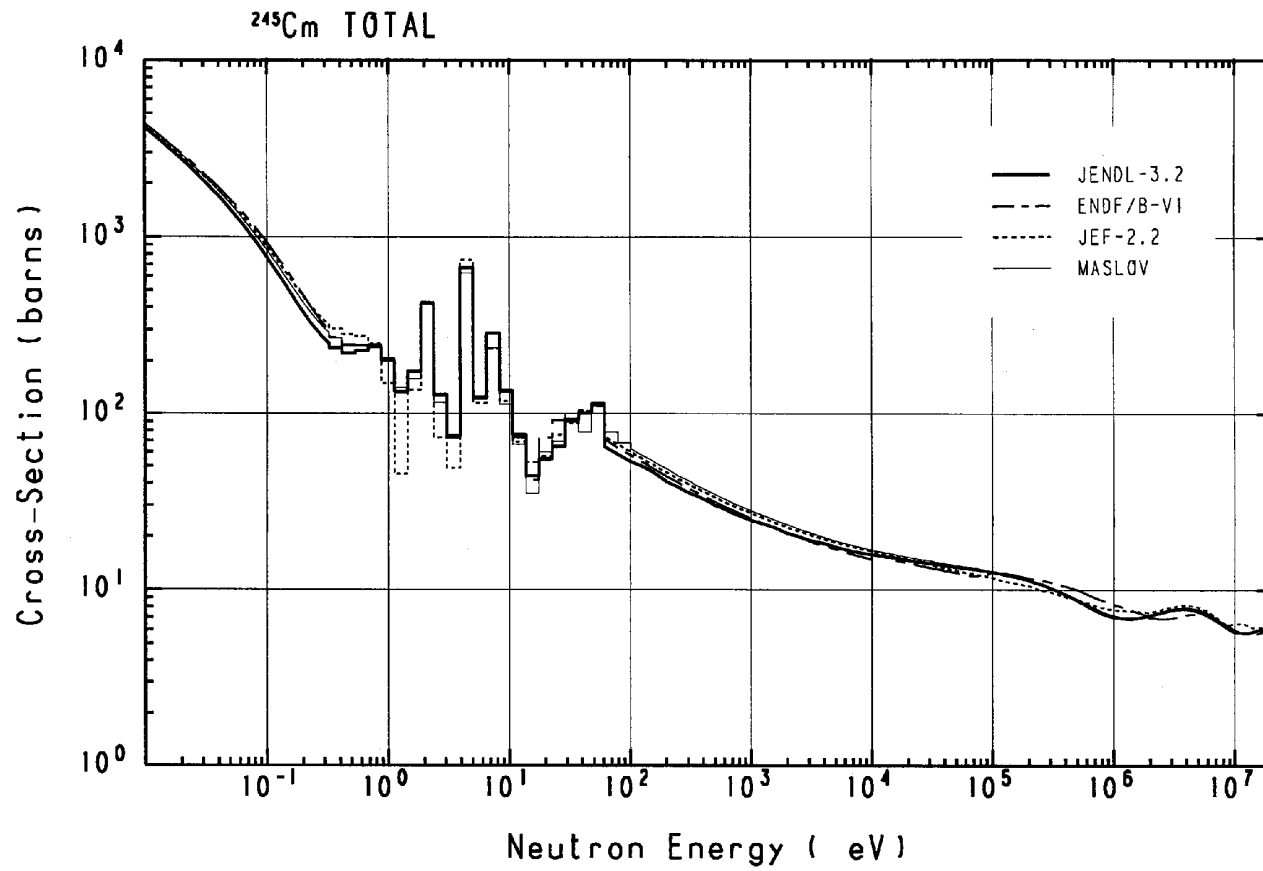


Figure 2.59. ^{237}Np number of neutrons per fission

Shown are the evaluated data for total ν and experimental data for total ν and ν_p

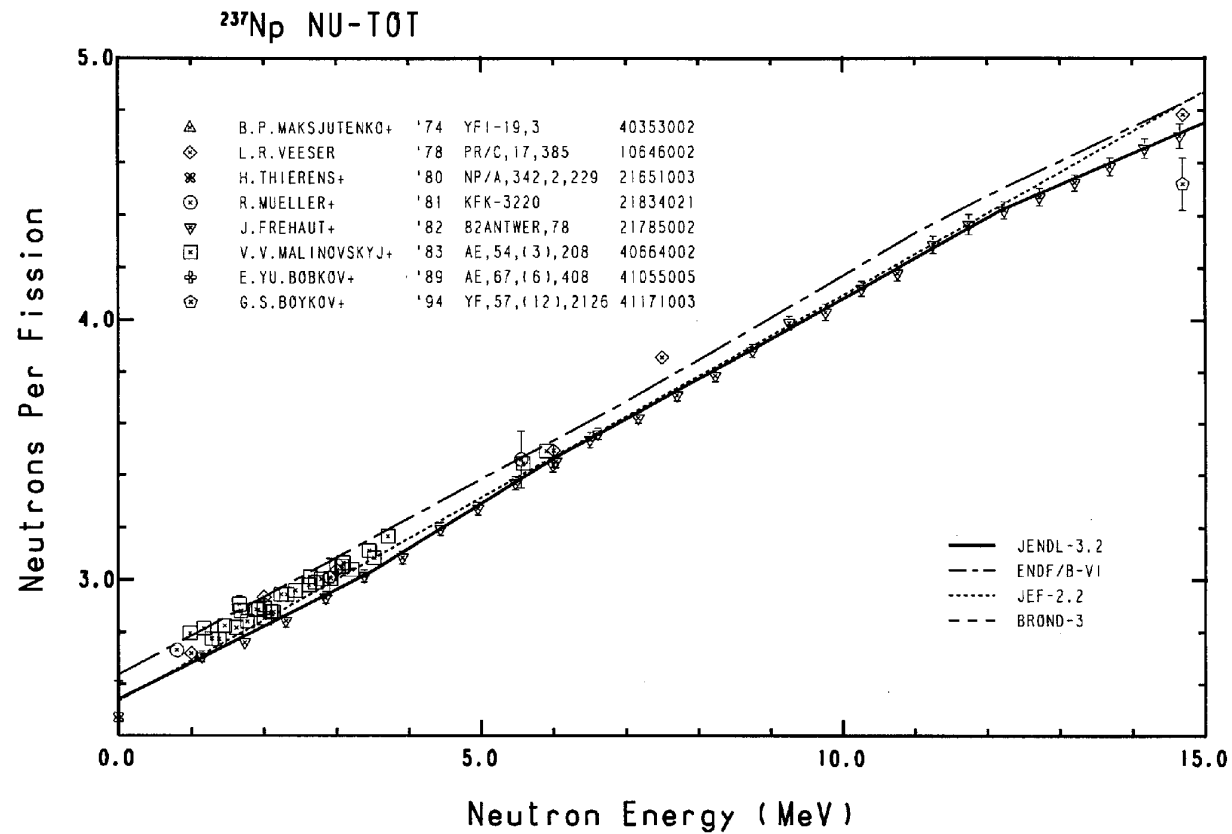


Figure 2.60. ^{241}Am number of neutrons per fission

Shown are the evaluated data for total ν and experimental data for total ν and ν_p

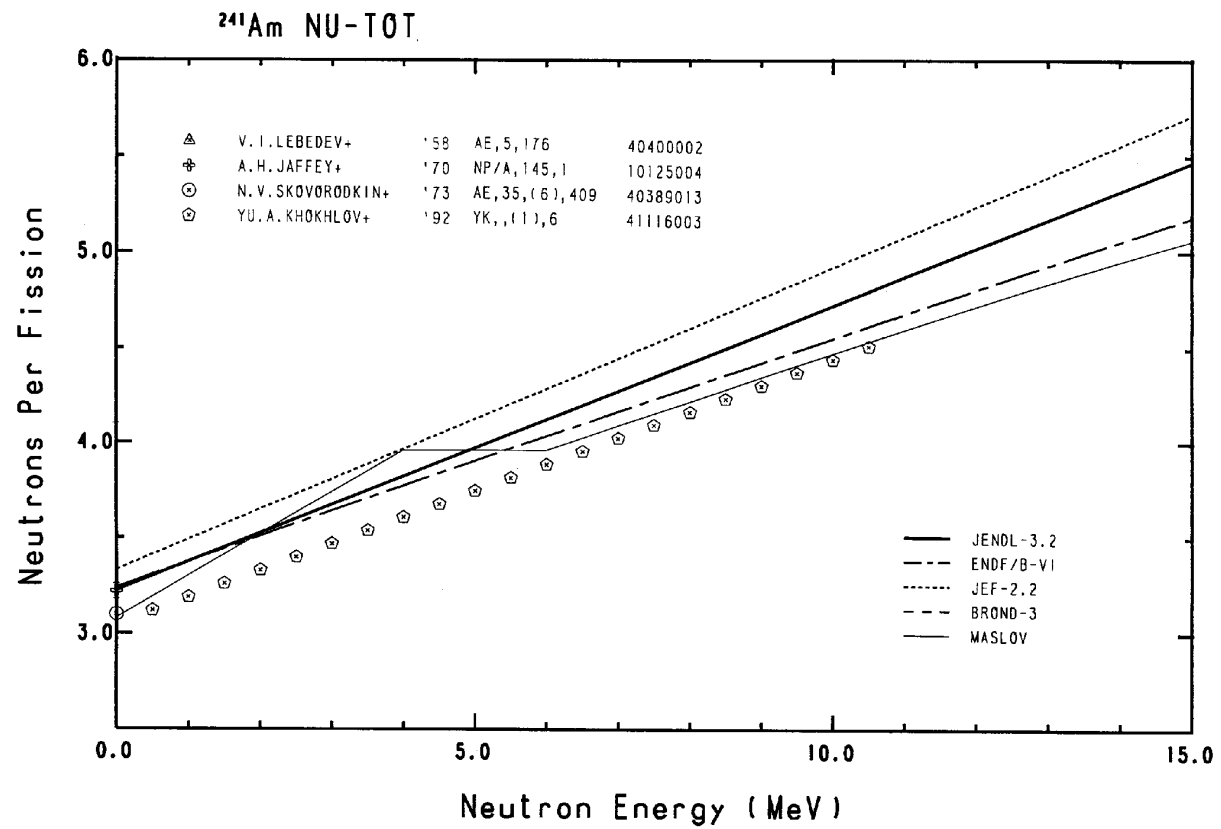


Figure 2.61. ^{243}Am number of neutrons per fission
Shown are the data for total ν

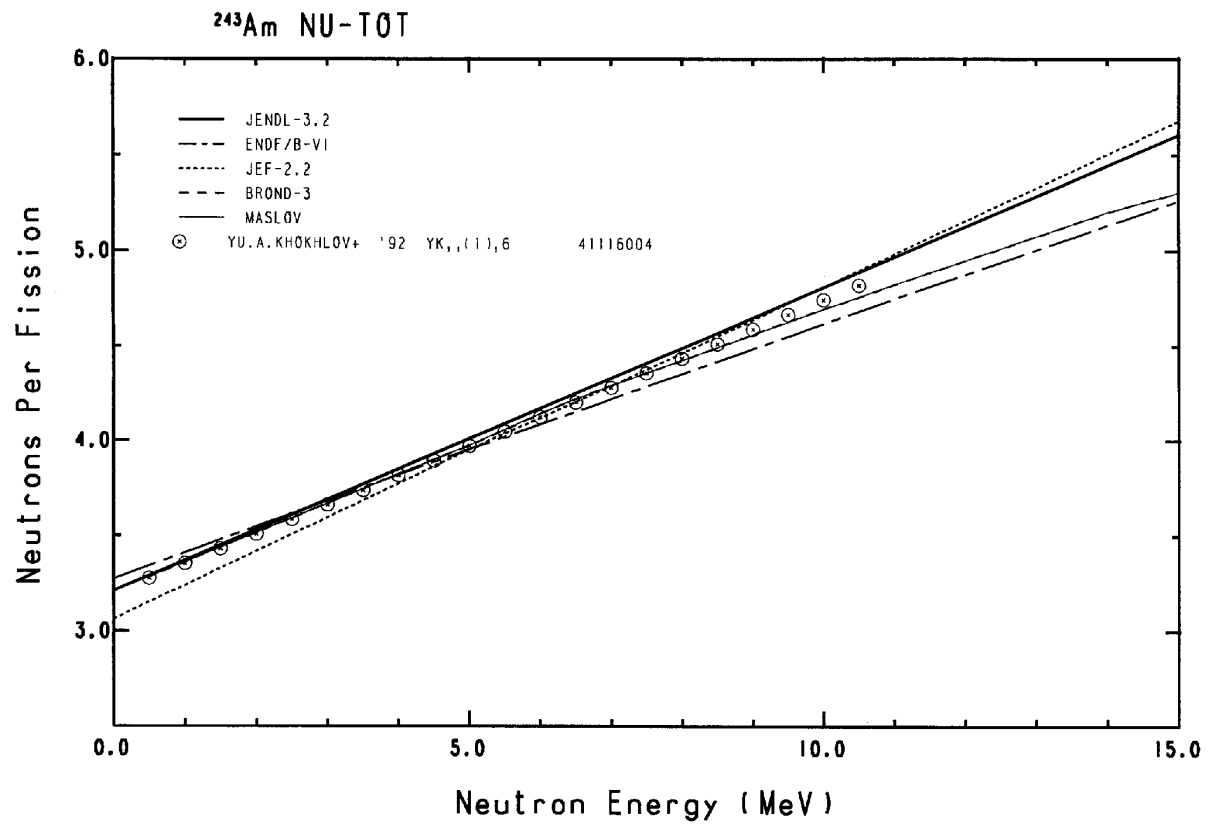


Figure 2.62. ^{242}Cm number of neutrons per fission

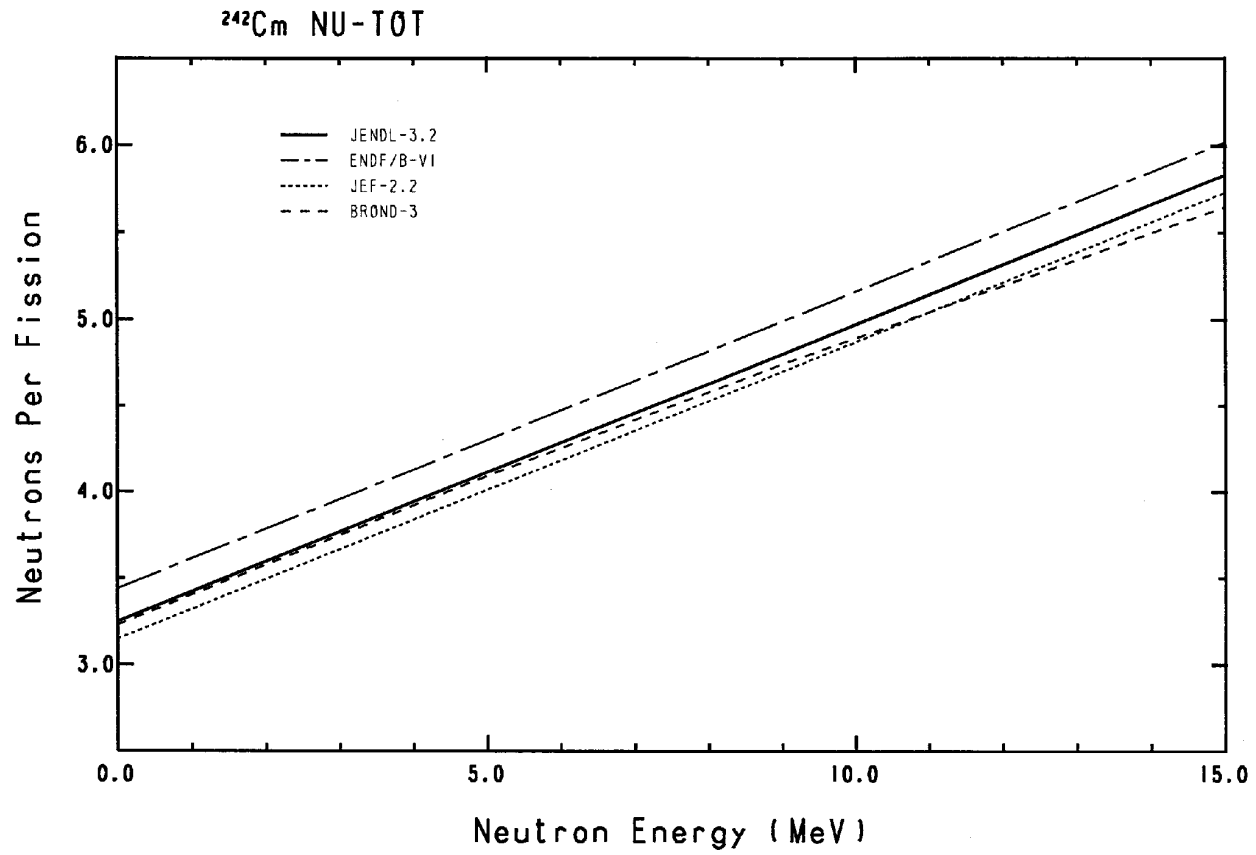


Figure 2.63. ^{243}Cm number of neutrons per fission
Shown are the evaluated data for total ν and experimental data for ν_p

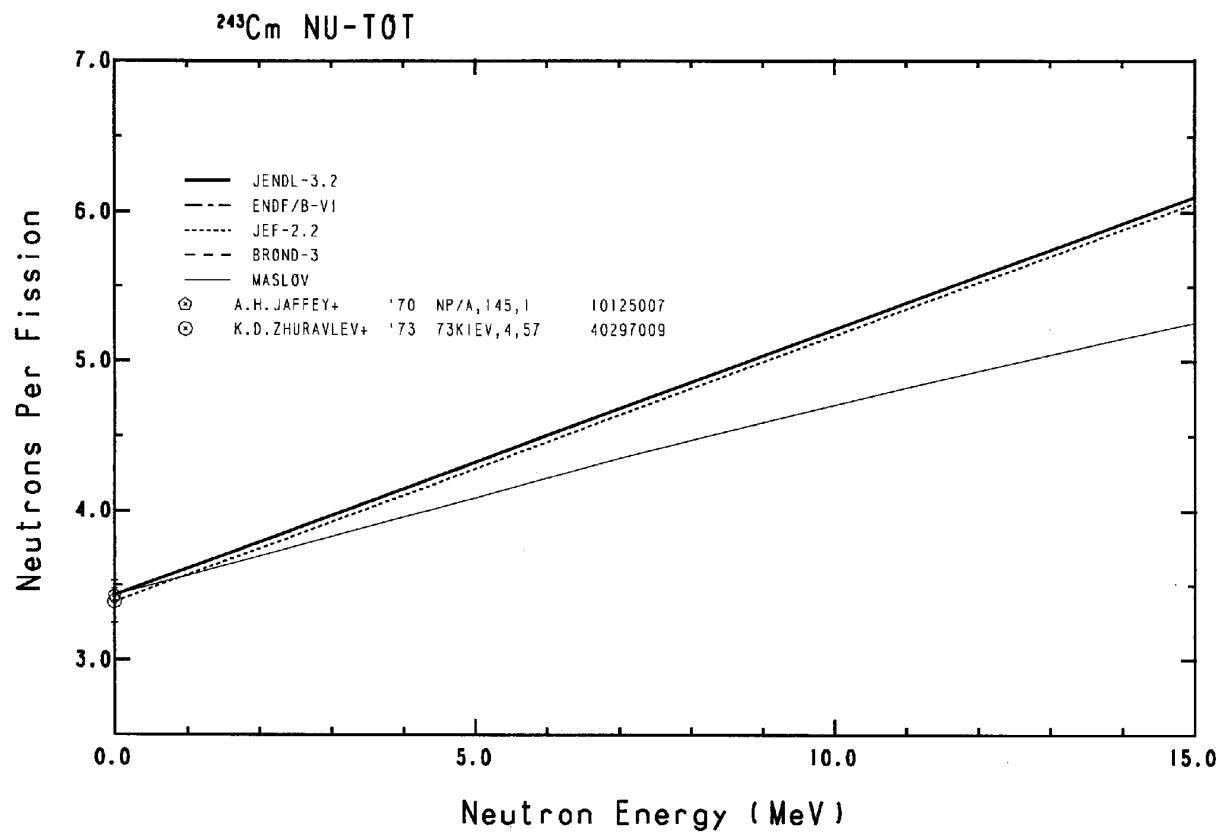


Figure 2.64. ^{244}Cm number of neutrons per fission

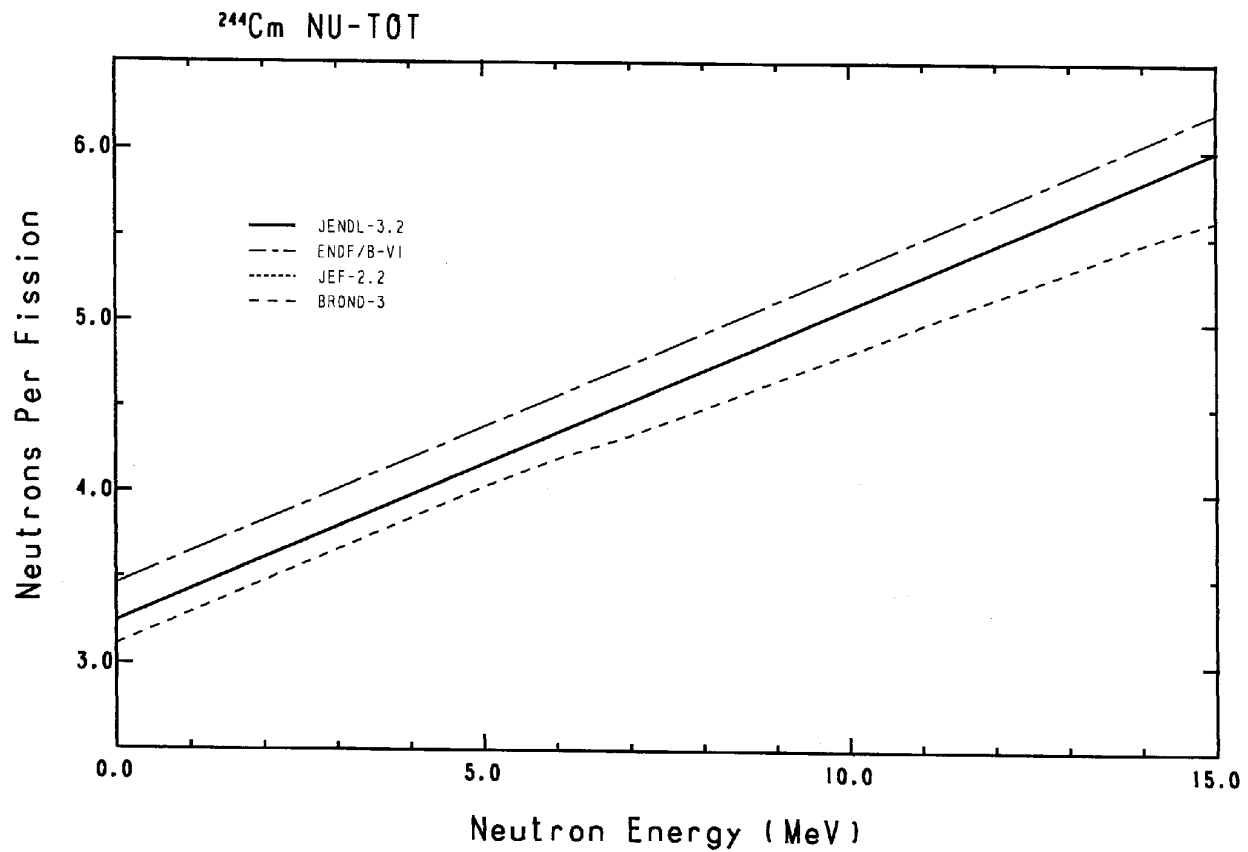


Figure 2.65. ^{245}Cm number of neutrons per fission

Shown are the evaluated data for total ν and experimental data for total ν and ν_p

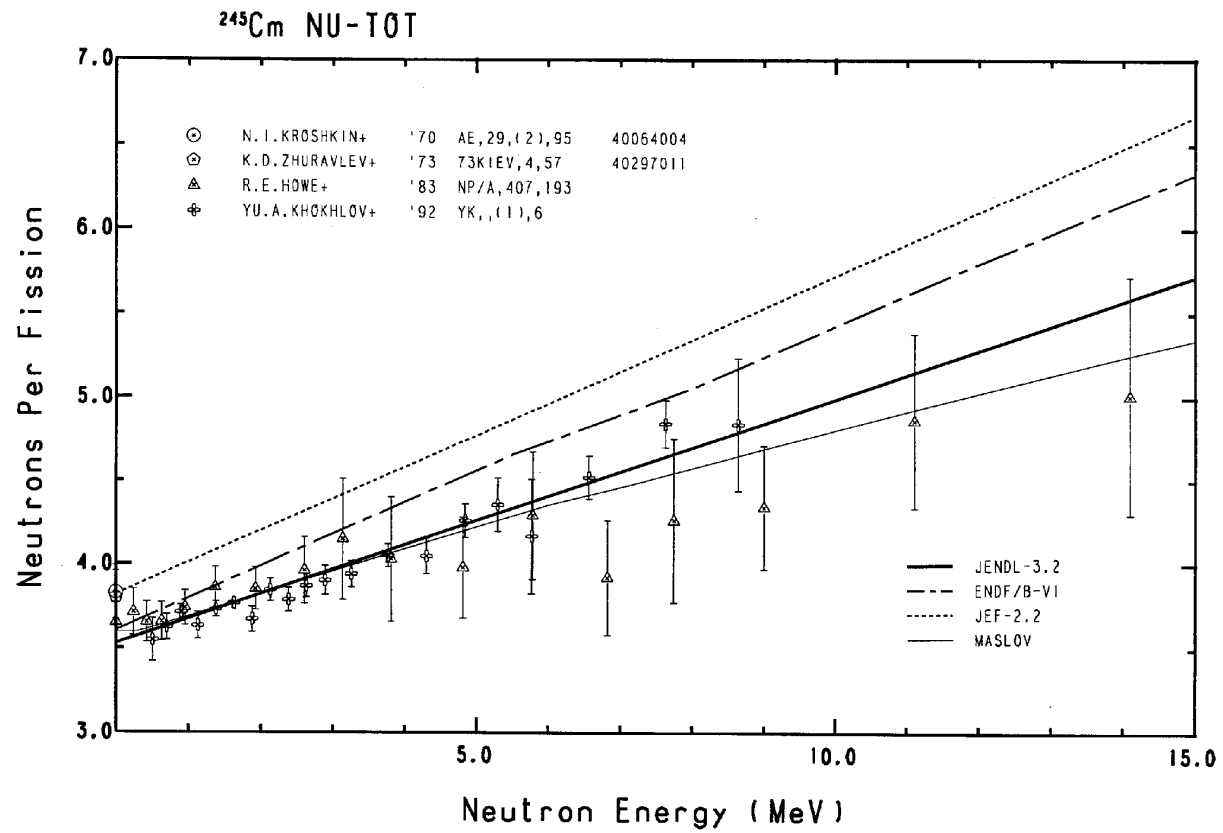


Figure 3.1. Neutron spectra in FCA-IX assemblies

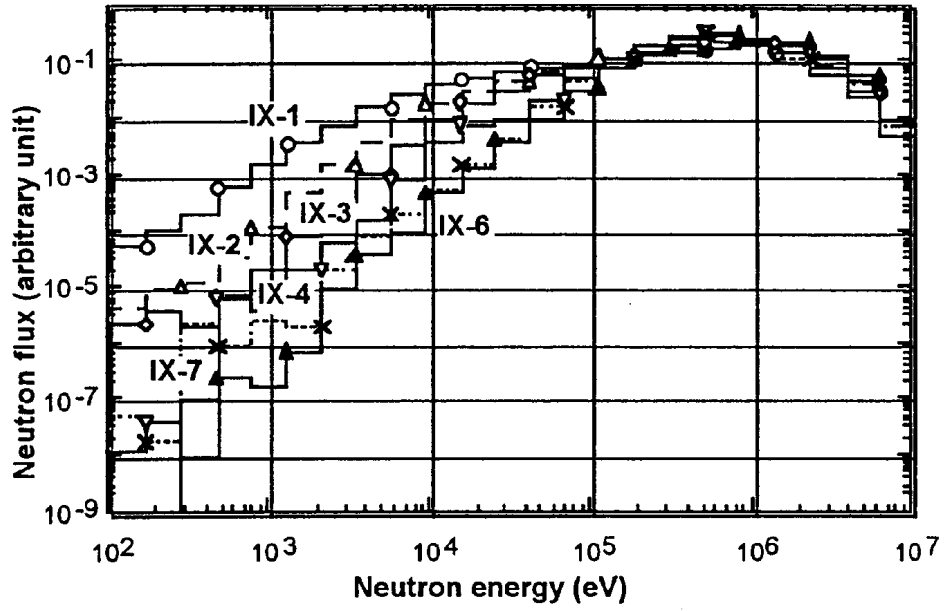


Figure 3.2. Comparison of burn-up reactivity change

